平均化法によるサブバンド適応フィルタとマイナー成分分析アルゴリズムの解析

AUTHOR(S):
酒井, 英昭

平均化法によるサブバンド適応フィルタとマイナー成分分析アルゴリズムの解析

(課題番号: 12650443)

平成12年度～平成13年度科学研究補助金(基盤研究(C)(2))
研究成果報告書

平成14年3月

研究代表者 酒井 英昭
(京都大学情報学研究科)

平均化法によるサブバンド適応フィルタとマイナー成分分析アルゴリズムの解析

(課題番号: 12650443)

平成12年度〜平成13年度科学研究補助金(基盤研究(C)(2))
研究成果報告書

平成14年3月

研究代表者 酒井 英昭
(京都大学情報学研究科)

はしがき

近年システム同定や適応フィルタ (ADF) の分野で適応アルゴリズムの平均的挙動を表す差分方程式や微分方程式に基づく性能解析の手法が注目されており，さまざまなシステムに応用されている．本研究では特にサブバンド ADF と複数のマイナー成分を適応的に抽出するアルゴリズムに平均化法を適用し，それらの性能解析を行なった．

サブバンド ADF は信号を複数の帯域に分割し，各帯域に ADF を配置することにより計算量の低減と収束速度の改善を計る手法であり，すでにさまざまな構成法が提案されている．しかし従来の手法では遅延が生じるので実時間処理を行なうシステムには不向きであった．そこで遅延のないサブバンド ADF が提案されており，アダマール変換を用いて拡張された遅延のないサブバンド ADF が研究代表者らによって提案された．これらのシステムではレート変換や複数のフィルタが存在するため，時間領域において平均化法を直接適用し解析を行うことは難しい．そこで離散フーリエ変換を対象とするアルゴリズムに適用し，アルゴリズムを周波数領域表現に変換した後，平均化法を適用するという手法を開発した．本手法によりアルゴリズムの安定条件や誤差信号の分散が見通しのよい形で得られた．さらに最近 Pradhan と Reddy によって提案された新しい構成のサブバンド ADF に本手法を適用し，その性能解析を行なった．

マイナー成分分析は信号成分のパラメータ推定問題に用いられる重要な手法である．従来，主成分分析で用いられた適応アルゴリズムの適応ゲインの符号を反転させたアルゴリズムが研究されてきたが，単一成分の抽出が主で複数成分の抽出に関しては十分な研究がなされていない．そこで本研究ではデフレーション法とグラムシュミットの直交化法を組み込むことにより，複数のマイナー成分を抽出するアルゴリズムを提案した．提案したアルゴリズムの性能解析を ODE 法により行ない，アルゴリズムが常に安定であることを示し，抽出したマイナー成分の誤差ベクトルの共分散行列を理論的に求めた．

以上の結果は現在それぞれ専門雑誌に投稿中であり，その原稿を元に本報告書に成果としてまとめた．後半にはすでに発表した論文の別刷りが添付されている．これらの成果を通じて，平均化法が種々の適応アルゴリズムの解析において非常に有効な手段であることを示すことができた．

研究組織

研究代表者　酒井 英昭　(京都大学大学院情報学研究科)
研究分担者　宮城 茂幸　(京都大学大学院情報学研究科)

交付決定額 (分配額) (金額単位: 千円)

平成 12 年度	900
平成 13 年度	1,000
総計	1,900

研究発表

1. S. Miyagi and H. Sakai, "Convergence Analysis of the Delayless Subband Adaptive Filter Based on the Frequency Domain Expression," Proceeding of ICASSP2000, Istanbul, Vol. 1, pp.368–371, May. 2000.
2. H. Sakai and S. Miyagi, "Performance Analysis of an Adaptive Algorithm for Minor Component Analysis," Proc. of EUSIPCO 2000, Vol.2, pp.853–856, Sep. 2000.
3. S. Miyagi and H. Sakai, "Performance Comparison between the Filtered-error LMS and the Filtered-X LMS Algorithms," Proc. of ISCAS2001, Sydney, Australia, Vol. II, pp. 661–664, May 2001.
4. H. Sakai and S. Miyagi, "Analysis of the Adaptive Filter Algorithm for Feedback-Type Active Noise Control," Proc. of ICASSP2001, Salt Lake City, Utah, Vol. VI, pp. 3841–3844, May 2001.
5. H.Sakai and S.Hori, "Stabilisation of Fast QRD Inverse-Updates Adaptive Filtering Algorithm," IEE Proc. Vision, Image Signal Processing, Vol.148, No.2, pp.107–114, Apr. 2001 .

関連発表

1. S. Ohno and H. Sakai, "Spectral Analysis of Subband Adaptive Digital Filters," IEEE Trans. Signal Processing, Vol. 48, pp.254–257, Jan. 2000.
2. S. Ohno and H. Sakai, "Studies on the Convergence Speed of Over-Sampled Subband Adaptive Digital Filter," IEICE Trans. Fundamentals of Electronics, Communications and Computer Sciences, Vol.E83-A, pp.1531–1538, Aug. 2000.

A New Method to Analyze Subband Adaptive Filters Based on the Frequency Domain Expressions

Abstract

A new method to analyze subband adaptive filters is proposed. This method is based on the frequency domain expressions of the adaptive algorithms in subband adaptive filters converted by the discrete Fourier transform. By combining this expression with the averaging method or the ordinary differential equation method, the stability condition and the excess mean square error can be evaluated. This method is applied to both the subband adaptive filter with delay recently proposed by Pradhan and Reddy and the delayless one. Simulation results show the validity of the theoretical results derived by our method.

Keywords: subband adaptive filter, delayless subband adaptive filter, ODE, averaging method, frequency domain analysis

1 Introduction

Recently there have been increasing interests in subband adaptive filters (SADFs). The conventional SADF contains a delay and there is the aliasing effect when using a non-ideal filter bank. A delayless subband adaptive filter (DLSADF) was proposed in [1] by using the transformation of the taps of the subband adaptive filters into the fullband ones. A modification using the Hadamard transform was proposed in [2] where it is shown that there is no aliasing effect even using the non-ideal filter bank. Recently a new structure of the SADF which has a delay but is free from the aliasing effect has been developed by Pradhan and Reddy[3]. They have stated that this new scheme improves the convergence rate. This has been shown in some simulations in which each step size of the fullband and subband adaptive filters is adjusted to the best possible value by simulations, that is, it yields the fastest convergence to a desired point. In this paper we adjust each step size so that the excess mean square error (EMSE) becomes the same. To do this, it is necessary to evaluate the EMSE theoretically. However this is a kind of complex task in the time-domain analysis, because some fixed filters, downsamplers and upsamplers are in the system. The theoretical analysis of the EMSE of SADFs has not been fully studied yet. Also, the analysis of the convergence performance in [3] is done for the subband adaptive filters, not for the corresponding fullband characteristics.

To analyze these properties in the SADF, a new approach is proposed. This approach is based on the frequency domain expression of the adaptive algorithms in the SADF combined with the averaging method[4]. Once all the tap vectors and signal vectors expressed in the time domain is converted into those in the frequency domain by using the discrete Fourier transform (DFT), the updating equation of the adaptive filter is expressed in the frequency domain accordingly. After that, the averaging method is applied to the expression. By using the property of the DFT, the coefficient matrix in the updating equation can be approximately diagonalized. Strictly speaking, this analysis method is a kind of approximation, however, can be extract a significant property of the adaptive algorithm such as a stability condition with a clear formula. On the other hand, by applying the ODE method[5] to the frequency domain expression, the covariance matrix of the tap vector of the adaptive filter can be evaluated. From this result, the variance of error signal or the excess mean square error can be explicitly derived.

The method is also applied to analyze delayless subband adaptive filters (DLSADFs). After deriving the general form of the stability condition by the averaging method and the variance of the error signal for the two band DLSADF by the ODE method, as a special case, we apply these formulas to the DLSADF with the Hadamard transform[2]. Some preliminary results about the analysis of this DLSADF by this method have been presented in [6].

2 The Averaging Method and the ODE method

Here we give a brief review of the averaging method in [4] and the ODE method in [5]. Consider the general adaptive algorithm

$$\boldsymbol{\theta}(n+1) = \boldsymbol{\theta}(n) + \mu \boldsymbol{h}(\boldsymbol{\theta}(n), \boldsymbol{x}(n)) \tag{1}$$

where $\boldsymbol{\theta}(n)$ is a parameter vector, $\boldsymbol{x}(n)$ is a stationary random input signal and μ is the adaptive gain. The averaged system corresponding to (1) is

$$\bar{\boldsymbol{\theta}}(n+1) = \bar{\boldsymbol{\theta}}(n) + \mu \tilde{\boldsymbol{h}}(\bar{\boldsymbol{\theta}}(n)) \tag{2}$$

with $\tilde{\boldsymbol{h}}(\boldsymbol{\theta}) = \mathrm{E}\left[\boldsymbol{h}(\boldsymbol{\theta}, \boldsymbol{x}(n))\right]$. Then the following theorem [4, p.234] is proven.

Theorem 1 *Fix an interval* $[0, T]$. *For (1) and the corresponding averaged system (2), under some appropriate regularity conditions, there exists* $c_T(\mu)$ *so that for a given* T

$$\max_{1 \le n \le T/\mu} \|\boldsymbol{\theta}(n) - \bar{\boldsymbol{\theta}}(n)\| \le c_T(\mu) \quad \textit{w.p. 1}$$
$$c_T(\mu) \to 0 \quad \textit{w.p. 1 as } \mu \to 0.$$

This theorem implies that the behavior of the averaged system is close to that of the corresponding original system when the step size μ is sufficiently small. From this fact, the convergence property of (1) can be examined by examining that of the averaged system (2).

On the other hand, the ODE corresponding to (1) is given by

$$\frac{\mathrm{d}\boldsymbol{\theta}(t)}{\mathrm{d}t} = \tilde{\boldsymbol{h}}(\boldsymbol{\theta}(t)).$$

It is assumed that a convergent point of the ODE exists and is denoted by $\boldsymbol{\theta}_*$. Under some regularity conditions, the following theorem holds [5, p.107].

Theorem 2 *If all the eigenvalues of the derivative matrix* $\boldsymbol{H}(\boldsymbol{\theta}_*)$ *defined by*

$$\boldsymbol{H}(\boldsymbol{\theta}_*) = \left.\frac{\partial \tilde{\boldsymbol{h}}(\boldsymbol{\theta})}{\partial \boldsymbol{\theta}^T}\right|_{\boldsymbol{\theta}=\boldsymbol{\theta}_*} \tag{3}$$

have negative real parts and if the matrix

$$\boldsymbol{S}(\boldsymbol{\theta}) = \sum_{n=-\infty}^{\infty} \mathrm{E}\left[\boldsymbol{h}(\boldsymbol{\theta}, \boldsymbol{x}(n))\boldsymbol{h}^\dagger(\boldsymbol{\theta}, \boldsymbol{x}(0))\right] \tag{4}$$

exists, $\mu^{-1/2}[\boldsymbol{\theta}(n) - \boldsymbol{\theta}_*]$ *converges asymptotically (*$n \to \infty$ *and* $\mu \to 0$*) to a zero mean normal distributed random vector weakly with a covariance matrix* $\boldsymbol{Y}$*, which is the solution of the Lyapunov equation*

$$\boldsymbol{H}(\boldsymbol{\theta}_*)\boldsymbol{Y} + \boldsymbol{Y}\boldsymbol{H}^\dagger(\boldsymbol{\theta}_*) = -\boldsymbol{S}(\boldsymbol{\theta}_*) \tag{5}$$

where † *denotes the transpose of the complex conjugate vector or matrix.*

By using above theorem, the covariance matrix of the parameter estimation error vector $\boldsymbol{\theta}(n) - \boldsymbol{\theta}_*$ can be evaluated.

3 Analysis of two band SADF

We briefly summarize the structure of the SADF proposed by Pradhan and Reddy[3] and explain the analysis technique based on the frequency domain expression with using the averaging method and ODE method. For simplicity of the analysis, we consider the two band case.

3.1 Structure of SADF

The block diagram of the two band SADF proposed by Pradhan and Reddy is shown in Fig. 1. $W_{\mathrm{opt}}(z)$ denotes the unknown system. $H_0(z)$ and $H_1(z)$ are the analysis filters in the lowpass band and the highpass band, respectively. $\downarrow 2$ is two-fold decimator. $G_0(z)$

and $G_1(z)$ are the adaptive filters in each subband. The desired signal $d(n)$ is generated by the input signal $x(n)$ filtered by $W_{\rm opt}(z)$ and the additive white noise $v(n)$ which is uncorrelated to $x(n)$. $y_0(k)$, $y_1(k)$ and $d_0(k)$, $d_1(k)$ denote the output signals and the decimated desired signals in each subband, respectively. To adjust the subband adaptive filters $G_0(z)$ and $G_1(z)$, the subband error signals $e_0(k)$, $e_1(k)$ and the decimated subband input signals $x_{00}(k)$, $x_{01}(k)$, $x_{10}(k)$ and $x_{11}(k)$ are used. In [3], the relation between the fullband adaptive filter $W(z)$ and the subband adaptive filters is given by

$$W(z) = G_0(z^2) + z^{-1}G_1(z^2), \tag{6}$$

so that $G_0(z)$ and $G_1(z)$ correspond to the polyphase components. Of course, the adaptive filters are time-varying and their transfer functions are not defined. But here for convenience, we use the above notations $W(z)$, $G_0(z)$ and $G_1(z)$.

The updating equations of the tap vectors of $G_0(z)$ and $G_1(z)$ is given by

$$\boldsymbol{g}_0(k+1) = \boldsymbol{g}_0(k) + \mu\left[\gamma_0 e_0(k)\boldsymbol{x}_{00}(k) + \gamma_1 e_1(k)\boldsymbol{x}_{10}(k)\right] \tag{7}$$

$$\boldsymbol{g}_1(k+1) = \boldsymbol{g}_1(k) + \mu\left[\gamma_0 e_0(k)\boldsymbol{x}_{01}(k) + \gamma_1 e_1(k)\boldsymbol{x}_{11}(k)\right] \tag{8}$$

where γ_0 and γ_1 are the weighting factors which are proportional to the inverse of σ_{x_0}, the variance of $x_0(n)$ and σ_{x_1}, that of $x_1(n)$, respectively. That is

$$\gamma_0 = \frac{\sigma_{x_1}^2}{\sigma_{x_0}^2 + \sigma_{x_1}^2}, \quad \gamma_1 = \frac{\sigma_{x_0}^2}{\sigma_{x_0}^2 + \sigma_{x_1}^2}. \tag{9}$$

The tap vector $\boldsymbol{g}_i(k)$, $i = 0, 1$ and the signal vectors are defined as

$$\begin{aligned} \boldsymbol{g}_i(k) &= \begin{bmatrix} g_{i,0}, & g_{i,1}, & \cdots, & g_{i,N_g-1} \end{bmatrix}^{\rm T} \\ \boldsymbol{x}_{i,j}(k) &= [\, x_{i,j}(k), \ x_{i,j}(k-1), \ \cdots, \ x_{i,j}(k-N_g+1) \,]^{\rm T} \quad (i,j = 0,1). \end{aligned}$$

From (6), the tap length of the fullband adaptive filter becomes $N = 2N_g$. We assume that the tap length of the unknown system $W_{\rm opt}(z)$ equals to N. In [3], the weighting factors γ_0 and γ_1 are determined from the overall samples used in the adaptation. Instead, here, $\sigma_{x_0}^2$ and $\sigma_{x_1}^2$ are estimated by

$$\begin{aligned} \sigma_{x_0}^2(n) &= \lambda\sigma_{x_0}^2(n-1) + (1-\lambda)x_0^2(n) \\ \sigma_{x_1}^2(n) &= \lambda\sigma_{x_1}^2(n-1) + (1-\lambda)x_1^2(n) \end{aligned}$$

where λ is a smoothing factor with $0 < (1-\lambda) \ll 1$ and these are used in (9) for determining γ_0 and γ_1.

For later discussions, other signal vectors and the tap vectors are defined as follows. The input signal vector $\boldsymbol{x}(n)$, the subband signal vector $\boldsymbol{x}_i(n)$, the noise signal vector

$\boldsymbol{v}(n)$, tap vectors $\boldsymbol{w}_{\mathrm{opt}}$, $\boldsymbol{w}(n)$, $\boldsymbol{h}_i$ and $\boldsymbol{z}$ corresponding to $W_{\mathrm{opt}}(z)$, $W(z)$, $H_i(z)$ and the delay operator z^{-1}, respectively are defined as

$$
\begin{aligned}
\boldsymbol{x}(n) &= [\ x(n),\ x(n-1),\ \cdots,\ x(n-N+1)\ ]^{\mathrm{T}} \\
\boldsymbol{x}_i(n) &= [\ x_i(n),\ x_i(n-1),\ \cdots,\ x_i(n-N+1)\ ]^{\mathrm{T}} \\
\boldsymbol{v}(n) &= [\ v(n),\ v(n-1),\ \cdots,\ v(n-N+1)\ ]^{\mathrm{T}} \\
\boldsymbol{w}_{\mathrm{opt}} &= [\ w_{\mathrm{opt},0},\ w_{\mathrm{opt},1},\ \cdots,\ w_{\mathrm{opt},N-1}\ ]^{\mathrm{T}} \\
\boldsymbol{w}(n) &= [\ w_0(n),\ w_1(n),\ \cdots,\ w_{N-1}(n)\ ]^{\mathrm{T}} \\
\boldsymbol{h}_i &= [\ h_{i,0},\ h_{i,1},\ \cdots,\ h_{i,N_h-1},\ \underbrace{0,\ \cdots,\ 0}_{N-N_h}\ ]^{\mathrm{T}} \\
\boldsymbol{z} &= [\ 0,\ 1,\ \underbrace{0,\ \cdots,\ 0}_{N-2}\ ]^{\mathrm{T}}.
\end{aligned}
$$

3.2 Frequency-domain Expressions of Signals and Filters

Capital bold letters $\boldsymbol{X}(n)$, $\boldsymbol{X}_i(n)$, $\boldsymbol{V}(n)$, $\boldsymbol{W}_{\mathrm{opt}}$, $\boldsymbol{W}(n)$, $\boldsymbol{H}_i$ and $\boldsymbol{Z}$ mean the N point discrete Fourier transformation (DFT) vectors of the $\boldsymbol{x}(n)$, $\boldsymbol{x}_i(n)$, $\boldsymbol{v}(n)$, $\boldsymbol{w}_{\mathrm{opt}}$, $\boldsymbol{w}(n)$, $\boldsymbol{h}_i$ and $\boldsymbol{z}$, respectively. By using the N point DFT matrix

$$
\boldsymbol{F} = \left[\exp\left(-\mathrm{i}\frac{2\pi lm}{N}\right)\right] \qquad l, m = 0, 1, \cdots, N-1,
$$

these are written as

$$
\begin{aligned}
&\boldsymbol{X}(n) \equiv [\ X_0(n),\ X_1(n),\ \cdots, X_{N-1}(n)\ ]^{\mathrm{T}} = \boldsymbol{F}\boldsymbol{x}(n) \\
&\boldsymbol{X}_i(n) \equiv [\ X_{i,0}(n),\ X_{i,1}(n),\ \cdots, X_{i,N-1}(n)\ ]^{\mathrm{T}} = \boldsymbol{F}\boldsymbol{x}_i(n) \\
&\boldsymbol{V}(n) \equiv [\ V_0(n),\ V_1(n),\ \cdots, V_{N-1}(n)\ ]^{\mathrm{T}} = \boldsymbol{F}\boldsymbol{v}_i(n) \\
&\boldsymbol{W}_{\mathrm{opt}} \equiv [\ W_{\mathrm{opt},0},\ W_{\mathrm{opt},1},\ \cdots, W_{\mathrm{opt},N-1}\ ]^{\mathrm{T}} = \boldsymbol{F}\boldsymbol{w}_{\mathrm{opt}} \\
&\boldsymbol{W}(n) \equiv [\ W_0(n),\ W_1(n),\ \cdots, W_{N-1}(n)\ ]^{\mathrm{T}} = \boldsymbol{F}\boldsymbol{w}(n) \\
&\boldsymbol{H}_i \equiv [\ H_{i,0},\ H_{i,1},\ \cdots, H_{i,N-1}\ ]^{\mathrm{T}} = \boldsymbol{F}\boldsymbol{h}_i \\
&\boldsymbol{Z} \equiv [\ Z_0,\ Z_1,\ \cdots, Z_{N-1}\ ]^{\mathrm{T}} = \boldsymbol{F}\boldsymbol{z}
\end{aligned}
$$

where $Z_m = \exp\{-\mathrm{i}2\pi m/N\}$. The error signal $e(n)$ is expressed as

$$
e(n) = -\boldsymbol{x}^{\dagger}(n)\Delta\boldsymbol{w} + v(n) \tag{10}
$$

where $\Delta\boldsymbol{w} = \boldsymbol{w}(n) - \boldsymbol{w}_{\mathrm{opt}}$ and $\dagger$ denotes the complex conjugate transpose of a vector or a matrix. By using the DFT matrix $\boldsymbol{F}$ with $\boldsymbol{F}^{\dagger}\boldsymbol{F} = N\boldsymbol{I}_N$ where $\boldsymbol{I}_N$ denotes an $N \times N$ identity matrix, (10) can be expressed as

$$
e(n) = -\frac{1}{N}\boldsymbol{X}^{\dagger}(n)\Delta\boldsymbol{W}(n) + v(n) \tag{11}
$$

where $\Delta \boldsymbol{W}(n) = \boldsymbol{F}\Delta \boldsymbol{w}(n) = \boldsymbol{W}(n) - \boldsymbol{W}_{\mathrm{opt}}$. From (11), the variance of the error signal is calculated as

$$\mathrm{E}[|e(n)|^2] = \frac{1}{N^2}\mathrm{E}[\boldsymbol{X}^{\dagger}(n)\Delta \boldsymbol{W}(n)\Delta \boldsymbol{W}^{\dagger}(n)\boldsymbol{X}(n)] + \sigma_v^2 \tag{12}$$

where σ_v^2 is the variance of additive white noise $v(n)$.

3.3 Frequency-domain Expression of the Adaptive Filter

In the time domain, (6) can be rewritten as the following equation,

$$\boldsymbol{w}(n) = \boldsymbol{U}\boldsymbol{g}_0(k) + \boldsymbol{z} \otimes (\boldsymbol{U}\boldsymbol{g}_1(k)), \quad k = n/2 \tag{13}$$

where $\otimes$ denotes the convolution and $\boldsymbol{U}$ is an $N \times N_g$ up-sampling matrix defined by

$$\boldsymbol{U} = \begin{bmatrix} 1 & 0 & 0 & \cdots & & & & 0 \\ 0 & 0 & 0 & \cdots & & & & 0 \\ 0 & 1 & 0 & 0 & \cdots & & & 0 \\ 0 & 0 & 0 & 0 & \cdots & & & 0 \\ 0 & 0 & 1 & 0 & \cdots & & & 0 \\ \vdots & & & & & & & \vdots \\ 0 & \cdots & & & & 0 & 1 & 0 \\ 0 & \cdots & & & & 0 & 0 & 0 \\ 0 & \cdots & & & & 0 & 0 & 1 \\ 0 & \cdots & & & & 0 & 0 & 0 \end{bmatrix}$$

as in [7]. We should note that the relation between the time index in the fullband and that in the subband $k = n/2$ holds due to the two fold decimators.

Applying the DFT matrix to (13), we get

$$\boldsymbol{W}(n) = \boldsymbol{F}(\boldsymbol{U}g_0(k)) + \boldsymbol{\Lambda}_Z \boldsymbol{F}(\boldsymbol{U}\boldsymbol{g}_1(k)) \tag{14}$$

where $\boldsymbol{\Lambda}_Z = \mathrm{diag}[\, Z_0,\ Z_1,\ \cdots,\ Z_{N-1}\,]$. In (14), the end effect due to finite length sequences is assumed to be small and is neglected.

By substituting (7) and (8) into (14), the updating equation for $\Delta \boldsymbol{W}(n) = \boldsymbol{W}(n) - \boldsymbol{W}_{\mathrm{opt}}$ is given by

$$\Delta \boldsymbol{W}(n) = \Delta \boldsymbol{W}(n-2) + \mu \sum_{i=0}^{1} \gamma_i \left[\boldsymbol{F}\boldsymbol{U}\boldsymbol{x}_{i,0}(k-1) + \boldsymbol{\Lambda}_Z \boldsymbol{F}\boldsymbol{U}\boldsymbol{x}_{i,1}(k-1)\right] e_i(k-1). \tag{15}$$

The error signal in each subband $e_i(k)$ is expressed as

$$e_i(k) \;=\; d_i(k) - y_i(k)$$

$$
\begin{aligned}
&= \sum_{l=0}^{N_h-1} h_{i,l} \left(\sum_{j=0}^{N-1} x(n-l-j) w_{\mathrm{opt},j} + v(n-l) \right) - \sum_{j=0}^{N-1} w_j(n) \sum_{l=0}^{N_h-1} x(n-l-j) h_{i,l} \\
&= -\boldsymbol{b}^\dagger(n)\boldsymbol{h}_i = -\frac{1}{N}\boldsymbol{B}^\dagger(n)\boldsymbol{H}_i \qquad (16)
\end{aligned}
$$

where

$$
\boldsymbol{b}(n) = \begin{bmatrix} \Delta\boldsymbol{w}^{\mathrm{T}}(n)\boldsymbol{x}(n) \\ \Delta\boldsymbol{w}^{\mathrm{T}}(n)\boldsymbol{x}(n-1) \\ \vdots \\ \Delta\boldsymbol{w}^{\mathrm{T}}(n)\boldsymbol{x}(n-N+1) \end{bmatrix} - \boldsymbol{v}(n) \qquad (17)
$$

and $\boldsymbol{B}(n) = \boldsymbol{F}\boldsymbol{b}(n)$. By using the property of the DFT matrix again, each subband signal vector is expressed as

$$
\begin{aligned}
\boldsymbol{x}_{i,0}(k) &= \boldsymbol{D}\boldsymbol{x}_i(n) = \frac{1}{N}\boldsymbol{D}\boldsymbol{F}^\dagger\boldsymbol{X}_i(n) \qquad (18) \\
\boldsymbol{x}_{i,1}(k) &= \boldsymbol{D}(\boldsymbol{z}\otimes\boldsymbol{x}_i(n)) = \frac{1}{N}\boldsymbol{D}\boldsymbol{F}^\dagger\Lambda_Z^\dagger\boldsymbol{X}_i(n) \qquad (19)
\end{aligned}
$$

where $\boldsymbol{D}$ is an $N_g \times N$ down-sampling matrix defined by $\boldsymbol{D} = \boldsymbol{U}^T$. Substituting (16), (18) and (19) into (15), we get the updating equation as

$$
\Delta\boldsymbol{W}(n) = \Delta\boldsymbol{W}(n-2) - \frac{\mu}{N^2}\sum_{i=0}^{1}\gamma_i\left[\boldsymbol{F}\boldsymbol{U}\boldsymbol{D}\boldsymbol{F}^\dagger + \Lambda_Z\boldsymbol{F}\boldsymbol{U}\boldsymbol{D}\boldsymbol{F}^\dagger\Lambda_Z^\dagger\right]\boldsymbol{X}_i(n-2)\boldsymbol{B}^\dagger(n-2)\boldsymbol{H}_i. \qquad (20)
$$

Since

$$
\boldsymbol{F}\boldsymbol{U}\boldsymbol{D}\boldsymbol{F}^\dagger = \frac{N}{2}\begin{pmatrix} \boldsymbol{I}_{N/2} & \boldsymbol{I}_{N/2} \\ \boldsymbol{I}_{N/2} & \boldsymbol{I}_{N/2} \end{pmatrix}, \qquad (21)
$$

we have

$$
\Lambda_Z\boldsymbol{F}\boldsymbol{U}\boldsymbol{D}\boldsymbol{F}^\dagger\Lambda_Z^\dagger = \frac{N}{2}\begin{pmatrix} \boldsymbol{I}_{N/2} & -\boldsymbol{I}_{N/2} \\ -\boldsymbol{I}_{N/2} & \boldsymbol{I}_{N/2} \end{pmatrix}.
$$

From this fact, $\boldsymbol{F}\boldsymbol{U}\boldsymbol{D}\boldsymbol{F}^\dagger + \Lambda_Z\boldsymbol{F}\boldsymbol{U}\boldsymbol{D}\boldsymbol{F}^\dagger\Lambda_Z^\dagger = N\boldsymbol{I}_N$ so that (20) reduces to

$$
\Delta\boldsymbol{W}(n) = \Delta\boldsymbol{W}(n-2) - \frac{\mu}{N}\sum_{i=0}^{1}\gamma_i\boldsymbol{X}_i(n-2)\boldsymbol{B}^\dagger(n-2)\boldsymbol{H}_i. \qquad (22)
$$

3.4 Stability Analysis by the Averaging Method

The averaged system corresponding to (22) is given by

$$
\Delta\bar{\boldsymbol{W}}(n) = \left(\boldsymbol{I}_N - \frac{\mu}{N}\sum_{i=0}^{1}\gamma_i\Lambda_{H_i}^\dagger\boldsymbol{Q}\Lambda_{H_i}\right)\Delta\bar{\boldsymbol{W}}(n-2) \qquad (23)
$$

where $\mathbf{\Lambda}_{H_i} = \mathrm{diag}[\ H_{i,0},\ H_{i,1},\ \cdots,\ H_{i,N-1}\ ]$ and $\boldsymbol{Q}$ is defined as

$$\begin{aligned}\boldsymbol{Q} &= \mathrm{diag}[\ Q_0,\ Q_1,\ \cdots,\ Q_{N-1}\ ] \\ & Q_m = NS_x(\omega_m), \quad \omega_m = \frac{2\pi m}{N},\end{aligned}$$

where $S_x(\omega)$ denotes the spectral density of the input signal $x(n)$. See Appendix A for the detailed derivation of (23). The matrix $\sum_{i=0}^{1} \gamma_i \mathbf{\Lambda}_{H_i}^{\dagger} \boldsymbol{Q} \mathbf{\Lambda}_{H_i}$ is diagonal and all its elements are positive. Therefore, this system is always stable for the positive small μ. This result can be easily generalized to the M-band case where the relevant matrix in (23) is replaced by $\sum_{i=0}^{M-1} \gamma_i \mathbf{\Lambda}_{H_i}^{\dagger} \boldsymbol{Q} \mathbf{\Lambda}_{H_i}$. If $M \gg 1$, the bandwidth is small so that the quantity $|H_{i,m}|^2 Q_m$ is approximately proportional to $\sigma_{x_i}^2$, the variance of the subband signal $x_i(n)$. Since γ_i is proportional to the inverse of $\sigma_{x_i}^2$, all the elements of the above matrix are same. This coincides with the result in [3]

3.5 Second Order Analysis

The ODE corresponding to (22) is given by

$$\frac{\mathrm{d}\Delta \boldsymbol{W}(t)}{\mathrm{d}t} = -\frac{1}{N} \sum_{i=0}^{1} \gamma_i \mathbf{\Lambda}_{H_i}^{\dagger} \boldsymbol{Q} \mathbf{\Lambda}_{H_i} \Delta \boldsymbol{W}(t)$$

with an equilibrium point $\Delta \boldsymbol{W}_* = \boldsymbol{0}$. The matrices $\boldsymbol{H}(\Delta \boldsymbol{W})$ and $\boldsymbol{S}(\Delta \boldsymbol{W}_*)$ are calculated as

$$\begin{aligned}\boldsymbol{H}(\Delta \boldsymbol{W}) &= -\frac{1}{N} \sum_{i=0}^{1} \gamma_i \mathbf{\Lambda}_{H_i}^{\dagger} \boldsymbol{Q} \mathbf{\Lambda}_{H_i} \\ \boldsymbol{S}(\Delta \boldsymbol{W}_*) &= \frac{2\sigma_v^2}{3} \sum_{i=0}^{1} \sum_{j=0}^{1} \gamma_i \gamma_j \mathbf{\Lambda}_{H_i}^{\dagger} \mathbf{\Lambda}_{H_j} \boldsymbol{Q} \mathbf{\Lambda}_{H_j}^{\dagger} \mathbf{\Lambda}_{H_i}.\end{aligned} \tag{24}$$

See Appendix B for the detailed derivation of $\boldsymbol{S}(\Delta \boldsymbol{W}_*)$. Since both matrices are diagonal matrices, the Lyapunov equation can be easily solved. As a result, we obtain

$$\begin{aligned}\boldsymbol{Y} &= \mathrm{diag}[\ Y_0,\ Y_1,\ \cdots,\ Y_{N-1}\ ] \\ Y_m &= \frac{\sigma_v^2 N}{3} \left[\gamma_0 |H_{0,m}|^2 + \gamma_1 |H_{1,m}|^2\right].\end{aligned}$$

Once the solution $\boldsymbol{Y}$ is obtained, the covariance matrix can be evaluated as

$$\mathrm{E}\left[\Delta \boldsymbol{W}(n) \Delta \boldsymbol{W}^{\dagger}(n)\right] = \mu \boldsymbol{Y}. \tag{25}$$

Since $\Delta \boldsymbol{W}(n)$ is slowly varying in contrast to $\boldsymbol{X}(n)$, we use the so-called the averaging principle[8]. By applying this to (12), the variance of the error signal can be obtained as

$$\mathrm{E}[|e(n)|^2] \simeq \frac{1}{N^2} \mathrm{Tr}\left[\mathrm{E}\left[\boldsymbol{X}(n) \boldsymbol{X}^{\dagger}(n)\right] \mathrm{E}\left[\Delta \boldsymbol{W}(n) \Delta \boldsymbol{W}^{\dagger}(n)\right]\right] + \sigma_v^2. \tag{26}$$

Since $\mathrm{E}\left[\boldsymbol{X}(n)\boldsymbol{X}^{\dagger}(n)\right] \simeq \boldsymbol{Q}$, by substituting (25) into (26), the variance of the error signal is finally evaluated as

$$\begin{aligned}\mathrm{E}[|e(n)|^2] &\simeq \sigma_v^2(1+\mu N\xi) \\ \xi &= \frac{1}{3N^2}\sum_{m=0}^{N-1} Q_m\left[\gamma_0|H_{0,m}|^2+\gamma_1|H_{1,m}|^2\right].\end{aligned}$$

By using the continuous frequency, this can be approximated as

$$\begin{aligned}\xi &\simeq \frac{1}{3}\cdot\frac{1}{2\pi}\int_{-\pi}^{\pi} S_x(\omega)\left(\gamma_0|H_0(\mathrm{e}^{\mathrm{i}\omega})|^2+\gamma_1|H_1(\mathrm{e}^{\mathrm{i}\omega})|^2\right)\mathrm{d}\omega \\ &= \frac{1}{3}\left(\gamma_0\sigma_{x0}^2+\gamma_1\sigma_{x1}^2\right)\end{aligned}$$

Substituting (9) into the above equation, ξ is roughly approximated as

$$\xi \simeq \frac{1}{3}\cdot\frac{2\sigma_{x0}^2\sigma_{x1}^2}{\sigma_{x0}^2+\sigma_{x1}^2}. \tag{27}$$

If $|H_0(\mathrm{e}^{\mathrm{i}\omega})|^2+|H_1(\mathrm{e}^{\mathrm{i}\omega})|^2=1$ is satisfied, then $\sigma_{x0}^2+\sigma_{x1}^2=\sigma_x^2$ where σ_x^2 is the variance of $x(n)$. Since the harmonic mean is less than or equal to the arithmetic mean, we have $\xi \leq \sigma_x^2/6$. Note that the corresponding ξ of the fullband adaptive filter is $\sigma_x^2/2$ [4]. Thus the excess mean square error of this SADF is at least reduced to 1/3 of that of the fullband one. For the M-band case the corresponding formula will be

$$\xi = \frac{1}{3}\left(\frac{1}{M}\sum_{j=0}^{M-1}\frac{1}{\sigma_{xj}^2}\right)^{-1}.$$

4 Analysis of DLSADFs

By using the technique in the previous section, we consider the stability condition and the excess mean square error of DLSADFs. First, we apply the method to a general DLSADF. After that we treat the DLSADF with the Hadamard transform in [2] as a special case. The preliminary results of this section were presented in [6].

4.1 Frequency-domain Expression of a DLSADF

In a two band DLSADF shown in Fig. 2, the subband adaptive filters $G_0(z)$ and $G_1(z)$ are converted into the fullband filter $W(z)$ with the following rule

$$W(z) = C_0(z)G_0(z^2) + C_1(z)G_1(z^2) \tag{28}$$

as in [9]. In the time domain, (28) can be rewritten as the following equation,

$$\boldsymbol{w}(n) = \boldsymbol{c}_0 \otimes (\boldsymbol{U}\boldsymbol{g}_0(k)) + \boldsymbol{c}_1 \otimes (\boldsymbol{U}\boldsymbol{g}_1(k)), \quad k = n/2 \tag{29}$$

Applying the DFT matrix $\boldsymbol{F}$ to (29), then the frequency-domain description of (29) is given by

$$\boldsymbol{W}(n) = \Lambda_{C_0}\boldsymbol{F}(\boldsymbol{U}\boldsymbol{g}_0(k)) + \Lambda_{C_1}\boldsymbol{F}(\boldsymbol{U}\boldsymbol{g}_1(k)) \tag{30}$$

with $\Lambda_{C_i} = \mathrm{diag}[\ C_{i,0},\ C_{i,1},\ \cdots,\ C_{i,N-1}\ ]\ \ (i = 0, 1)$ where each diagonal element of Λ_{C_i} corresponds to each element of $\boldsymbol{C}_i = \boldsymbol{F}\boldsymbol{c}_i$ and $\boldsymbol{c}_i$ is the tap vector of $C_i(z)$. Two tap vectors of the subband adaptive filters are updated by the following LMS algorithm,

$$\boldsymbol{g}_i(k+1) = \boldsymbol{g}_i(k) + \mu\boldsymbol{x}'_i(k)e'_i(k), \quad i = 0, 1. \tag{31}$$

We have the following relations for the decimated input signal $x'_i(k)$ and the decimated error signal $e'_i(k)$ in each subband:

$$\begin{aligned} \boldsymbol{x}'_i(k) &= \boldsymbol{D}\boldsymbol{x}_i(n) = \boldsymbol{D}\boldsymbol{F}^{\dagger}\boldsymbol{X}_i(n)/N && (32)\\ e'_i(k) &= e_i(n) = (\boldsymbol{d}(n) - \boldsymbol{y}(n))^{\dagger}\boldsymbol{h}_i = \boldsymbol{B}'^{\dagger}(n)\boldsymbol{H}_i/N && (33) \end{aligned}$$

where $\boldsymbol{B}'(n) = \boldsymbol{F}(\boldsymbol{d}(n) - \boldsymbol{y}(n))$. Both $\boldsymbol{d}(n)$ and $\boldsymbol{y}(n)$ are defined as $\boldsymbol{d}(n) = [\ d(n),\ d(n-1),\ \cdots,\ d(n-N+1)\ ]$ and $\boldsymbol{y}(n) = [\ y(n),\ y(n-1),\ \cdots,\ y(n-N+1)\ ]$. Substituting (31), (32) and (33) into (30), the following recursive equations for $\Delta\boldsymbol{W}(n)$ is obtained,

$$\begin{aligned} \Delta\boldsymbol{W}(n) &= \Delta\boldsymbol{W}(n-2) + \mu\boldsymbol{K}'(\boldsymbol{X}(n-2), \Delta\boldsymbol{W}(n-2)) && (34)\\ \boldsymbol{K}'(\boldsymbol{X}(n), \Delta\boldsymbol{W}(n)) &\equiv \frac{1}{N^2}\sum_{i=0}^{1}\Lambda_{C_i}\boldsymbol{F}\boldsymbol{U}\boldsymbol{D}\boldsymbol{F}^{\dagger}\boldsymbol{X}_i(n)\boldsymbol{B}'^{\dagger}(n)\boldsymbol{H}_i. && (35) \end{aligned}$$

4.2 Stability Condition of DLSADFs

By using the similar approximation method in Appendix A, the averaged system corresponding to (34) is given by

$$\Delta\bar{\boldsymbol{W}}(n) = \Delta\bar{\boldsymbol{W}}(n-2) - \frac{\mu}{N^2}\sum_{i=0}^{1}\Lambda_{C_i}\boldsymbol{F}\boldsymbol{U}\boldsymbol{D}\boldsymbol{F}^{\dagger}\Lambda_{H_i}^{\dagger}\Lambda_{H_i}\boldsymbol{Q}\Delta\bar{\boldsymbol{W}}(n-2) \tag{36}$$

where the derivation is omitted. Due to (21), (36) is reduced to

$$\Delta\bar{\boldsymbol{W}}(n) = \left(\boldsymbol{I}_N - \frac{\mu}{2N}\boldsymbol{A}\boldsymbol{Q}\right)\Delta\bar{\boldsymbol{W}}(n-2) \tag{37}$$

where $\boldsymbol{A}$ is defined as

$$\boldsymbol{A} = \frac{2}{N}\sum_{i=0}^{1}\Lambda_{C_i}\boldsymbol{F}\boldsymbol{U}\boldsymbol{D}\boldsymbol{F}^{\dagger}\Lambda_{H_i}^{\dagger}\Lambda_{H_i} = \begin{bmatrix} \boldsymbol{A}_{11} & \boldsymbol{A}_{12}\\ \boldsymbol{A}_{21} & \boldsymbol{A}_{22} \end{bmatrix} \tag{38}$$

with

$$\boldsymbol{A}_{11} = \sum_i \mathrm{diag}\left[C_{i,0}|H_{i,0}|^2,\ C_{i,1}|H_{i,1}|^2,\ \cdots,\ C_{i,N/2-1}|H_{i,N/2-1}|^2\right]$$

$$
\begin{aligned}
\boldsymbol{A}_{12} &= \sum_i \mathrm{diag}\left[C_{i,0}|H_{i,N/2}|^2,\ C_{i,1}|H_{i,N/2+1}|^2,\ \cdots,\ C_{i,N/2-1}|H_{i,N-1}|^2\right] \\
\boldsymbol{A}_{21} &= \sum_i \mathrm{diag}\left[C_{i,N/2}|H_{i,0}|^2,\ C_{i,N/2+1}|H_{i,1}|^2,\ \cdots,\ C_{i,N-1}|H_{i,N/2-1}|^2\right] \\
\boldsymbol{A}_{22} &= \sum_i \mathrm{diag}\left[C_{i,N/2}|H_{i,N/2}|^2,\ C_{i,N/2+1}|H_{i,N/2+1}|^2,\ \cdots,\ C_{i,N-1}|H_{i,N-1}|^2\right].
\end{aligned}
$$

Since $\boldsymbol{A}$ is no longer diagonal, the situation becomes complex compared with that of the previous section.

For (37) to be stable, the real parts of all the eigenvalues of the matrix $\boldsymbol{AQ}$ must be positive for a small positive μ. Let us examine whether all the roots of the characteristic equation of the matrix $\boldsymbol{AQ}$ are on the right-half plane in the complex plane or not. We define the following vectors whose elements are all zero except the m-th and $(m+N/2)$-th elements,

$$
\begin{aligned}
\boldsymbol{p}_m &= [\,0,\ \cdots,\ 0,\ t_m,\ 0,\ \cdots,\ t_{m+N/2},\ 0,\ \cdots,\ 0\,]^{\mathrm{T}} \\
\boldsymbol{p}_{m+N/2} &= [\,0,\ \cdots,\ 0,\ \bar{t}_m,\ 0,\ \cdots,\ \bar{t}_{m+N/2},\ 0,\ \cdots,\ 0\,]^{\mathrm{T}} \\
& \quad m = 0,\ 1,\ \cdots,\ N/2-1.
\end{aligned}
$$

The characteristic equation of the matrix $\boldsymbol{AQ}$ is obtained from $\boldsymbol{AQp}_m = \lambda \boldsymbol{p}_m$ and $\boldsymbol{AQp}_{m+N/2} = \lambda \boldsymbol{p}_{m+N/2}$ as

$$
\begin{aligned}
f_m(\lambda) = {} & \left(\lambda - Q_m \sum_i C_{i,m}|H_{i,m}|^2\right)\left(\lambda - Q_{m+N/2}\sum_i C_{i,m+N/2}|H_{i,m+N/2}|^2\right) \\
& - Q_m Q_{m+N/2} \sum_i C_{i,m}|H_{i,N/2+m}|^2 \sum_j C_{j,N/2+m}|H_{j,m}|^2 = 0.
\end{aligned} \tag{39}
$$

These $\boldsymbol{p}_m$ are eigenvectors corresponding to eigenvalues λ_m ($m = 0,\ 1,\ \cdots,\ N-1$). Generally speaking, $|H_{0,m+N/2}|^2 = |H_{1,m}|^2$ and $|H_{1,m+N/2}|^2 = |H_{0,m}|^2$ hold in the filter bank such as the quadrature mirror filter (QMF) bank or the conjugate quadrature filter (CQF) bank. If we assume that $C_i(z)$ is the QMF bank, from $C_0(z) = C_1(-z)$, $C_{0,m+N/2} = C_{1,m}$ and $C_{1,m+N/2} = C_{0,m}$ hold. From this assumption, (39) is rewritten as

$$
\begin{aligned}
f_m(\lambda) &= \lambda^2 - (Q_m + Q_{m+N/2})\zeta_m \lambda + Q_m Q_{m+N/2}(\zeta_m^2 - \eta_m^2) \qquad (40) \\
\zeta_m &= C_{0,m}|H_{0,m}|^2 + C_{1,m}|H_{1,m}|^2 \\
\eta_m &= C_{0,m}|H_{1,m}|^2 + C_{1,m}|H_{0,m}|^2.
\end{aligned}
$$

From [10, p.250], the stability condition of a general second order polynomial with complex coefficients $f(z)$ is given by $\nabla_2 = -a_1 < 0$ and $\nabla_4 = a_1^2 b_2 - a_2^2 - a_1 a_2 b_1 > 0$ where $f(\mathrm{i}z) = -z^2 + b_1 z + b_2 + \mathrm{i}(a_1 z + a_2)$. In the present case, for (40) by setting $\zeta_m = \alpha_m + \mathrm{i}\beta_m$ and $\zeta_m^2 - \eta_m^2 = \kappa_m + \mathrm{i}\epsilon_m$, we have $a_1 = -(Q_m + Q_{m+N/2})\alpha_m$, $a_2 = Q_m Q_{m+N/2}\epsilon_m$,

$b_1 = (Q_m + Q_{m+N/2})\beta_m$ and $b_2 = Q_m Q_{m+N/2}\kappa_m$. Hence the stability conditions become

$$\begin{aligned} &-(Q_m + Q_{m+N/2})\alpha_m < 0 \\ &Q_m Q_{m+N/2}\left[(Q_m + Q_{m+N/2})^2\alpha_m(\alpha_m\kappa_m + \beta_m\epsilon_m) - Q_m Q_{m+N/2}\epsilon_m^2\right] > 0. \end{aligned} \tag{41}$$

Q_m is real and positive so that $Q_m + Q_{m+N/2} > 0$, $(Q_m + Q_{m+N/2})^2/(Q_m Q_{m+N/2}) \geq 4$. Hence (41) is satisfied if

$$\alpha_m > 0, \quad 4\alpha_m(\alpha_m\kappa_m + \beta_m\epsilon_m) > \epsilon_m^2 \quad (m = 0, 1, \cdots, N/2-1) \tag{42}$$

If the above inequalities are satisfied, all the eigenvalues λ_m $(m = 0, 1, \cdots, N-1)$ are in the right-half plane so that $\Delta\boldsymbol{W}(n)$ asymptotically converges to $\mathbf{0}$. Since $\Delta\boldsymbol{w}(n) = (1/N)\boldsymbol{F}^{\dagger}\Delta\boldsymbol{W}(n)$, $\Delta\boldsymbol{w}(n)$ also converges to $\mathbf{0}$.

Next let us consider the stability of the DLSADF using the Hadamard transform as a special case. In this configuration, we set $\boldsymbol{c}_0 = 1/2[1,\ 1,\ 0,\ \cdots,\ 0]^{\mathrm{T}}$ and $\boldsymbol{c}_1 = 1/2[1,\ -1,\ 0,\ \cdots,\ 0]^{\mathrm{T}}$ so that we obtain each element of $\boldsymbol{C}_0$ and $\boldsymbol{C}_1$ as

$$C_{0,m} = \frac{1}{2}\left(1 + \mathrm{e}^{-\mathrm{i}\frac{2\pi m}{N}}\right), \quad C_{1,m} = \frac{1}{2}\left(1 - \mathrm{e}^{-\mathrm{i}\frac{2\pi m}{N}}\right).$$

In this case, (42) becomes

$$\begin{aligned} &\tfrac{1}{2}(1+\phi_m) > 0 \\ &\phi_m\left[(1+\phi_m)^2 + \psi_m^2\right] > 0 \end{aligned} \qquad (m = 0, 1, \cdots, N/2-1) \tag{43}$$

where $\phi_m = \cos(2\pi m/N)\left(|H_{0,m}|^2 - |H_{1,m}|^2\right)$, $\psi_m = \sin(2\pi m/N)\left(|H_{0,m}|^2 - |H_{1,m}|^2\right)$ and the power complementary property $|H_{0,m}|^2 + |H_{1,m}|^2 = 1$ are used. Since in the lowpass band $|H_{0,m}|^2 > |H_{1,m}|^2$ and in the highpass band $|H_{0,m}|^2 < |H_{1,m}|^2$, ϕ_m is always positive except at the point whose corresponding frequency is $\pi/2$. This point can be avoided if we assume that $N = 4q+2$ where q is a positive integer. Thus the stability condition (43) is satisfied. If this is not the case, we append an appropriate number of zeros to the SADF taps $\boldsymbol{g}_i(k)$. But the modes close to $\pi/2$ cause the slow convergence if the magnitude of the frequency response of the unknown system is not small around this frequency $\pi/2$. This explains the slow convergence seen in the example in Fig.3 of [2].

4.3 Second Order Analysis of DLSADFs

The equilibrium point of the ODE corresponding to (37) is $\Delta\boldsymbol{W}_* = \mathbf{0}$, and if the two conditions in (42) are satisfied, the derivative matrix $\boldsymbol{H}(\Delta\boldsymbol{W}) = -\boldsymbol{A}\boldsymbol{Q}/(2N)$ is a stable matrix. The matrix $\boldsymbol{S}$ at the equilibrium point $\Delta\boldsymbol{W}_*$ is obtained as

$$\boldsymbol{S}(\Delta\boldsymbol{W}_*) = \sigma_v^2\boldsymbol{A}\boldsymbol{Q}\boldsymbol{A}^{\dagger}/6.$$

The derivation is similar to that of (24) in Appendix B and is omitted. By substituting $\boldsymbol{H}(\Delta \boldsymbol{W}_*)$ and $\boldsymbol{S}(\Delta \boldsymbol{W}_*)$ into the Lyapunov equation (5), noting that $\boldsymbol{H}(\Delta \boldsymbol{W}_*)$ and $\boldsymbol{S}(\Delta \boldsymbol{W}_*)$ have the same structure with that of $\boldsymbol{A}$ in (38), the solution is given by the following form,

$$\boldsymbol{Y} = \frac{\sigma_v^2 N}{3}\begin{bmatrix} \boldsymbol{Y}_a & \boldsymbol{Y}_b \\ \boldsymbol{Y}_c & \boldsymbol{Y}_d \end{bmatrix}$$

where

$$\begin{aligned}
\boldsymbol{Y}_a &= \mathrm{diag}[\, Y_{a,0},\ Y_{a,1},\ \cdots,\ Y_{a,N/2-1}\,] \\
\boldsymbol{Y}_b &= \boldsymbol{Y}_c^\dagger = \mathrm{diag}[\, Y_{b,0},\ Y_{b,1},\ \cdots,\ Y_{b,N/2-1}\,] \\
\boldsymbol{Y}_d &= \mathrm{diag}[\, Y_{d,0},\ Y_{d,1},\ \cdots,\ Y_{d,N/2-1}\,].
\end{aligned}$$

From this result, the variance of the error signal is formally evaluated as

$$\begin{aligned}
\mathrm{E}[|e(n)|^2] &\simeq \sigma_v^2(1+\mu N\xi') \\
\xi' &= \frac{\mu}{3N^2}\left(\sum_{m=0}^{N/2-1} Q_m Y_{a,m} + \sum_{m=0}^{N/2-1} Q_{m+N/2} Y_{d,m}\right).
\end{aligned} \tag{44}$$

If $C_0(z)$, $H_0(z)$ and $C_1(z)$, $H_1(z)$ are close to the ideal lowpass filter and highpass filter, respectively, $\boldsymbol{A}$ is approximated to a diagonal matrix so that ξ is easily calculated as

$$\xi' \simeq \frac{1}{6N^2}\sum_{m=0}^{N-1}\frac{Q_m|\sum_{i=0}^{1} C_{i,m}|H_{i,m}|^2|^2}{\sum_{i=0}^{1}\mathrm{Re}[C_{i,m}]|H_{i,m}|^2}.$$

This is roughly approximated as

$$\xi' \simeq \frac{1}{6}\cdot\frac{1}{2\pi}\int_{-\pi}^{\pi} S_x(\omega)\mathrm{d}\omega \simeq \frac{\sigma_x^2}{6}. \tag{45}$$

5 Simulation Results

5.1 Verifying the Stability

By some simulations, we verify whether theoretical stability condition in the DLSADF is correct or not. We use a 128 tap FIR filter as an unknown system. The step size μ, the variance of the additive Gaussian white noise σ_v^2 and the analysis filter bank are fixed to 0.001, 1.0×10^{-4} and 32 tap QMF bank, respectively. The input signal is assumed to be Gaussian white noise with zero mean and unit variance. Under this configuration, we check the stability condition (42) and perform simulations. These results are listed in Table.1. The first column denotes a code name of the filter $C_i(z)$ $(i = 0, 1)$ in [12]. All the cases except "Hadamard" do not satisfy the two conditions in (43). These results coincide with the empirical results.

5.2 Evaluating Excess Mean Square Errors

We evaluate the excess mean square errors of the two band Pradhan's SADF and of the two band DLSADF with the Hadamard transform. The same FIR filter in the previous simulations is used as the unknown system. Both the step size μ and the variance of additive white noise σ_v^2 are fixed to 1.0×10^{-4}. Two input signals are considered. One is the Gaussian white noise with zero mean and unit variance. The other is the first order lowpass AR process with innovation variance 1.0 and AR coefficient 0.9 so that $\sigma_x^2 = 5.2632$. $(1 - \lambda)$ is fixed to 0.01.

Table 2 shows the simulation results under the above configuration. All the empirical results are obtained by taking the averages over independent 10 runs. All these results coincide well to the theoretical ones where we note that since $C_i(z)$'s of the DLSADF using the Hadamard transform are far from ideal, we use (44) to evaluate ξ' numerically. But the rough estimate in (45) still gives good results. For the white input signal, ξ of the Pradhan's SADF is close to that of the DLSADF with the Hadamard transform. On the other hand, for the colored input signal, we can see that ξ of the Pradhan's SADF is considerably reduced. In this case, μ of the Pradhan's SADF can be theoretically increased up to about 20 times larger than that of the fullband ADF with the same EMSE.

Fig. 3 shows the mean square error (MSE) curves of the Pradhan's SADF and the fullband ADF. In this simulation, the above first order AR process is used as the input signal. Other parameters except the step size μ are just the same with the above simulations. μ of the Pradhan's SADF is fixed to 2.0×10^{-2}. Then ξ is evaluated as 0.13361 so that $\mu\xi$ becomes 2.6722×10^{-3}. When μ of the fullband ADF is set to 7.2×10^{-4}, then ξ becomes 3.6985. As a result, $\mu\xi$ is 2.6629×10^{-3} which almost equals to that of Pradhan's SADF. The ratio of both μs is 27.8 which almost coincides with the theoretical one, 23.1. The Pradhan's SADF and the fullband ADF converge to the desired point at 5000 and 7000, respectively. From this fact, we conclude that the convergence rate is improved by the Pradhan's SADF.

6 Conclusion

We have proposed a new method to analyze SADFs based on the frequency domain expression with combined the averaging method and the ODE method. As an analysis example, our method has been applied to the Pradhan's SADF. From this analysis, we have theoretically shown that the Pradhan's SADF is always stable and its EMSE is reduced compared with the usual fullband adaptive filter. As another example our method has been also applied to the DLSADF with the Hadamard transform. We have found a mode that is related to slow convergence rate in some cases. The corresponding EMSE is larger than that of the Pradhan's SADF at the expense of the delaylessness.

Appendix

A Derivation of (23)

To derive (23), we evaluate the average of $\boldsymbol{X}_i(n)\boldsymbol{B}^\dagger(n)$ for fixed $\Delta\bar{\boldsymbol{W}}$ in (22).

From (17), the m-th element of $\boldsymbol{B}(n)$ is expressed as

$$\sum_{p=0}^{N-1} \Delta w_p(n) \mathrm{e}^{\mathrm{i}\frac{2\pi mp}{N}} \sum_{l=p}^{N-1+p} x(n-l)\mathrm{e}^{-\mathrm{i}\frac{2\pi ml}{N}} - V_m(n) \tag{46}$$

Next, we describe $\boldsymbol{X}_i(n)$ by using the input signal $x(n)$. Since $\boldsymbol{x}_i(n)$ $(i=0,1)$ are the output of the lowpass filter and the highpass filter respectively, we have

$$\boldsymbol{x}_i(n) = \left[\, \boldsymbol{h}_i^{\mathrm{T}}\boldsymbol{x}(n),\ \boldsymbol{h}_i^{\mathrm{T}}\boldsymbol{x}(n-1),\ \cdots,\ \boldsymbol{h}_i^{\mathrm{T}}\boldsymbol{x}(n-(N-1)) \,\right]^{\mathrm{T}}. \tag{47}$$

By applying the N point DFT matrix $\boldsymbol{F}$ to $\boldsymbol{x}_i(n)$, the m-th element of $\boldsymbol{X}_i(n)$ is calculated as

$$\sum_{p=0}^{N_h-1} h_{i,p}\mathrm{e}^{\mathrm{i}\frac{2\pi mp}{N}} \sum_{l=p}^{N-1+p} x(n-l)\mathrm{e}^{-\mathrm{i}\frac{2\pi ml}{N}} \tag{48}$$

From (46) and (48), the $(m,\ k)$-th element of matrix $\boldsymbol{X}_i(n)\boldsymbol{B}^\dagger(n)$ can be described as

$$\begin{aligned} &\sum_{p=0}^{N_h-1} h_{i,p}\mathrm{e}^{\mathrm{i}\frac{2\pi mp}{N}} \sum_{p'=0}^{N-1} \Delta w_{p'}(n)\mathrm{e}^{-\mathrm{i}\frac{2\pi kp'}{N}} \\ &\quad\times \sum_{l=p}^{N-1+p}\sum_{l'=p'}^{N-1+p'} x(n-l)x(n-l')\mathrm{e}^{-\mathrm{i}\frac{2\pi(ml-kl')}{N}} \\ &\quad- \sum_{p=0}^{N_h-1} h_{i,p}\mathrm{e}^{\mathrm{i}\frac{2\pi mp}{N}} \sum_{l=p}^{N-1+p} x(n-l)\mathrm{e}^{-\mathrm{i}\frac{2\pi ml}{N}} V_k^*(n) \end{aligned} \tag{49}$$

where * denotes the complex conjugate operation. Taking the average of (49), the second term in (49) is zero due to the uncorrelatedness of $\boldsymbol{V}(n)$ and $\boldsymbol{x}(n)$ so that (49) for fixed $\Delta\bar{w}_{p'}$ is expressed as

$$\begin{aligned} &\sum_{p=0}^{N_h-1} h_{i,p}\mathrm{e}^{\mathrm{i}\frac{2\pi mp}{N}} \sum_{p'=0}^{N-1} \Delta\bar{w}_{p'}\mathrm{e}^{-\mathrm{i}\frac{2\pi kp'}{N}} \\ &\quad \underbrace{\times\, \mathrm{E}\left[\sum_{l=p}^{N-1+p}\sum_{l'=p'}^{N-1+p'} x(n-l)x(n-l')\mathrm{e}^{-\mathrm{i}\omega_m l}\mathrm{e}^{-\mathrm{i}(-\omega_k)l'}\right]}_{A_{pp'}} \end{aligned} \tag{50}$$

where $\omega_m = 2\pi m/N$ and $\omega_k = 2\pi k/N$. The sum with respect to l is equal to the sum for $0 \le l \le N-1$ minus the sum for $0 \le l \le p-1$ plus $N \le l \le N-1+p$. Since latter two sums are of $O(N_h)$, and can be discarded under the assumption $N_h \ll N$, $A_{pp'}$ is approximated as

$$A_{pp'} \simeq \mathrm{E}\left[\sum_{l=0}^{N-1}\sum_{l'=p'}^{N-1+p'} x(n-l)x(n-l')\mathrm{e}^{-\mathrm{i}\omega_m l}\mathrm{e}^{-\mathrm{i}(-\omega_k)l'}\right].$$

If we set

$$\begin{aligned} d_1^{(N)}(\omega_m) &= \sum_{l=-\infty}^{\infty} h_1(l)x(n-l)\mathrm{e}^{-\mathrm{i}\omega_m l} \\ d_2^{(N)}(\omega_k) &= \sum_{l'=-\infty}^{\infty} h_2(l')x(n-l')\mathrm{e}^{-\mathrm{i}\omega_k l'} \end{aligned}$$

where

$$\begin{aligned} h_1(l) &= \begin{cases} 1 & 0 \le l \le N-1 \\ 0 & \text{otherwise} \end{cases} \\ h_2(l') &= \begin{cases} 1 & p' \le l' \le N-1+p' \\ 0 & \text{otherwise} \end{cases}, \end{aligned}$$

we have

$$A_{pp'} = \mathrm{E}\left[d_1^{(N)}(\omega_m)d_2^{(N)}(-\omega_k)\right].$$

Then the theorem in [11, p.92, Theorem 4.3.1], which evaluates the cumulants of the finite Fourier transform of r dimensional time series, can be applied to $A_{pp'}$. As a result, $A_{pp'}$ is approximated as

$$A_{pp'} = H_{12}^{(N)}(\omega_m - \omega_k)S_x(\omega_m) + o(N)$$

where $S_x(\omega)$ is the spectral density of the input signal $x(n)$ and

$$H_{12}^{(N)}(\omega) = \sum_l h_1(l)h_2(l)\mathrm{e}^{-\mathrm{i}\omega l} = \sum_{l=p'}^{N-1} e^{-\mathrm{i}\omega l}.$$

For $\omega_m \ne \omega_k$, $A_{pp'}$ is of $o(N)$. Since $H_{12}^{(N)}(0) = (N-p')$, $A_{pp'}$ is approximated as

$$A_{pp'} \simeq (N-p')S_x(\omega_m)\delta_{mk}.$$

By substituting the above equation into (50), the k-th diagonal element of the matrix $\boldsymbol{X}_i(n)\boldsymbol{B}^\dagger(n)$ is written as

$$\sum_{p=0}^{N_h-1} h_{i,p}\mathrm{e}^{\mathrm{i}\frac{2\pi kp}{N}} \underbrace{\sum_{p'=0}^{N-1} \Delta\bar{w}_{p'}(n)\frac{N-p'}{N}\mathrm{e}^{-\mathrm{i}\frac{2\pi kp'}{N}}}_{A'_k} \cdot NS_x(\omega_m)\delta_{mk} \tag{51}$$

Putting $\Delta\bar{w}_{p'}(n) = 0$ for $-(N-1) \leq p' \leq -1$. A'_k can be rewritten as

$$A'_k = \sum_{p'=-(N-1)}^{N-1} \Delta\bar{w}_{p'}(n) \frac{N-|p'|}{N} \mathrm{e}^{-\mathrm{i}\frac{2\pi k p'}{N}} \tag{52}$$

where $f_N(p') = (N - |p'|)/N$ is called the Bartlett window. Since (52) is the DFT of the product of $\Delta\bar{w}_{p'}(n)$ and $f_N(p')$, it is also expressed by the convolution of $\Delta\bar{W}(\omega)$ and the Fejer kernel $F_N(\omega) = \sin^2(N\omega/2)/(2\pi N \sin^2(\omega/2))$ as

$$A'_k \simeq \int_0^{2\pi} \Delta\bar{W}(\nu) F_N(\omega_k - \nu) \mathrm{d}\nu \tag{53}$$

where $\Delta\bar{W}(\omega)$ and $F_N(\omega)$ are the DFT of $\Delta\bar{w}_{p'}(n)$ and $f_N(p')$, respectively. When N is sufficiently large, $F_N(\omega)$ is close to a delta function[11]. Then (53) can be further approximated as

$$A'_k \simeq \Delta\bar{W}(\omega_k) = \Delta\bar{W}_k(n). \tag{54}$$

Using the above equation, (51) can be approximated by $\delta_{mk} H^*_{i,k} \Delta\bar{W}_k(n) Q_k$. Hence, $\mathrm{E}[\boldsymbol{X}_i(n)\boldsymbol{B}^\dagger(n)]$ is asymptotically close to the following diagonal matrix,

$$\mathrm{E}[\boldsymbol{X}_i(n)\boldsymbol{B}^\dagger(n)] \simeq \boldsymbol{\Lambda}^\dagger_{H_i} \boldsymbol{Q} \boldsymbol{\Lambda}_{\Delta\bar{W}(n)}. \tag{55}$$

where $\boldsymbol{\Lambda}_{\Delta\bar{W}(n)} = \mathrm{diag}[\, \Delta\bar{W}_0(n),\ \Delta\bar{W}_1(n),\ \cdots,\ \Delta\bar{W}_{N-1}(n)\,]$ and $\boldsymbol{Q} = \mathrm{diag}[\, Q_0,\ Q_1,\ \cdots,\ Q_{N-1}\,]$, $Q_m \equiv N S_x(\omega_m)$. By taking the average of (22) for fixed $\Delta\bar{\boldsymbol{W}}(n)$ and substituting (55) into it, (23) is obtained.

B Derivation of (24)

From the definition of matrix $\boldsymbol{S}$, we have

$$S(\Delta\boldsymbol{W}) = \frac{1}{N^2} \sum_{n=-\infty}^{\infty} \sum_{i=0}^{1}\sum_{j=0}^{1} \gamma_i\gamma_j \mathrm{E}\left[\boldsymbol{X}_i(n)\boldsymbol{B}^\dagger(n)\boldsymbol{H}_i\boldsymbol{H}^\dagger_j\boldsymbol{B}(0)\boldsymbol{X}^\dagger_j(0)\right].$$

Let us calculate the term

$$\sum_{n=-\infty}^{\infty} \mathrm{E}\left[\boldsymbol{X}_i(n)\boldsymbol{B}^\dagger(n)\boldsymbol{H}_i\boldsymbol{H}^\dagger_j\boldsymbol{B}(0)\boldsymbol{X}^\dagger_j(0)\right] \tag{56}$$

at the equilibrium point $\Delta\boldsymbol{W}_* = \boldsymbol{0}$. Since only the second term in (49) remains for $\Delta\boldsymbol{W} = \boldsymbol{0}$, the (m, m') element of (56) is expressed as

$$\sum_{n=-\infty}^{\infty} \sum_{p=0}^{N_h-1} h_{i,p} \mathrm{e}^{\mathrm{i}\frac{2\pi m p}{N}} \sum_{p'=0}^{N_h-1} h_{j,p} \mathrm{e}^{-\mathrm{i}\frac{2\pi m' p'}{N}} \sum_{l=p}^{N-1+p} \sum_{l'=p'}^{N-1+p'} x(n-l)x(-l')\mathrm{e}^{-\mathrm{i}\frac{2\pi m l}{N}} \mathrm{e}^{\mathrm{i}\frac{2\pi m' l'}{N}}$$
$$\times \sum_{k=0}^{N-1}\sum_{k'=0}^{N-1} V^*_k(n) H_{i,k} V_{k'}(0) H^*_{j,k'}$$

Taking the average of the above quantity, it becomes

$$\sum_{n=-\infty}^{\infty} H_{i,m}^* H_{j,m'} \underbrace{\mathrm{E}\left[\sum_{l=p}^{N-1+p} \sum_{l'=p'}^{N-1+p'} x(n-l)x(-l')\mathrm{e}^{-\mathrm{i}\frac{2\pi ml}{N}}\mathrm{e}^{\mathrm{i}\frac{2\pi m'l'}{N}}\right]}_{A'_{pp'}} \sum_{k=0}^{N-1}\sum_{k'=0}^{N-1} \mathrm{E}\left[V_k^*(n)V_{k'}(0)\right] H_{i,k}H_{j,k'}^*. \tag{57}$$

We use the same method in Appendix A to evaluate $A'_{pp'}$. Since $0 \le p, p' \le N_h - 1$ and $N_h \ll N$, we have $A'_{pp'} \simeq A'_{0,0}$. Also, the length of the overlap of the windows is $N - |n|$ for $-(N-1) \le n \le N-1$ and 0 otherwise, we have

$$A'_{00} \simeq \begin{cases} (N-|n|)\delta_{mm'}S_x(\omega_m)\mathrm{e}^{-\mathrm{i}\omega_m n} & (|n| \le N-1) \\ 0 & (\text{otherwise}) \end{cases}. \tag{58}$$

Also, the term $\mathrm{E}\left[V_k^*(n)V_{k'}(0)\right]$ in (57) is given by

$$\mathrm{E}\left[V_k^*(n)V_{k'}(0)\right] = \mathrm{E}\left[\sum_{u=-n}^{-n+N-1} v(-u)\mathrm{e}^{-\mathrm{i}(-\omega_k)u} \sum_{u'=0}^{N-1} v(-u')\mathrm{e}^{-\mathrm{i}\omega_{k'}u'}\right]\mathrm{e}^{\mathrm{i}\omega_k n}$$

so that

$$\mathrm{E}\left[V_k^*(n)V_{k'}(0)\right] \simeq (N-|n|)\delta_{kk'}S_v(\omega_k)\mathrm{e}^{\mathrm{i}\omega_k n} \tag{59}$$

where $S_v(\omega)$ is the spectral density of $v(n)$. By substituting (58) and (59) into (57), we have

$$(57) \simeq N^2\delta_{mm'}H_{i,m}^*H_{j,m}S_x(\omega_m)\sum_{k=0}^{N-1} H_{i,k}H_{j,k}^*S_v(\omega_k) \sum_{n=-(N-1)}^{N-1} f^2(n)\mathrm{e}^{-\mathrm{i}(\omega_m-\omega_k)n}$$

where $f(n)$ is the Bartlett window introduced in Appendix A. The sum with respect to n is approximated by $(2N/3)\delta_{mk}$ as $N \to \infty$. Hence, the $(m+1, m'+1)$ element of (56) is given by

$$(57) \simeq \frac{2}{3}N^2\delta_{mm'}H_{i,m}^*H_{j,m}Q_mH_{i,m}H_{j,m}^*S_v(\omega_m).$$

For simplicity, we assume that $\{v(n)\}$ is white with the variance σ_v^2, then we have

$$(56) \simeq \frac{2}{3}N^2\sigma_v^2\mathbf{\Lambda}_{H_i}^\dagger\mathbf{\Lambda}_{H_i}\boldsymbol{Q}\mathbf{\Lambda}_{H_j}^\dagger\mathbf{\Lambda}_{H_j}.$$

Finally, we find that $\boldsymbol{S}(\Delta\boldsymbol{W}_*)$ can be approximated by the following matrix,

$$\boldsymbol{S}(\Delta\boldsymbol{W}_*) \simeq \frac{2\sigma_v^2}{3}\sum_{i=0}^{1}\sum_{j=0}^{1}\gamma_i\gamma_j\mathbf{\Lambda}_{H_i}^\dagger\mathbf{\Lambda}_{H_i}\boldsymbol{Q}\mathbf{\Lambda}_{H_j}^\dagger\mathbf{\Lambda}_{H_j}.$$

References

[1] D. R. Morgan and J. C. Thi, "A delayless subband adaptive filter architecture," *IEEE Trans. Signal Processing*, vol. 43, pp.1819–1830, Aug. 1995.

[2] N. Hirayama, H. Sakai, and S. Miyagi, "Delayless subband adaptive filtering using the Hadamard transform," *IEEE Trans. Signal Processing*, vol. 47, pp.1731–1734, June 1999.

[3] S. S. Pradhan and V. U. Reddy, "A new approach to subband adaptive filtering," *IEEE Trans. Signal Processing*, vol. 47, pp. 655–664, March 1999.

[4] V. Solo and X. Kong, *Adaptive Signal Processing Algorithms – Stability and Performance –*. Englewood Cliffs, NJ: Prentice Hall, 1995.

[5] A. Benveniste, M. Métivier and P. Priouret, *Adaptive Algorithms and Stochastic Approximations.* Berlin Heidelberg: Springer-Verlag, 1990.

[6] S. Miyagi and H. Sakai, "Convergence analysis of the delayless subband adaptive filter based on the frequency domain expression," in *Proc. IEEE ICASSP 2000*, Istanbul, Turkey, pp. 368-371.

[7] K. Nishikawa and H. Kiya, "Conditions for convergence of a deleyless subband adaptive filter and its efficient implementation," *IEEE Trans. on Signal Processing*, vol. 46, pp.1158–1167, Apr. 1998.

[8] C. G. Samson and V. U. Reddy, "Fixed point error analysis of the normalized ladder algorithm," *IEEE Trans. Acoustic Speech and Signal Processing*, vol. ASSP-31, pp.1177–1191, Oct. 1983.

[9] S. Ohno and H. Sakai, "On delayless subband adaptive filtering by subband/fullband transforms," *IEEE Signal Processing Letters*, vol. 6, pp.236–239, Sept. 1999.

[10] F. R. Gantmacher, *The Theory of Matrices Vol 2.* New York, Chelsea Pubrishing Company, 1974.

[11] D. R. Brillinger, *Time Series – Data Analysis and Theory –*. New York: Holt, Rinehart and Wintston, 1975.

[12] R. E. Crochiere and L. R. Rabiner, *Multirate Digital Signal Processing.* Englewood Cliffs, NJ: Prentice Hall, 1983.

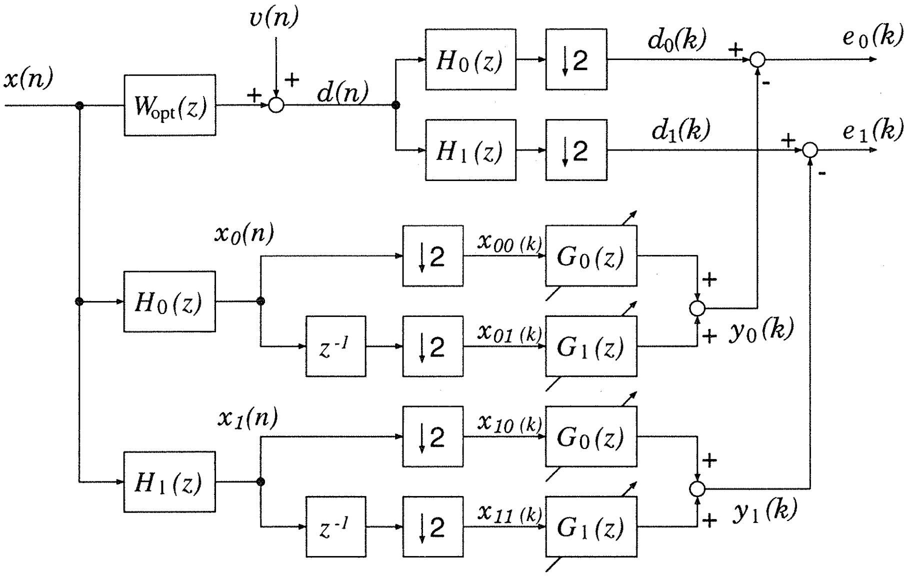

Figure 1: Block diagram of the two band subband adaptive filter proposed by Pradhan and Reddy.

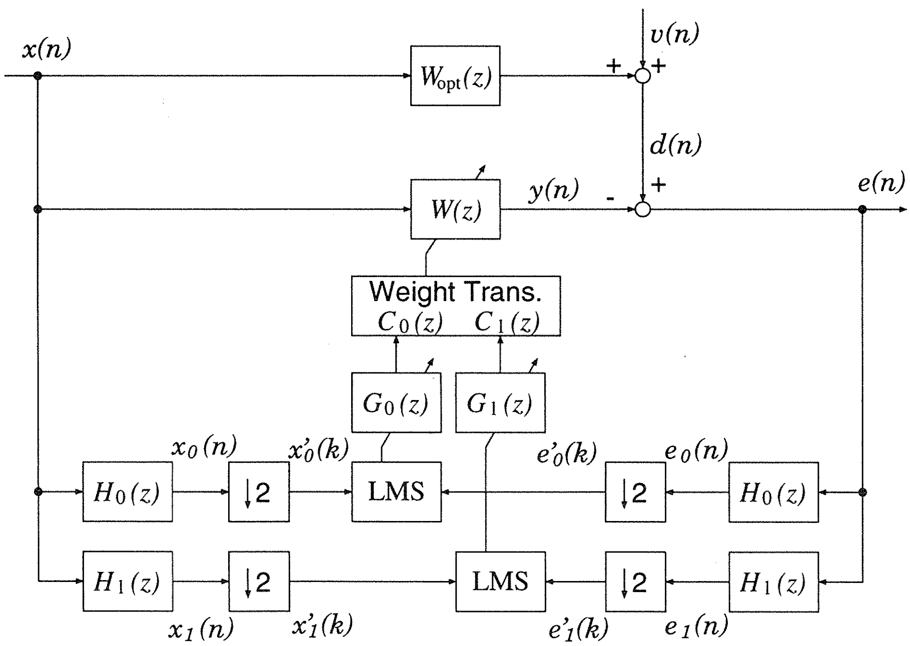

Figure 2: Block diagram of the two band delayless subband adaptive filter.

$C_i(z)$	stability		
	theoretical		empirical
	1st condition	2nd condition	
Hadamard	satisfied	marginal	stable
8A	not satisfied	not satisfied	unstable
12A	not satisfied	not satisfied	unstable
16A	not satisfied	not satisfied	unstable

Table 1: Stability checking of the two band delayless subband adaptive filter

	ξ			
	Gaussian white noise		1st order AR	
	theoretical	empirical	theoretical	empirical
Pradhan's SADF	0.16660	0.18094	0.11384	0.085254
DLSADF with Hadmard transform	0.28804	0.20271	0.93975	0.78206

Table 2: Comparison of ξ of the Pradhan's two band SADF with that of the DLSADF with the Hadamard transform.

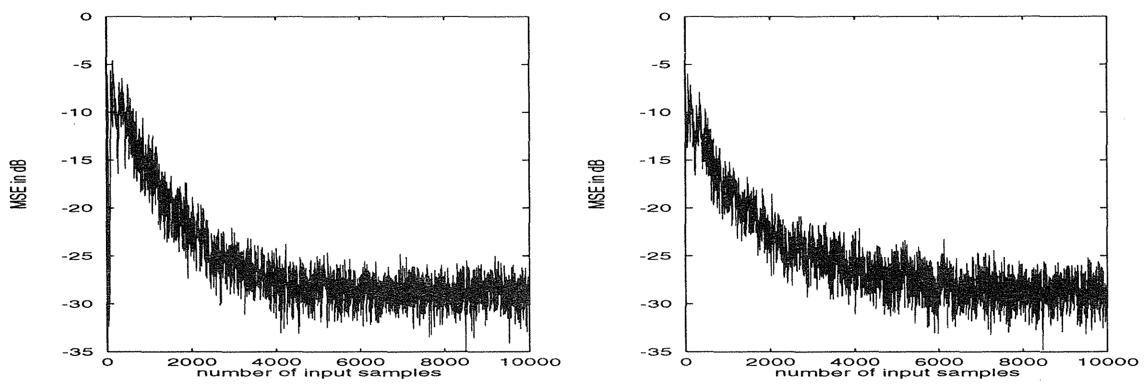

Figure 3: MSE curves showing the convergence rate under the condition with having the same EMSE, where step sizes are 0.02 and 0.00072 for the Pradhan's SADF and the usual fullband ADF, respectively.

Second Order Analysis of a Multiple Minor Components Extraction Algorithm by the Averaging Method

Keywords: minor component analysis, adaptive algorithm, averaging method, second order analysis

Abstract

In this paper, we derive the asymptotic distribution of a multiple minor components extraction algorithm based on the algorithm proposed by Douglas,*et al.* for the extraction of the eigenvalue corresponding to the minimum eigenvalue of the covariance matrix of the input vector. Our algorithm extracts multiple minor components by applying the deflation technique and the GS (Gram-Schmidt) orthogonalization. By using the ODE (Ordinary Differential Equation) theory based on the averaging method and solving the related Lyapunov equation, we derive the asymptotic distribution of our minor components extraction algorithm.

1 Introduction

Minor component analysis plays important roles in many applications, such as MUSIC algorithm and Pisarenko frequency estimation. Several adaptive algorithms for minor component extraction have been proposed. Thompson/Owsley algorithm [1] is originally an estimator for the eigenvector corresponding to the largest eigenvalue. This algorithm can be used for minor component analysis by replacing the adaptive gain μ by $-\mu$. An equivalent algorithm has been proposed by Reddy*et al.* [2]. Oja has suggested an LMS type algorithm with a negative adaptive gain from a neural network point of view [3]. The PASTd algorithm which was originally used in principal component analysis in [4] has been modified for multiple minor components extraction by Sakai and Shimizu [5].

The properties of these algorithms have not been fully analyzed. Solo and Kong [6] have compared Reddy's algorithm with Oja's algorithm by means of the averaging method. Also, Yang [7] derived the asympotic distribution of the PAST algorithm by using the ODE (Ordinary Differential Equation) method in [8]. Also, a similar performance analysis is made by Delmas and Cardoso [9].

The algorithm in [4] uses Oja's algorithm as a fundamental building block for extraction of a single minor component. In this paper, we use a more stable algorithm by Douglas, Kung, Amari [10] and derive the asymptotic distoribution of the algorithm.

Our algorithm is based on the deflation technique and the orthogonalization. In order to derive the asymptotic distributions, we also use the ODE method. And by the computer simulations, we compare the empirical covariances of our algorithm with the theoretical values.

2 Minor Component Analysis

Single minor component analysis is extracting the eigenvector corresponding to the minimum eigenvalue of the covariance matrix of the input vector $\boldsymbol{x}(k)$ where $\boldsymbol{x}(k)$ is an n-dimensional stochastic input signal and is assumed to be real with zero mean and the covariance matrix $\boldsymbol{C}$

$$\boldsymbol{C} = \mathrm{E}[\boldsymbol{x}(k)\boldsymbol{x}^T(k)]. \tag{1}$$

The eigenvalues of $\boldsymbol{C}$ are given by

$$\lambda_n \geq \lambda_{n-1} \geq \cdots \geq \lambda_r > \cdots > \lambda_2 > \lambda_1 > 0 \tag{2}$$

and the eigenvectors corresponding to the eigenvalues are $\boldsymbol{u}_n, \cdots, \boldsymbol{u}_1$, respectively. For notational simplicity we use the reversed ordering with the usual convention. Then $\boldsymbol{C}$ is expressed as

$$\boldsymbol{C} = \boldsymbol{U}\Lambda\boldsymbol{U}^T = \sum_{i=1}^{n} \lambda_i \boldsymbol{u}_i \boldsymbol{u}_i^T$$

where

$$\boldsymbol{U} = [\boldsymbol{u}_1, \cdots, \boldsymbol{u}_n], \qquad \boldsymbol{U}\boldsymbol{U}^T = \boldsymbol{I}, \qquad \Lambda = \mathrm{diag}[\lambda_1, \cdots, \lambda_n].$$

We use the following adaptive algorithm with a sufficiently small positive constant gain μ for extracting $\boldsymbol{u}_1$ corresponding to the minimum eigenvalue λ_1 due to Douglas *et al.*[10]:

$$\boldsymbol{v}_1(k) \;=\; \boldsymbol{v}_1(k-1) - \mu \boldsymbol{A}_1(k)\boldsymbol{v}_1(k-1) \tag{3}$$

where

$$\boldsymbol{A}_1(k) \;=\; \| \boldsymbol{v}_1(k-1) \|^4 \, \boldsymbol{x}(k)\boldsymbol{x}^T(k) - \boldsymbol{I}\{\boldsymbol{v}_1^T(k-1)\boldsymbol{x}(k)\}^2. \tag{4}$$

This algorithm is slightly different from those used in [5] and [6]. The reason why we choose this will become apparent later. From(3),(4) and A, we have

$$\boldsymbol{h}_1(\boldsymbol{v}_1, \boldsymbol{x}) = -\Big[\|\boldsymbol{v}_1\|^4 \boldsymbol{x}\boldsymbol{x}^T - \boldsymbol{I}(\boldsymbol{v}_1^T\boldsymbol{x})^2\Big]\boldsymbol{v}_1.$$

Taking the expectation with respect to $\boldsymbol{x}$, the ODE of $\boldsymbol{v}_1(k)$ is given by

$$\dot{\boldsymbol{v}}_1 = \tilde{\boldsymbol{h}}_1(\boldsymbol{v}_1) \equiv -\left(\|\boldsymbol{v}_1\|^4 \boldsymbol{C} - \boldsymbol{I}\boldsymbol{v}_1^T\boldsymbol{C}\boldsymbol{v}_1\right)\boldsymbol{v}_1. \tag{5}$$

Thus for the Lyapunov function $L(\boldsymbol{v}_1) = (\|\boldsymbol{v}_1\|^2 - 1)^2$,

$$\dot{L}(\boldsymbol{v}_1) = -4\|\boldsymbol{v}_1\|^2\boldsymbol{v}_1^T\boldsymbol{C}\boldsymbol{v}_1(\|\boldsymbol{v}_1\|^2 - 1)^2 < 0.$$

This means that $\|\boldsymbol{v}_n\| \to 1$. Using the argument in [5], we have $\boldsymbol{v}_1(k) \to \boldsymbol{u}_1$. So the vector $\boldsymbol{v}_1(k)$ in the algorithm (3) converges to the eigenvector $\boldsymbol{u}_1$ corresponding to the minimum eigenvalue λ_1 of $\boldsymbol{C}$. Next, we consider extracting multiple minor components by using the deflation technique. First, we state about the second minor component and extend to the i-th minor component.

The algorithm of the second minor component extraction is as follows

- deflation step

$$\boldsymbol{x}_2(k) = \left(\boldsymbol{I} - \boldsymbol{v}_1(k)\boldsymbol{v}_1^T(k)\right)\boldsymbol{x}(k) \tag{6}$$

- updating the weight vector

$$\boldsymbol{\psi}_2(k) = \boldsymbol{v}_2(k-1) - \mu\boldsymbol{A}_2(k)\boldsymbol{v}_2(k-1) \tag{7}$$

where

$$\boldsymbol{A}_2(k) = \| \boldsymbol{v}_2(k-1) \|^4 \boldsymbol{x}_2(k)\boldsymbol{x}_2^T(k) - \boldsymbol{I}\{\boldsymbol{v}_2^T(k-1)\boldsymbol{x}_2(k)\}^2$$

and $\boldsymbol{C}_2 = \mathrm{E}[\boldsymbol{x}_2(k)\boldsymbol{x}_2^T(k)]$

- orthogonalization step

$$\boldsymbol{v}_2(k) = \left(\boldsymbol{I} - \frac{\boldsymbol{v}_1(k)\boldsymbol{v}_1^T(k)}{\| \boldsymbol{v}_1(k) \|^2}\right)\boldsymbol{\psi}_2(k) \tag{8}$$

By using the "deflated" vector $\boldsymbol{x}_2(k)$ and the orthogonalization, $\boldsymbol{v}_2(k)$ converges to the eigenvector corresponding to the eigenvalue λ_2. The orthogonalization step which is not necessary for principal component analysis is needed. This is because the covariance matrix $\boldsymbol{C}_2$ of the "deflated" vector $\boldsymbol{x}_2$ is given by

$$\begin{aligned} \boldsymbol{C}_2 &\to \boldsymbol{C} - 2\boldsymbol{u}_1\boldsymbol{u}_1^T\boldsymbol{C} + \boldsymbol{u}_1^T\boldsymbol{C}\boldsymbol{u}_1\boldsymbol{u}_1\boldsymbol{u}_1^T = \boldsymbol{C} - \lambda_1\boldsymbol{u}_1\boldsymbol{u}_1^T \\ &= 0 \cdot \boldsymbol{u}_1\boldsymbol{u}_1^T + \lambda_2\boldsymbol{u}_2\boldsymbol{u}_2^T + \cdots + \lambda_n\boldsymbol{u}_n\boldsymbol{u}_n^T. \end{aligned}$$

From this calculation, the eigenvalues of the covariance matrix $\boldsymbol{C}_2$ are $\lambda_1, \cdots, \lambda_{n-1}, 0$. So, λ_2 is not the smallest and the orthogonalization is needed to prevent that $\boldsymbol{v}_2(k)$ converges to $\boldsymbol{u}_1$ again. By (8) $\boldsymbol{v}_1^T(k)\boldsymbol{v}_2(k) = 0$ is ensured.

Similarly, the i-th ($i = 2, \cdots, n$) minor component is extracted by the following algorithm.

- deflation step

$$\boldsymbol{x}_1(k) = \boldsymbol{x}(k) \tag{9}$$

$$\boldsymbol{x}_i(k) = \Big(\boldsymbol{I} - \sum_{j=1}^{i-1} \boldsymbol{v}_j(k)\boldsymbol{v}_j^T(k)\Big)\boldsymbol{x}(k). \tag{10}$$

- updating the weight vector

$$\boldsymbol{\psi}_i(k) = \boldsymbol{v}_i(k-1) - \mu \boldsymbol{A}_i(k)\boldsymbol{v}_i(k-1) \tag{11}$$

- orthogonalization

$$\boldsymbol{v}_i(k) = \Big(\boldsymbol{I} - \sum_{j=1}^{i-1} \frac{\boldsymbol{v}_j(k)\boldsymbol{v}_j^T(k)}{\| \boldsymbol{v}_j(k) \|^2}\Big)\boldsymbol{\psi}_i(k) \tag{12}$$

where

$$\boldsymbol{A}_i(k) = \| \boldsymbol{v}_i(k-1) \|^4 \boldsymbol{x}_i(k)\boldsymbol{x}_i^T(k) - \boldsymbol{I}\{\boldsymbol{v}_i^T(k-1)\boldsymbol{x}_i(k)\}^2 \tag{13}$$

and $\boldsymbol{C}_i = \mathrm{E}[\boldsymbol{x}_i(k)\boldsymbol{x}_i^T(k)]$

3 The Second Order Analysis

In this section, we will derive the ODE of the above minor components extraction algorithm (8)-(12). First we consider the case of the single minor conponent extraction algorithm and extend the result to multiple minor component analysis.

First, we derive the ODE of the single minor component extraction algorithm and calculate $\boldsymbol{H}(\boldsymbol{u}_1)$, $\boldsymbol{S}(\boldsymbol{u}_1)$ and the covariance matrix $\boldsymbol{D}$ in Appendix A.

The derivative matrix $\boldsymbol{H}(\boldsymbol{v}_1)$ is calculated from (5) as

$$\begin{aligned}
\boldsymbol{H}(\boldsymbol{v}_1) &= \frac{\partial}{\partial \boldsymbol{v}_1^T}\tilde{\boldsymbol{h}}_1(\boldsymbol{v}_1) \\
&= -\|\boldsymbol{v}_1\|^4\boldsymbol{C} - 4\|\boldsymbol{v}_1\|^2\boldsymbol{C}\boldsymbol{v}_1\boldsymbol{v}_1^T + \boldsymbol{I}(\boldsymbol{v}_1^T\boldsymbol{C}\boldsymbol{v}_1) + 2\boldsymbol{v}_1\boldsymbol{v}_1^T\boldsymbol{C}. \qquad (14)
\end{aligned}$$

The derivative matrix at the equilibrium point $\boldsymbol{u}_1$ is

$$\boldsymbol{H}(\boldsymbol{u}_1) = -2\lambda_1\boldsymbol{u}_1\boldsymbol{u}_1^T + \sum_{j=2}^{n-1}(-\lambda_j + \lambda_1)\boldsymbol{u}_j\boldsymbol{u}_j^T. \tag{15}$$

This means that the eigenvalues of $\boldsymbol{H}(\boldsymbol{u}_1)$ are all negative. But for the algorithm in [3], $-2\lambda_1$ is replaced by $2\lambda_1$. This violates the assumption about (46) in A. This is why we use the algorithm (3), (4).

In order to compute the matrix $\boldsymbol{S}(\boldsymbol{v}_1)$, we further assume that $\boldsymbol{x}(k)$ is independently, identically and normally distributed. This allows us to simplify (45) in A to the expression

$$\boldsymbol{S}(\boldsymbol{v}_1) = \mathrm{E}[\boldsymbol{h}_1(\boldsymbol{v}_1, \boldsymbol{x}(0))\boldsymbol{h}_1^T(\boldsymbol{v}_1, \boldsymbol{x}(0))]$$

and the high order moments can be easily calculated. After some calculations, $\boldsymbol{S}_{11} = \boldsymbol{S}(\boldsymbol{u}_1)$ is obtained as

$$\boldsymbol{S}_{11} = \lambda_1 \boldsymbol{C} - \lambda_1^2 \boldsymbol{u}_1 \boldsymbol{u}_1^T. \tag{16}$$

By solving the Lyapunov equation $\boldsymbol{H}(\boldsymbol{u}_1)\boldsymbol{D}_{11} + \boldsymbol{D}_{11}\boldsymbol{H}^T(\boldsymbol{u}_1) = -\boldsymbol{S}_{11}$, we obtain the covariance matrix $\boldsymbol{D}_{11}$ as

$$\boldsymbol{D}_{11} = \frac{1}{2}\sum_{j=2}^{n} \frac{\lambda_j \lambda_1}{\lambda_j - \lambda_1} \boldsymbol{u}_j \boldsymbol{u}_j^T. \tag{17}$$

Next, we will derive the ODE of the i-th minor component extraction by using the deflation technique $i-1$ times. But in deriving the ODE, complicated calculations are needed. So,we simplify (11), (12) by some approximations. Here we have $\boldsymbol{\psi}_1(k) = \boldsymbol{v}_1(k)$ and after some approximation, we can simplify (11), (12) as

$$\begin{aligned} \boldsymbol{v}_i(k) &\approx \boldsymbol{\psi}_i(k) - \sum_{j=1}^{i-1} \frac{\boldsymbol{\psi}_j(k)\boldsymbol{\psi}_j^T(k)}{\| \boldsymbol{\psi}_j(k) \|^2} \boldsymbol{\psi}_i(k) & (18) \\ &\approx \boldsymbol{v}_i(k-1) + \mu \boldsymbol{h}_i(\boldsymbol{v}_1(k-1), \cdots \boldsymbol{v}_i(k-1), \boldsymbol{x}_i(k)) & (19) \end{aligned}$$

where

$$\begin{aligned} \boldsymbol{h}_i(\boldsymbol{v}_1, \cdots, \boldsymbol{v}_i, \boldsymbol{x}_i(k)) &\equiv -\boldsymbol{A}_i(k)\boldsymbol{v}_i + \sum_{j=1}^{i-1} \frac{\boldsymbol{v}_j \boldsymbol{v}_j^T}{\|\boldsymbol{v}_j\|^2} \boldsymbol{A}_i(k)\boldsymbol{v}_i + \sum_{j=1}^{i-1} \frac{\boldsymbol{A}_j(k)\boldsymbol{v}_j \boldsymbol{v}_j^T}{\|\boldsymbol{v}_j\|^2} \boldsymbol{v}_i \\ &+ \sum_{j=1}^{i-1} \frac{\boldsymbol{v}_j \boldsymbol{v}_j^T \boldsymbol{A}_j^T(k)}{\|\boldsymbol{v}_j\|^2} \boldsymbol{v}_i - 2\sum_{j=1}^{i-1} \frac{\boldsymbol{v}_j^T \boldsymbol{A}_j^T(k) \boldsymbol{v}_j}{\|\boldsymbol{v}_j\|^4} \boldsymbol{v}_j \boldsymbol{v}_j^T \boldsymbol{v}_i & (20) \\ &\equiv (S1) + (S2) + (S3) + (S4) + (S5) \end{aligned}$$

$$\boldsymbol{A}_i(k) = \|\boldsymbol{v}_i\|^4 \boldsymbol{x}_i(k)\boldsymbol{x}_i^T(k) - \boldsymbol{I}(\boldsymbol{v}_i^T \boldsymbol{x}_i(k))^2. \tag{21}$$

The details of the derivation are presented in Appendix B. Then by taking the expectation of (21) with respect to $\boldsymbol{x}_i(k)$ the ODE is given by

$$\begin{aligned} \dot{\boldsymbol{v}}_i &= \tilde{\boldsymbol{h}}_i(\boldsymbol{v}_1, \cdots, \boldsymbol{v}_i) \\ &\equiv -\boldsymbol{A}_i \boldsymbol{v} + \sum_{j=1}^{i-1} \frac{\boldsymbol{v}_j \boldsymbol{v}_j^T}{\|\boldsymbol{v}_j\|^2} \boldsymbol{A}_i \boldsymbol{v}_i + \sum_{j=1}^{i-1} \frac{\boldsymbol{A}_j \boldsymbol{v}_j \boldsymbol{v}_j^T}{\|\boldsymbol{v}_j\|^2} \boldsymbol{v}_i + \sum_{j=1}^{i-1} \frac{\boldsymbol{v}_j \boldsymbol{v}_j^T \boldsymbol{A}_j^T}{\|\boldsymbol{v}_j\|^2} \boldsymbol{v}_i \\ &\quad -2\sum_{j=1}^{i-1} \frac{\boldsymbol{v}_j^T \boldsymbol{A}_j \boldsymbol{v}_j}{\|\boldsymbol{v}_j\|^4} \boldsymbol{v}_j \boldsymbol{v}_j^T \boldsymbol{v}_i \equiv (H1) + (H2) + (H3) + (H4) + (H5) & (22) \end{aligned}$$

$$\boldsymbol{A}_i = \| \boldsymbol{v}_i \|^4 \boldsymbol{C}_i - \boldsymbol{I}(\boldsymbol{v}_i^T \boldsymbol{C}_i \boldsymbol{v}_i). \tag{23}$$

Next we define the vectors

$$\boldsymbol{v}^T = [\boldsymbol{v}_1^T, \cdots, \boldsymbol{v}_r^T], \quad \boldsymbol{u}^T = [\boldsymbol{u}_1^T, \cdots, \boldsymbol{u}_r^T] \tag{24}$$

and the derivative matrix as

$$\boldsymbol{H}(\boldsymbol{v}) = \begin{pmatrix} \frac{\partial}{\partial \boldsymbol{v}_1^T}\tilde{\boldsymbol{h}}_1(\boldsymbol{v}_1) & \cdots & \frac{\partial}{\partial \boldsymbol{v}_r^T}\tilde{\boldsymbol{h}}_1(\boldsymbol{v}_1) \\ \vdots & & \vdots \\ \frac{\partial}{\partial \boldsymbol{v}_1^T}\tilde{\boldsymbol{h}}_r(\boldsymbol{v}_1, \cdots, \boldsymbol{v}_r) & \cdots & \frac{\partial}{\partial \boldsymbol{v}_r^T}\tilde{\boldsymbol{h}}_r(\boldsymbol{v}_1, \cdots, \boldsymbol{v}_r) \end{pmatrix}. \tag{25}$$

We define each block of the derivative matrix (25) at the equilibrium point as

$$\begin{aligned} \boldsymbol{H}_{pq} &= \left(\boldsymbol{H}(\boldsymbol{u})\right)_{pq} \\ &= \left.\frac{\partial \tilde{\boldsymbol{h}}_p(\boldsymbol{v}_1, \cdots, \boldsymbol{v}_p)}{\partial \boldsymbol{v}_q^T}\right|_{\boldsymbol{v}=\boldsymbol{u}} \quad (p, q = 1, \cdots, r). \end{aligned} \tag{26}$$

After some calculations, each block of the derivative matrix is obtained as

$$\boldsymbol{H}_{pq} = \begin{cases} \sum\limits_{j=p+1}^{n} (-\lambda_j + \lambda_p)\boldsymbol{u}_j\boldsymbol{u}_j^T - 2\lambda_p\boldsymbol{u}_p\boldsymbol{u}_p^T & (p = q) \\ (\lambda_p - \lambda_q)\boldsymbol{u}_q\boldsymbol{u}_p^T & (p > q) \\ \boldsymbol{0} & (p < q). \end{cases} \tag{27}$$

The details of the derivation of (27) are in Appendix C. Also, $\boldsymbol{S}(\boldsymbol{u})$ corresponding to (45) in A is calculated as

$$\begin{aligned} \boldsymbol{S}_{pq} &= \left(\boldsymbol{S}(\boldsymbol{v})\right)_{pq} \equiv E[\boldsymbol{h}_p(\boldsymbol{u}_1, \cdots, \boldsymbol{u}_p, \boldsymbol{x}_p(0))\boldsymbol{h}_q^T(\boldsymbol{u}_1, \cdots, \boldsymbol{u}_q, \boldsymbol{x}_q(0))] \\ &= \begin{cases} \lambda_p\boldsymbol{C} - \lambda_p^2\boldsymbol{u}_p\boldsymbol{u}_p^T & (p = q) \\ -\lambda_p\lambda_q\boldsymbol{u}_q\boldsymbol{u}_p^T & (p \neq q). \end{cases} \end{aligned} \tag{28}$$

The details of the derivation of (28) are in D.

4 Calculation of the Estimation Error Covariance Matrix

From Appendix A, the covariance matrix $\boldsymbol{D}$ is given by solving the Lyapunov equation

$$\boldsymbol{H}(\boldsymbol{u})\boldsymbol{D} + \boldsymbol{D}\boldsymbol{H}^T(\boldsymbol{u}) = -\boldsymbol{S}(\boldsymbol{u}) \tag{29}$$

Let the (i, j)th block of $\boldsymbol{D}$ be denoted by $\boldsymbol{D}_{ij}$ $(i, j = 1, \cdots, r)$. Since from (27), $\boldsymbol{H}(\boldsymbol{u})$ is a block lower triangular matrix, (29) can be rewritten in the following Lyapunov equation about $\boldsymbol{D}_{pq}$

$$\begin{aligned}\boldsymbol{H}_{pp}\boldsymbol{D}_{pq}+\boldsymbol{D}_{pq}\boldsymbol{H}_{qq}^T &= -\sum_{i=1}^{p-1}\boldsymbol{H}_{pi}\boldsymbol{D}_{iq}-\sum_{k=1}^{q-1}\boldsymbol{D}_{pk}\boldsymbol{H}_{qk}^T-\boldsymbol{S}_{pq} \\ &\equiv -\tilde{\boldsymbol{S}}_{pq}\end{aligned} \tag{30}$$

for $q=1,\cdots,p$; $p=1,\cdots,r$. Thus we can obtain $\boldsymbol{D}_{11},\boldsymbol{D}_{21},\boldsymbol{D}_{22},\cdots,\boldsymbol{D}_{r1},\cdots,\boldsymbol{D}_{rr}$ in this order, since $\tilde{\boldsymbol{S}}_{pq}$ in the right hand side of (30) is already given when we solve (30) about $\boldsymbol{D}_{pq}$.

Applying the vec operation which transforms a matrix into a column vector to (30), we have

$$\boldsymbol{\Phi}_{pq}\mathrm{vec}\ \boldsymbol{D}_{pq}=-\mathrm{vec}\ \tilde{\boldsymbol{S}}_{pq} \tag{31}$$

where

$$\boldsymbol{\Phi}_{pq}=\boldsymbol{I}\otimes\boldsymbol{H}_{pp}+\boldsymbol{H}_{qq}\otimes\boldsymbol{I} \tag{32}$$

and $\otimes$ denotes the Kronecker product. In (31) we use the identity

$$\mathrm{vec}\ (\boldsymbol{ABC})=(\boldsymbol{C}^T\otimes\boldsymbol{A})\mathrm{vec}\ \boldsymbol{B} \tag{33}$$

in [11]. From (27) the eigenvectors of $\boldsymbol{H}_{pp}$ are $\boldsymbol{u}_1,\boldsymbol{u}_2,\cdots,\boldsymbol{u}_n$ with the corresponding nonpositive eigenvalues μ_i^p $(i=1,\cdots,n)$ as

$$\mu_i^p=\begin{cases}0 & (i=1,\cdots,p-1)\\ -2\lambda_p & (i=p)\\ -\lambda_i+\lambda_p & (i=p+1,\cdots,n)\end{cases} \tag{34}$$

Since the eigenvalues of $\boldsymbol{\Phi}_{pq}$ are $\mu_i^p+\mu_j^q$ with the corresponding eigenvectors $\boldsymbol{u}_j\otimes\boldsymbol{u}_i$ $(i,j=1,\cdots,n)$, from (34) we note that $\mu_i^p+\mu_j^q=0$ for $i=1,\cdots,p-1$, and $j=1,\cdots,q-1$ so that the null space $\mathcal{N}(\boldsymbol{\Phi}_{pq})$ is spanned by $\boldsymbol{u}_j\otimes\boldsymbol{u}_i$ $(i=1,\cdots,p-1;j=1,\cdots,q-1)$. Let one particular solution of (31) be vec $\boldsymbol{D}_{pq}^0$. Then using (32), any solution of (30) can be expressed as

$$\boldsymbol{D}_{pq}=\boldsymbol{D}_{pq}^0+\sum_{i=1}^{p-1}\sum_{j=1}^{q-1}\alpha_{ij}^{pq}\boldsymbol{u}_i\boldsymbol{u}_j^T. \tag{35}$$

Using this expression for $\boldsymbol{D}_{iq}$ $(i=1,\cdots,p-1)$, $\boldsymbol{D}_{pk}$ $(k=1,\cdots,q-1)$ and substituting these into the right hand side of (30),we note that the indeterminate term in (35) does not contribute to $\tilde{\boldsymbol{S}}_{pq}$ in (30), since, for example, from (27)

$$\sum_{i=1}^{p-1}(\lambda_p-\lambda_i)\boldsymbol{u}_i\boldsymbol{u}_p^T\sum_{l=1}^{i-1}\sum_{j=1}^{p-1}\alpha_{lj}^{ip}\boldsymbol{u}_l\boldsymbol{u}_j^T=\mathbf{O}$$

and similarly for the other terms.

Next we prove by mathematical induction that a particular solution $\boldsymbol{D}^0_{pq}$ is given by

$$\boldsymbol{D}^0_{pq} = \begin{cases} \dfrac{1}{2}\displaystyle\sum_{j=p+1}^{n} \frac{\lambda_j \lambda_p}{\lambda_j - \lambda_p}\boldsymbol{u}_j\boldsymbol{u}_j^T & (p = q) \\ -\dfrac{1}{2}\dfrac{\lambda_p\lambda_q}{\lambda_p - \lambda_q}\boldsymbol{u}_q\boldsymbol{u}_p^T & (p > q) \\ \dfrac{1}{2}\dfrac{\lambda_p\lambda_q}{\lambda_p - \lambda_q}\boldsymbol{u}_q\boldsymbol{u}_p^T & (p < q). \end{cases} \tag{36}$$

Obviously from (17), (36) is true for $p = 1$. Assume that $\boldsymbol{D}^0_{21}, \boldsymbol{D}^0_{22}, \cdots, \boldsymbol{D}^0_{p1} \cdots, \boldsymbol{D}^0_{p\ q-1}$ are given by (36). Then $\tilde{\boldsymbol{S}}_{pq}$ in (30) for $p > q$ is given by

$$\begin{aligned} \tilde{\boldsymbol{S}}_{pq} &= \sum_{i=1}^{q-1}(\lambda_p - \lambda_i)\boldsymbol{u}_i\boldsymbol{u}_p^T\boldsymbol{D}^0_{iq} + (\lambda_p - \lambda_q)\boldsymbol{u}_q\boldsymbol{u}_p^T\boldsymbol{D}^0_{q,q} \\ &+ \sum_{i=q+1}^{p-1}(\lambda_p - \lambda_i)\boldsymbol{u}_i\boldsymbol{u}_p^T\boldsymbol{D}^0_{iq} + \sum_{k=1}^{q-1}\boldsymbol{D}^0_{pk}(\lambda_q - \lambda_k)\boldsymbol{u}_k\boldsymbol{u}_k^T \\ &+ \boldsymbol{S}_{pq} = 0 + \frac{1}{2}\lambda_p\lambda_q\boldsymbol{u}_q\boldsymbol{u}_p^T + 0 + 0 - \lambda_p\lambda_q\boldsymbol{u}_q\boldsymbol{u}_p^T \\ &= -\frac{1}{2}\lambda_p\lambda_q\boldsymbol{u}_q\boldsymbol{u}_p^T. \end{aligned}$$

For $q = p$, from (28) we have

$$\begin{aligned} \tilde{\boldsymbol{S}}_{pp} &= -\lambda_p\sum_{k=1}^{p-1}\lambda_k\boldsymbol{u}_k\boldsymbol{u}_k^T + \lambda_p\boldsymbol{C} - \lambda_p^2\boldsymbol{u}_p\boldsymbol{u}_p^T \\ &= \lambda_p\sum_{k=p+1}^{n}\lambda_k\boldsymbol{u}_k\boldsymbol{u}_k^T \end{aligned}$$

Hence it is easily checked that $\boldsymbol{D}^0_{pq}$ and $\boldsymbol{D}^0_{pp}$ in (36) satisfy the Lyapunov equation $\boldsymbol{H}_{pp}\boldsymbol{D}_{pq} + \boldsymbol{D}_{pq}\boldsymbol{H}^T_{qq} = -\tilde{\boldsymbol{S}}_{pq}$ in (30) for $p > q$ and $p = q$, respectively.

Finally we find the coefficients α^{pq}_{ij} of the indeterminate term in (35) by using the orthogonality constraints between the extracted minor component vectors $\boldsymbol{v}_1(k), \cdots, \boldsymbol{v}_r(k)$, that is,

$$\boldsymbol{v}_m^T(k)\boldsymbol{v}_p(k) = 0 \quad (m = 1, \cdots, p-1; p = 2, \cdots, r) \tag{37}$$

Let the estimation errors be $\Delta\boldsymbol{v}_i(k) = \boldsymbol{v}_i(k) - \boldsymbol{u}_i (i = 1, \cdots, r)$.Then from (37) we have the constraint

$$\boldsymbol{u}_m^T\Delta\boldsymbol{v}_p(k) + \boldsymbol{u}_p^T\Delta\boldsymbol{v}_m(k) \approx 0 \tag{38}$$

where the second order terms about the estimation errors are discarded because these are of order μ where $\Delta\boldsymbol{v}_i(k)$ is of order $\mu^{1/2}$. Multiplying $\Delta\boldsymbol{v}_q^T(k)$ to (38) from the right and taking the expectation, we have

$$\boldsymbol{u}_m^T \boldsymbol{D}_{pq} + \boldsymbol{u}_p^T \boldsymbol{D}_{mq} = \boldsymbol{0}^T \ (m = 1, \cdots, p-1). \tag{39}$$

But from (35) and (36),we have

$$\begin{aligned} \boldsymbol{u}_m^T \boldsymbol{D}_{pq} &= -\frac{1}{2}\frac{\lambda_p \lambda_q}{\lambda_p - \lambda_q}\delta_{mq}\boldsymbol{u}_p^T + \sum_{i=1}^{p-1}\sum_{j=1}^{q-1}\alpha_{ij}^{pq}\delta_{mi}\boldsymbol{u}_j^T \\ \boldsymbol{u}_p^T \boldsymbol{D}_{mq} &= \frac{1}{2}\frac{\lambda_p \lambda_q}{\lambda_p - \lambda_q}\boldsymbol{u}_p^T \delta_{mq}. \end{aligned}$$

Hence from (39)

$$\sum_{j=1}^{q-1} \alpha_{mj}^{pq} \boldsymbol{u}_j^T = \boldsymbol{0}^T \Rightarrow \alpha_{mj}^{pq} = \boldsymbol{0} \ (m = 1, \cdots, p-1; j = 1, \cdots, q-1).$$

This means that the indeterminate term in $\boldsymbol{D}_{pq}$ is actually zero. For $p = q$, from (35) and (36), we have

$$\boldsymbol{u}_m^T \boldsymbol{D}_{pq} = \sum_{i=1}^{p-1}\sum_{j=1}^{q-1}\alpha_{ij}^{pp}\delta_{mi}\boldsymbol{u}_j^T, \ \boldsymbol{u}_p^T \boldsymbol{D}_{mp} = \frac{1}{2}\frac{\lambda_m \lambda_p}{\lambda_m - \lambda_p}\boldsymbol{u}_m^T.$$

Hence

$$\begin{aligned} &\frac{1}{2}\frac{\lambda_m \lambda_p}{\lambda_m - \lambda_p}\boldsymbol{u}_m^T + \sum_{j=1}^{p-1}\alpha_{mj}^{pp}\boldsymbol{u}_j^T = \boldsymbol{0}^T \\ &\Longrightarrow \alpha_{mm}^{pp} = \frac{1}{2}\frac{\lambda_m \lambda_p}{\lambda_p - \lambda_m}, \ \alpha_{mj}^{pp} = 0 \ (j \neq m) \end{aligned}$$

Thus the final expression for $\boldsymbol{D}_{pq}$ is given by

$$\boldsymbol{D}_{pq} = \begin{cases} \frac{1}{2}\sum_{j=1, j\neq p}^{n} \frac{\lambda_j \lambda_p}{|\lambda_j - \lambda_p|}\boldsymbol{u}_j \boldsymbol{u}_j^T & (p = q) \\ -\frac{1}{2}\frac{\lambda_p \lambda_q}{\lambda_p - \lambda_q}\boldsymbol{u}_q \boldsymbol{u}_p^T & (p > q) \\ \frac{1}{2}\frac{\lambda_p \lambda_q}{\lambda_p - \lambda_q}\boldsymbol{u}_q \boldsymbol{u}_p^T & (p < q). \end{cases} \tag{40}$$

From (40) we note that all the "auto"-covariance matrices $\boldsymbol{D}_{pp}$ have similar expressions and there remain a "weak" correlation between each pair of the extracted minor components.

5 Simulation Results

The covariances of the eigenvectors estimated by the algorithm (9) - (13) and are compared with the theoretical result . In this simulation, we test the case for $r = 3$, that is, consider for the algorithm extracting the first, the second and the third minor components. The input signal vector with zero mean and covariance matrix $\boldsymbol{C} = \mathrm{diag}[0.9,\ 0.8,\ \cdots\ 0.1,\ 0.01]$ is used. The adaptive gain μ is set to 0.001. The variance of each element of the eigenvectors corresponding to the first, the second and the third eigenvalues at $k = 100000$ are estimated from 30 trial sets. These result are listed in Table 3. These simulation results are roughly close to the theoretical values. This implies that the analysis with ODE approach gives a reasonable result.

	$\boldsymbol{u}_1$		$\boldsymbol{u}_2$		$\boldsymbol{u}_3$	
	simulation	theoretical	simulation	theoretical	simulation	theoretical
10	4.370×10^{-3}	5.056×10^{-3}	5.776×10^{-2}	5.625×10^{-2}	1.367×10^{-1}	1.286×10^{-1}
9	3.715×10^{-3}	5.063×10^{-3}	5.244×10^{-2}	5.714×10^{-2}	1.422×10^{-1}	1.333×10^{-1}
8	4.089×10^{-3}	5.725×10^{-3}	4.094×10^{-2}	5.833×10^{-2}	1.129×10^{-1}	1.400×10^{-1}
7	5.743×10^{-3}	5.085×10^{-3}	7.324×10^{-2}	6.000×10^{-2}	1.149×10^{-1}	1.500×10^{-1}
6	5.762×10^{-3}	5.102×10^{-3}	6.904×10^{-2}	6.250×10^{-2}	1.756×10^{-1}	1.667×10^{-1}
5	6.097×10^{-3}	5.128×10^{-3}	7.442×10^{-2}	6.667×10^{-2}	1.620×10^{-1}	2.000×10^{-1}
4	4.424×10^{-3}	5.172×10^{-3}	7.505×10^{-2}	7.500×10^{-2}	2.546×10^{-1}	3.000×10^{-1}
3	7.398×10^{-3}	5.263×10^{-3}	1.088×10^{-1}	1.000×10^{-1}	2.660×10^{-4}	0
2	5.039×10^{-3}	5.556×10^{-3}	6.956×10^{-4}	0	1.075×10^{-1}	1.000×10^{-1}
1	1.199×10^{-3}	0	4.921×10^{-3}	5.556×10^{-3}	7.291×10^{-3}	5.263×10^{-3}

Table 3: The estimated and theoretical variances of the eigenvectors by using the deflation technique. The adaptive gain is $\mu = 0.001$. The iteration number is 100000.

6 Conclusion

In this paper, we derive the asymptotic distributions of the multiple minor components extraction algorithm which is based on the algorithm proposed by Douglas et al. with the ODE method. By the computer simulations, we show that the asymptotic distributions derived by our calculation are close to the theoretical value.

Appendix

A The ODE Method

The general form of an adaptive algorithm is represented as

$$\boldsymbol{\theta}(k) = \boldsymbol{\theta}(k-1) + \mu(k)\boldsymbol{h}(\boldsymbol{\theta}(k-1), \boldsymbol{x}(k)) \tag{41}$$

where $\boldsymbol{\theta}(k)$ is a parameter vector to be recursively updated, $\boldsymbol{x}(k)$ is a stationary random input vector representing on-line observations of the system and $\mu(k)$ is a small scalar gain sequence. The ODE associated with this algorithm is introduced as follows:

$$\frac{\mathrm{d}\boldsymbol{\theta}(t)}{\mathrm{d}t} = \boldsymbol{h}(\boldsymbol{\theta}(t)) \tag{42}$$

with

$$\tilde{\boldsymbol{h}}(\boldsymbol{\theta}) = \mathrm{E}\left[\boldsymbol{h}(\boldsymbol{\theta}, \boldsymbol{x}(k))\right]. \tag{43}$$

We further define the derivative matrix

$$\boldsymbol{H}(\boldsymbol{\theta}) = \frac{\partial \tilde{\boldsymbol{h}}(\boldsymbol{\theta})}{\partial \boldsymbol{\theta}^T}. \tag{44}$$

Suppose the constant gain case $\mu(k) = \mu$. The following properties have been proved in [8] under some regularity assumptions. Assume that $\boldsymbol{\theta}(t) \rightarrow \boldsymbol{\theta}_*(t \rightarrow \infty)$ as then we can say that $\boldsymbol{\theta}(k) \rightarrow \boldsymbol{\theta}_*(k \rightarrow \infty), \mu \rightarrow 0$ with probability one. Also,if all the eigenvalues of $\boldsymbol{H}(\boldsymbol{\theta}_*)$ have negative real parts and if the matrix

$$\boldsymbol{S}(\boldsymbol{\theta}) = \sum_{k=-\infty}^{\infty} \mathrm{E}\left[\boldsymbol{h}(\boldsymbol{\theta}, \boldsymbol{x}(k))\boldsymbol{h}^T(\boldsymbol{\theta}, \boldsymbol{x}(0))\right] \tag{45}$$

exists, $\mu^{-1/2}[\boldsymbol{\theta}(k) - \boldsymbol{\theta}_*]$ converges asymptotically $(k \rightarrow \infty, \mu \rightarrow 0)$ to a zero mean normal distributed random vector weakly (in probability) with the covariance matrix which is the solution of the Lyapunov equation

$$\boldsymbol{H}(\boldsymbol{\theta}_*)\boldsymbol{D} + \boldsymbol{D}\boldsymbol{H}^T(\boldsymbol{\theta}_*) = -\boldsymbol{S}(\boldsymbol{\theta}_*). \tag{46}$$

B Derivation of (19)

From (12)

$$\boldsymbol{v}_i(k) = \boldsymbol{\psi}_i(k) - \frac{\boldsymbol{v}_1(k)\boldsymbol{v}_1^T(k)}{\|\boldsymbol{v}_1(k)\|^2}\boldsymbol{\psi}_i(k) - \sum_{j=2}^{i-1} \frac{\boldsymbol{v}_j(k)\boldsymbol{v}_j^T(k)}{\|\boldsymbol{v}_j(k)\|^2}\boldsymbol{\psi}_i(k). \tag{47}$$

Here we consider the third term of (47). Using (12) we have

$$\begin{aligned}
&\sum_{j=2}^{i-1} \frac{\boldsymbol{v}_j(k)\boldsymbol{v}_j^T(k)}{\|\boldsymbol{v}_j(k)\|^2}\boldsymbol{\psi}_i(k) \\
&= \sum_{j=2}^{i-1} \frac{1}{\|\boldsymbol{v}_j(k)\|^2}\Bigg[\boldsymbol{\psi}_j(k)\boldsymbol{\psi}_j^T(k)\boldsymbol{\psi}_i(k) - \sum_{l=1}^{j-1} \frac{\boldsymbol{v}_l(k)\boldsymbol{v}_l^T(k)}{\|\boldsymbol{v}_l(k)\|^2}\boldsymbol{\psi}_j(k)\boldsymbol{\psi}_j^T(k)\boldsymbol{\psi}_i(k) \\
&\quad - \boldsymbol{\psi}_j(k)\boldsymbol{\psi}_j^T(k)\sum_{l=1}^{j-1} \frac{\boldsymbol{v}_l(k)\boldsymbol{v}_l^T(k)}{\|\boldsymbol{v}_l(k)\|^2}\boldsymbol{\psi}_i(k) + \sum_{l=1}^{j-1} \frac{\boldsymbol{v}_l(k)\boldsymbol{v}_l^T(k)}{\|\boldsymbol{v}_l(k)\|^2}\boldsymbol{\psi}_j(k)\boldsymbol{\psi}_j^T(k)\sum_{l=1}^{j-1} \frac{\boldsymbol{v}_l(k)\boldsymbol{v}_l^T(k)}{\|\boldsymbol{v}_l(k)\|^2}\boldsymbol{\psi}_i(k)\Bigg].
\end{aligned} \tag{48}$$

First we calculate the quantity $\boldsymbol{v}_l^T \boldsymbol{A}_l \boldsymbol{v}_j$ $(1 \le l < j)$ where we define

$$\begin{aligned}
\boldsymbol{A}_1 &= \|\boldsymbol{v}_1\|^4 \boldsymbol{C} - \boldsymbol{I}\Big(\boldsymbol{v}_1^T \boldsymbol{C} \boldsymbol{v}_1\Big) \\
\boldsymbol{A}_l &= \|\boldsymbol{v}_l\|^4 \Big(\boldsymbol{I} - \sum_{m=1}^{l-1} \boldsymbol{v}_m \boldsymbol{v}_m^T\Big) \boldsymbol{C} \Big(\boldsymbol{I} - \sum_{m=1}^{l-1} \boldsymbol{v}_m \boldsymbol{v}_m^T\Big) \\
&\quad - \boldsymbol{I}\Big[\boldsymbol{v}_l^T \Big(\boldsymbol{I} - \sum_{m=1}^{l-1} \boldsymbol{v}_m \boldsymbol{v}_m^T\Big) \boldsymbol{C} \Big(\boldsymbol{I} - \sum_{m=1}^{l-1} \boldsymbol{v}_m \boldsymbol{v}_m^T\Big) \boldsymbol{v}_l\Big].
\end{aligned}$$

Then we have

$$\begin{aligned}
\boldsymbol{v}_l^T \boldsymbol{A}_l \boldsymbol{v}_j = \|\boldsymbol{v}_l\|^4 \Big[&\boldsymbol{v}_l^T \boldsymbol{C} \boldsymbol{v}_j - \boldsymbol{v}_l^T \sum_{m=1}^{l-1} \boldsymbol{v}_m \boldsymbol{v}_m^T \boldsymbol{C} \boldsymbol{v}_j - \boldsymbol{v}_l^T \boldsymbol{C} \sum_{m=1}^{l-1} \boldsymbol{v}_m \boldsymbol{v}_m^T \boldsymbol{v}_j \\
&+ \boldsymbol{v}_l^T \sum_{m=1}^{l-1} \boldsymbol{v}_m \boldsymbol{v}_m^T \boldsymbol{C} \sum_{m=1}^{l-1} \boldsymbol{v}_m \boldsymbol{v}_m^T \boldsymbol{v}_j\Big] - \boldsymbol{I}\Big[\boldsymbol{v}_l^T \Big(\boldsymbol{I} - \sum_{m=1}^{l-1} \boldsymbol{v}_m \boldsymbol{v}_m^T\Big) \boldsymbol{C} \Big(\boldsymbol{I} - \sum_{m=1}^{l-1} \boldsymbol{v}_m \boldsymbol{v}_m^T\Big) \boldsymbol{v}_l\Big] \boldsymbol{v}_l^T \boldsymbol{v}_j.
\end{aligned}$$

Hence, $\boldsymbol{v}_l^T \boldsymbol{A}_l \boldsymbol{v}_j$ and $\boldsymbol{v}_l^T \boldsymbol{A}_j \boldsymbol{v}_j$ become zero for $l < j$ at the equilibrium point . Using these results at the equilibrium point, we have

$$\begin{aligned}
\boldsymbol{v}_1^T(k) \boldsymbol{\psi}_j(k) &= \Big(\boldsymbol{v}_1(k-1) - \mu \boldsymbol{A}_1(k) \boldsymbol{v}_1(k-1)\Big)^T \Big(\boldsymbol{v}_j(k-1) - \mu \boldsymbol{A}_j(k) \boldsymbol{v}_j(k-1)\Big) \\
&\approx \boldsymbol{v}_1^T(k-1) \boldsymbol{v}_j(k-1) \\
&\quad - \mu\Big(\boldsymbol{v}_1^T(k-1) \boldsymbol{A}_1(k) \boldsymbol{v}_j(k-1) + \boldsymbol{v}_1^T(k-1) \boldsymbol{A}_j(k) \boldsymbol{v}_j(k-1)\Big) \\
&\to \boldsymbol{u}_1^T \boldsymbol{u}_j - \mu\Big(\boldsymbol{u}_1^T \boldsymbol{A}_1 \boldsymbol{u}_j + \boldsymbol{u}_1^T \boldsymbol{A}_j \boldsymbol{u}_j\Big) = 0 \qquad (2 \le j)
\end{aligned} \tag{49}$$

where in the second line we discard the term of order μ^2. We can generalize these results as

$$\begin{aligned}
\boldsymbol{v}_l^T(k) \boldsymbol{\psi}_j(k) &= \boldsymbol{\psi}_l^T(k) \left(\boldsymbol{I} - \sum_{m=1}^{l-1} \frac{\boldsymbol{v}_m(k) \boldsymbol{v}_m^T(k)}{\|\boldsymbol{v}_m(k)\|^2}\right) \boldsymbol{\psi}_j(k) \\
&= \boldsymbol{\psi}_l^T(k) \boldsymbol{\psi}_j(k) - \boldsymbol{\psi}_l^T(k) \sum_{m=1}^{l-1} \frac{\boldsymbol{v}_m(k) \boldsymbol{v}_m^T(k)}{\|\boldsymbol{v}_m(k)\|^2} \boldsymbol{\psi}_j(k) \\
&\approx \boldsymbol{\psi}_l^T(k) \boldsymbol{\psi}_j(k) \\
&\approx \boldsymbol{v}_l^T(k-1) \boldsymbol{v}_j(k-1) - \mu\Big(\boldsymbol{v}_l^T(k-1) \boldsymbol{A}_l(k) \boldsymbol{v}_j(k-1) \\
&+ \boldsymbol{v}_l^T(k-1) \boldsymbol{A}_j(k) \boldsymbol{v}_j(k-1)\Big) \\
&\to \boldsymbol{u}_l^T \boldsymbol{u}_j - \mu\Big(\boldsymbol{u}_l^T \boldsymbol{A}_l \boldsymbol{u}_j + \boldsymbol{u}_l^T \boldsymbol{A}_j \boldsymbol{u}_j\Big) = 0 \quad (l < j).
\end{aligned} \tag{50}$$

In (50) the product of $\boldsymbol{\psi}_l^T(k) \boldsymbol{v}_m(k)$ and $\boldsymbol{v}_m^T(k) \boldsymbol{\psi}_j(k)$ appears and from (49) these two terms are zero at the equilibrium point, so that in computing the derivative matrix $\boldsymbol{H}(\boldsymbol{v})$ the derivative of this product is also zero at the equilibrium point. Hence we can discard this product. Also,

$$\begin{aligned}
&\boldsymbol{\psi}_j^T(k) \boldsymbol{\psi}_i(k) \Big(\boldsymbol{v}_j(k-1) - \mu \boldsymbol{A}_j(k) \boldsymbol{v}_j(k-1)\Big)^T \Big(\boldsymbol{v}_i(k-1) - \mu \boldsymbol{A}_i(k) \boldsymbol{v}_i(k-1)\Big) \\
&\to \boldsymbol{u}_j^T \boldsymbol{u}_i - \mu\Big(\boldsymbol{u}_j^T \boldsymbol{A}_j \boldsymbol{u}_i + \boldsymbol{u}_j^T \boldsymbol{A}_i \boldsymbol{u}_i\Big) = 0 \quad (j < i).
\end{aligned}$$

Using these results and the following approximation,

$$\boldsymbol{v}_l^T(k)\boldsymbol{\psi}_j(k)\boldsymbol{\psi}_j^T(k)\boldsymbol{\psi}_i(k) \approx 0, \boldsymbol{\psi}_j^T(k)\boldsymbol{v}_l(k)\boldsymbol{v}_l^T(k)\boldsymbol{\psi}_j(k) \approx 0, \tag{51}$$

we simplify (48). As stated before, these approximations have no effect on calculating $\boldsymbol{H}(\boldsymbol{u})$. Using these approximations, only the first term in (48) remains, and we simplify (48) as

$$\sum_{j=2}^{i-1} \frac{\boldsymbol{v}_j(k)\boldsymbol{v}_j^T(k)}{\|\boldsymbol{v}_j(k)\|^2}\boldsymbol{\psi}_i(k) \approx \sum_{j=2}^{i-1} \frac{\boldsymbol{\psi}_j(k)\boldsymbol{\psi}_j^T(k)\boldsymbol{\psi}_i(k)}{\|\boldsymbol{v}_j(k)\|^2}. \tag{52}$$

Also, the following simplification is obtained.

$$\frac{1}{\|\boldsymbol{v}_j(k)\|^2} \approx \frac{1}{\|\boldsymbol{\psi}_j(k)\|^2}, \tag{53}$$

since

$$\begin{aligned}
&\|\boldsymbol{\psi}_j(k) - \sum_{l=1}^{j-1} \frac{\boldsymbol{v}_l(k)\boldsymbol{v}_l^T(k)}{\|\boldsymbol{v}_l(k)\|^2}\boldsymbol{\psi}_j(k)\|^2 = \|\boldsymbol{\psi}_j(k)\|^2 \\
-\ & 2\boldsymbol{\psi}_j^T(k)\sum_{l=1}^{j-1} \frac{\boldsymbol{v}_l(k)\boldsymbol{v}_l^T(k)}{\|\boldsymbol{v}_l(k)\|^2}\boldsymbol{\psi}_j(k) + \|\sum_{l=1}^{j-1} \frac{\boldsymbol{v}_l(k)\boldsymbol{v}_l^T(k)}{\|\boldsymbol{v}_l(k)\|^2}\boldsymbol{\psi}_j(k)\|^2 \\
\approx\ & \|\boldsymbol{\psi}_j(k)\|^2
\end{aligned}$$

where again we use (51). From (52) and (53), we simplify (47) with $\boldsymbol{v}_1(k) = \boldsymbol{\psi}_1(k)$ as follows.

$$\begin{aligned}
&\boldsymbol{v}_i(k) \approx \boldsymbol{\psi}_i(k) - \sum_{j=1}^{i-1} \frac{\boldsymbol{\psi}_j(k)\boldsymbol{\psi}_j^T(k)}{\|\boldsymbol{\psi}_j(k)\|^2}\boldsymbol{\psi}_i(k) \qquad (54)\\
&= \boldsymbol{v}_i - \mu\boldsymbol{A}_i\boldsymbol{v}_i - \sum_{j=1}^{i-1} \frac{(\boldsymbol{v}_j - \mu\boldsymbol{A}_j\boldsymbol{v}_j)(\boldsymbol{v}_j - \mu\boldsymbol{A}_j\boldsymbol{v}_j)^T}{\|\boldsymbol{v}_j - \mu\boldsymbol{A}_j\boldsymbol{v}_j\|^2}(\boldsymbol{v}_i - \mu\boldsymbol{A}_i\boldsymbol{v}_i) \\
&\approx \boldsymbol{v}_i - \mu\boldsymbol{A}_i\boldsymbol{v}_i - \sum_{j=1}^{i-1} \frac{\boldsymbol{v}_j\boldsymbol{v}_j^T\boldsymbol{v}_i}{\|\boldsymbol{v}_j\|^2 - 2\mu\boldsymbol{v}_j^T\boldsymbol{A}_j\boldsymbol{v}_j} \\
&+\mu\sum_{j=1}^{i-1} \frac{\boldsymbol{A}_j\boldsymbol{v}_j\boldsymbol{v}_j^T\boldsymbol{v}_i + \boldsymbol{v}_j\boldsymbol{v}_j^T\boldsymbol{A}_j\boldsymbol{v}_i}{\|\boldsymbol{v}_j\|^2 - 2\mu\boldsymbol{v}_j^T\boldsymbol{A}_j\boldsymbol{v}_j} + \mu\sum_{j=1}^{i-1} \frac{\boldsymbol{v}_j\boldsymbol{v}_j^T\boldsymbol{A}_i\boldsymbol{v}_i}{\|\boldsymbol{v}_j\|^2 - 2\mu\boldsymbol{v}_j^T\boldsymbol{A}_j\boldsymbol{v}_j} \\
&= \boldsymbol{v}_i + \mu\Big[-\Big(\boldsymbol{I} - \sum_{j=1}^{i-1} \frac{\boldsymbol{v}_j\boldsymbol{v}_j^T}{\|\boldsymbol{v}_j\|^2}\Big)\boldsymbol{A}_i \\
&+\sum_{j=1}^{i-1}\Big(\frac{\boldsymbol{A}_j\boldsymbol{v}_j\boldsymbol{v}_j^T + \boldsymbol{v}_j\boldsymbol{v}_j^T\boldsymbol{A}_j^T}{\|\boldsymbol{v}_j\|^2}\Big) - 2\sum_{j=1}^{i-1}\Big(\frac{\boldsymbol{v}_j^T\boldsymbol{A}_j\boldsymbol{v}_j}{\|\boldsymbol{v}_j\|^4}\Big)\boldsymbol{v}_j\boldsymbol{v}_j^T\Big]\boldsymbol{v}_i
\end{aligned}$$

where from the second line we drop the time index $k-1$ for simplicity. Thus we have shown (19).

C Derivation of (27)

From (22) $\tilde{\boldsymbol{h}}_i(\boldsymbol{v}_1, \cdots, \boldsymbol{v}_i)$ consists of five terms (H1)-(H5). We simplify each term and calculate the corresponding derivative at the equilibrium point. That is,

$$
\begin{aligned}
\text{(H1)} &= \|\boldsymbol{v}_i\|^4\Big(\boldsymbol{I} - \sum_{j=1}^{i-1}\boldsymbol{v}_j\boldsymbol{v}_j^T\Big)\boldsymbol{C}\Big(\boldsymbol{I} - \sum_{j=1}^{i-1}\boldsymbol{v}_j\boldsymbol{v}_j^T\Big)\boldsymbol{v}_i \\
&\quad +(\boldsymbol{v}_i^T\Big(\boldsymbol{I} - \sum_{j=1}^{i-1}\boldsymbol{v}_j\boldsymbol{v}_j^T\Big)\Big(\boldsymbol{I} - \sum_{j=1}^{i-1}\boldsymbol{v}_j\boldsymbol{v}_j^T\Big)\boldsymbol{C}\Big(\boldsymbol{I} - \sum_{j=1}^{i-1}\boldsymbol{v}_j\boldsymbol{v}_j^T\Big)\Big(\boldsymbol{I} - \sum_{j=1}^{i-1}\boldsymbol{v}_j\boldsymbol{v}_j^T\Big)\boldsymbol{v}_i)\boldsymbol{v}_i \\
&\simeq -\|\boldsymbol{v}_i\|^4\Big[\boldsymbol{C}\boldsymbol{v}_i - \boldsymbol{C}\Big(\sum_{j=1}^{i-1}\boldsymbol{v}_j\boldsymbol{v}_j^T\Big)\boldsymbol{v}_i - \Big(\sum_{j=1}^{i-1}\boldsymbol{v}_j\boldsymbol{v}_j^T\Big)\boldsymbol{C}\boldsymbol{v}_i \\
&+ \Big(\sum_{j=1}^{i-1}\boldsymbol{v}_j\boldsymbol{v}_j^T\Big)\boldsymbol{C}\Big(\sum_{j=1}^{i-1}\boldsymbol{v}_j\boldsymbol{v}_j^T\Big)\boldsymbol{v}_i\Big] + \boldsymbol{v}_i^T\boldsymbol{C}\boldsymbol{v}_i\boldsymbol{v}_i
\end{aligned}
$$

where as above the terms containing $(\boldsymbol{v}_i^T\boldsymbol{v}_j)^2$ $(0 \le j \le i-1)$ are discarded. Then we have

$$
\left.\frac{\partial(\text{H1})}{\partial \boldsymbol{v}_i^T}\right|_{\boldsymbol{v}=\boldsymbol{u}} = -4\lambda_i\boldsymbol{u}_i\boldsymbol{u}_i^T - \boldsymbol{C} + \sum_{j=1}^{i-1}\lambda_j\boldsymbol{u}_j\boldsymbol{u}_j^T + 2\lambda_i\boldsymbol{u}_i\boldsymbol{u}_i^T + \lambda_i\boldsymbol{I}
$$

$$
\left.\frac{\partial(\text{H1})}{\partial \boldsymbol{v}_k^T}\right|_{\boldsymbol{v}=\boldsymbol{u}} = \lambda_i\boldsymbol{u}_k\boldsymbol{u}_i^T \quad (k < i).
$$

Similarly,

$$
\begin{aligned}
\text{(H2)} &\simeq \sum_{j=1}^{i-1}\frac{\boldsymbol{v}_j\boldsymbol{v}_j^T}{\|\boldsymbol{v}_j\|^2}\|\boldsymbol{v}_i\|^4\Big[\boldsymbol{C}\boldsymbol{v}_i - \boldsymbol{C}\Big(\sum_{j=1}^{i-1}\boldsymbol{v}_j\boldsymbol{v}_j^T\Big)\boldsymbol{v}_i - \Big(\sum_{j=1}^{i-1}\boldsymbol{v}_j\boldsymbol{v}_j^T\Big)\boldsymbol{C}\boldsymbol{v}_i \\
&\quad +\Big(\sum_{j=1}^{i-1}\boldsymbol{v}_j\boldsymbol{v}_j^T\Big)\boldsymbol{C}\Big(\sum_{j=1}^{i-1}\boldsymbol{v}_j\boldsymbol{v}_j^T\Big)\boldsymbol{v}_i\Big] - \sum_{j=1}^{i-1}\frac{\boldsymbol{v}_j\boldsymbol{v}_j^T}{\|\boldsymbol{v}_j\|^2}\boldsymbol{v}_i^T\boldsymbol{C}\boldsymbol{v}_i\boldsymbol{v}_i
\end{aligned}
$$

Hence,

$$
\left.\frac{\partial(\text{H2})}{\partial \boldsymbol{v}_i^T}\right|_{\boldsymbol{v}=\boldsymbol{u}} = -\lambda_i\sum_{j=1}^{i-1}\boldsymbol{u}_j\boldsymbol{u}_j^T, \quad \left.\frac{\partial(\text{H2})}{\partial \boldsymbol{v}_i^T}\right|_{\boldsymbol{v}=\boldsymbol{u}} = -\lambda_i\boldsymbol{u}_k\boldsymbol{u}_i^T \quad (k < i)
$$

Also

$$
\begin{aligned}
\text{(H3)} &= \sum_{j=1}^{i-1}\Big[\|\boldsymbol{v}_j\|^2\Big(\boldsymbol{I} - \sum_{l=1}^{j-1}\boldsymbol{v}_l\boldsymbol{v}_l^T\Big)\boldsymbol{C}\Big(\boldsymbol{I} - \sum_{l=1}^{j-1}\boldsymbol{v}_l\boldsymbol{v}_l^T\Big)\boldsymbol{v}_j\boldsymbol{v}_j^T\boldsymbol{v}_i \\
&\quad - \frac{\boldsymbol{v}_j^T\Big(\boldsymbol{I} - \sum_{l=1}^{j-1}\boldsymbol{v}_l\boldsymbol{v}_l^T\Big)\boldsymbol{C}\Big(\boldsymbol{I} - \sum_{l=1}^{j-1}\boldsymbol{v}_l\boldsymbol{v}_l^T\Big)\boldsymbol{v}_j\boldsymbol{v}_j\boldsymbol{v}_j^T\boldsymbol{v}_i}{\|\boldsymbol{v}_j\|^2}\Big] \\
&\simeq \sum_{j=1}^{i-1}\Big[\|\boldsymbol{v}_j\|^2\boldsymbol{C}\boldsymbol{v}_j\boldsymbol{v}_j^T\boldsymbol{v}_i - \frac{1}{\|\boldsymbol{v}_j\|^2}\boldsymbol{v}_j^T\boldsymbol{C}\boldsymbol{v}_j\boldsymbol{v}_j\boldsymbol{v}_j^T\boldsymbol{v}_i\Big] \\
\text{(H4)} &\simeq \sum_{j=1}^{i-1}\Big[\|\boldsymbol{v}_j\|^2\boldsymbol{v}_j\boldsymbol{v}_j^T\boldsymbol{C}\boldsymbol{v}_i - \frac{1}{\|\boldsymbol{v}_j\|^2}\boldsymbol{v}_j^T\boldsymbol{C}\boldsymbol{v}_j\boldsymbol{v}_j\boldsymbol{v}_j^T\boldsymbol{v}_i\Big]
\end{aligned}
$$

Hence,

$$\left.\frac{\partial(\mathrm{H3})}{\partial \boldsymbol{v}_i^T}\right|_{\boldsymbol{v}=\boldsymbol{u}} = 0, \quad \left.\frac{\partial(\mathrm{H4})}{\partial \boldsymbol{v}_i^T}\right|_{\boldsymbol{v}=\boldsymbol{u}} = 0$$

$$\left.\frac{\partial(\mathrm{H3})}{\partial \boldsymbol{v}_k^T}\right|_{\boldsymbol{v}=\boldsymbol{u}} = 0, \quad \left.\frac{\partial(\mathrm{H4})}{\partial \boldsymbol{v}_k^T}\right|_{\boldsymbol{v}=\boldsymbol{u}} = (\lambda_i - \lambda_k)\boldsymbol{u}_k\boldsymbol{u}_i^T \ (k < i)$$

Finally,

$$(\mathrm{H5}) \simeq -2\sum_{j=1}^{i-1}\left\{\boldsymbol{v}_j^T\boldsymbol{C}\boldsymbol{v}_j\boldsymbol{v}_j\boldsymbol{v}_j^T\boldsymbol{v}_i - \frac{1}{||\boldsymbol{v}_j||^2}\boldsymbol{v}_j^T\boldsymbol{C}\boldsymbol{v}_j\boldsymbol{v}_j^T\boldsymbol{v}_j\boldsymbol{v}_j\boldsymbol{v}_j^T\boldsymbol{v}_i\right\}$$

So

$$\left.\frac{\partial(\mathrm{H5})}{\partial \boldsymbol{v}_i^T}\right|_{\boldsymbol{v}=\boldsymbol{u}} = 0, \quad \left.\frac{\partial(\mathrm{H5})}{\partial \boldsymbol{v}_k^T}\right|_{\boldsymbol{v}=\boldsymbol{u}} = 0 \quad (k < i).$$

Combining the above results,we have

$$\begin{aligned}&\left.\frac{\partial}{\partial \boldsymbol{v}_i^T}\tilde{\boldsymbol{h}}_i(\boldsymbol{v}_1, \cdots, \boldsymbol{v}_i)\right|_{\boldsymbol{v}=\boldsymbol{u}}\\ &= (-\lambda_n + \lambda_i)\boldsymbol{u}_n\boldsymbol{u}_n^T + \cdots + (-\lambda_{i+1} + \lambda_i)\boldsymbol{u}_{i+1}\boldsymbol{u}_{i+1}^T - 2\lambda_i\boldsymbol{u}_i\boldsymbol{u}_i^T\end{aligned}$$

$$\left.\frac{\partial}{\partial \boldsymbol{v}_k^T}\tilde{\boldsymbol{h}}_i(\boldsymbol{v}_1, \cdots, \boldsymbol{v}_i)\right|_{\boldsymbol{v}=\boldsymbol{u}} = (\lambda_i - \lambda_k)\boldsymbol{u}_k\boldsymbol{u}_i^T \quad (k < i)$$

D Derivation of (28)

First from (10) we simplify the expression of each term in (20) at $\boldsymbol{v} = \boldsymbol{u}$. Then we have

$$\begin{aligned}
(\mathrm{S1}) &= -\Big[||\boldsymbol{u}_i||^4\Big(\boldsymbol{I} - \sum_{j=1}^{i-1}\boldsymbol{u}_j\boldsymbol{u}_j^T\Big)\boldsymbol{x}\boldsymbol{x}^T\Big(\boldsymbol{I} - \sum_{j=1}^{i-1}\boldsymbol{u}_j\boldsymbol{u}_j^T\Big) - \boldsymbol{I}\Big(\boldsymbol{u}_i^T(\boldsymbol{I} - \sum_{j=1}^{i-1}\boldsymbol{u}_j\boldsymbol{u}_j^T)\boldsymbol{x}\Big)^2\Big]\boldsymbol{u}_i\\
&= -\boldsymbol{x}\boldsymbol{x}^T\boldsymbol{u}_i + \Big(\sum_{j=1}^{i-1}\boldsymbol{u}_j\boldsymbol{u}_j^T\Big)\boldsymbol{x}\boldsymbol{x}^T\boldsymbol{u}_i + \Big(\boldsymbol{u}_i^T\boldsymbol{x}\Big)^2\boldsymbol{u}_i,\\
(\mathrm{S2}) &= \Big(\sum_{j=1}^{i-1}\boldsymbol{u}_j\boldsymbol{u}_j^T\Big)\Big(\boldsymbol{I} - \sum_{l=1}^{i-1}\boldsymbol{u}_l\boldsymbol{u}_l^T\Big)\boldsymbol{x}\boldsymbol{x}^T\Big(\boldsymbol{I} - \sum_{l=1}^{i-1}\boldsymbol{u}_l\boldsymbol{u}_l^T\Big)\boldsymbol{u}_i = 0,\\
(\mathrm{S4}) &= \sum_{j=1}^{i-1}\frac{\boldsymbol{u}_j\boldsymbol{u}_j^T\Big[||\boldsymbol{u}_j||^4\boldsymbol{x}_j\boldsymbol{x}_j^T - \boldsymbol{I}(\boldsymbol{u}_j^T\boldsymbol{x}_j)^2\Big]}{||\boldsymbol{u}_j||^2}\boldsymbol{u}_i = \sum_{j=1}^{i-1}\boldsymbol{u}_j\boldsymbol{u}_j^T\boldsymbol{x}\boldsymbol{x}^T\boldsymbol{u}_i,\\
(\mathrm{S3}) &= 0, \qquad (\mathrm{S5}) = 0.
\end{aligned}$$

So, (S1) and (S4) remain where $\boldsymbol{x}$ denotes $\boldsymbol{x}(0)$ for simplicity and (S1) + (S4) $\equiv \boldsymbol{L}_i$ becomes

$$\boldsymbol{L}_i = -(\boldsymbol{x}^T\boldsymbol{u}_i)\boldsymbol{x} + 2(\boldsymbol{x}^T\boldsymbol{u}_i)(\sum_{j=1}^{i-1}\boldsymbol{u}_j\boldsymbol{u}_j^T)\boldsymbol{x} + (\boldsymbol{x}^T\boldsymbol{u}_i)^2\boldsymbol{u}_i.$$

Hence,

$$\boldsymbol{L}_p\boldsymbol{L}_q^T = \Big[(\boldsymbol{x}^T\boldsymbol{u}_p)(\boldsymbol{x}^T\boldsymbol{u}_q)\boldsymbol{x}\boldsymbol{x}^T - 2(\boldsymbol{x}^T\boldsymbol{u}_p)(\boldsymbol{x}^T\boldsymbol{u}_q)\boldsymbol{x}\boldsymbol{x}^T(\sum_{k=1}^{q-1}\boldsymbol{u}_k\boldsymbol{u}_k^T)$$

$$-(\boldsymbol{x}^T\boldsymbol{u}_p)(\boldsymbol{x}^T\boldsymbol{u}_q)^2\boldsymbol{x}\boldsymbol{u}_q^T\Big] + \Big[-2(\boldsymbol{x}^T\boldsymbol{u}_p)(\boldsymbol{x}^T\boldsymbol{u}_q)(\sum_{j=1}^{p-1}\boldsymbol{u}_j\boldsymbol{u}_j^T\boldsymbol{x})\boldsymbol{x}^T$$

$$+4(\boldsymbol{x}^T\boldsymbol{u}_p)(\boldsymbol{x}^T\boldsymbol{u}_q)(\sum_{j=1}^{p-1}\boldsymbol{u}_j\boldsymbol{u}_j^T)\boldsymbol{x}\boldsymbol{x}^T(\sum_{k=1}^{q-1}\boldsymbol{u}_k\boldsymbol{u}_k^T) + 2(\boldsymbol{x}^T\boldsymbol{u}_p)(\boldsymbol{x}^T\boldsymbol{u}_q)^2(\sum_{j=1}^{p-1}\boldsymbol{u}_j\boldsymbol{u}_j^T)\boldsymbol{x}\boldsymbol{u}_q^T\Big]$$

$$+\Big[-(\boldsymbol{x}^T\boldsymbol{u}_p)^2(\boldsymbol{x}^T\boldsymbol{u}_q)\boldsymbol{u}_p\boldsymbol{x}^T + 2(\boldsymbol{x}^T\boldsymbol{u}_p)^2(\boldsymbol{x}^T\boldsymbol{u}_q)\boldsymbol{u}_p\boldsymbol{x}^T(\sum_{k=1}^{q-1}\boldsymbol{u}_k\boldsymbol{u}_k^T) + (\boldsymbol{x}^T\boldsymbol{u}_p)^2(\boldsymbol{x}^T\boldsymbol{u}_q)^2\boldsymbol{u}_p\boldsymbol{x}_q^T\Big].$$

Using the well-known properties of fouth-order moments of Gaussian random variables, for $p = q$ we have

$$\begin{aligned}
\boldsymbol{S}_{pp} &= \Big[\{\boldsymbol{u}_p^T\boldsymbol{C}\boldsymbol{u}_p\boldsymbol{C} + 2\boldsymbol{C}\boldsymbol{u}_p\boldsymbol{u}_p^T\boldsymbol{C}\} - 2\boldsymbol{u}_p^T\boldsymbol{C}\boldsymbol{u}_p\Big(\sum_{j=1}^{p-1}\boldsymbol{C}\boldsymbol{u}_j\boldsymbol{u}_j^T\Big) - 3\boldsymbol{u}_p^T\boldsymbol{C}\boldsymbol{u}_p\boldsymbol{C}\boldsymbol{u}_p\boldsymbol{u}_p^T\Big] \\
&\quad +\Big[-2\boldsymbol{u}_p^T\boldsymbol{C}\boldsymbol{u}_p\Big(\sum_{j=1}^{p-1}\boldsymbol{u}_j\boldsymbol{u}_j^T\Big)\boldsymbol{C} + 4\boldsymbol{u}_p^T\boldsymbol{C}\boldsymbol{u}_p\Big(\sum_{j=1}^{p-1}\boldsymbol{u}_j^T\boldsymbol{C}\boldsymbol{u}_j\boldsymbol{u}_j\boldsymbol{u}_j^T\Big) + \boldsymbol{0}\Big] \\
&\quad +\Big[-3\boldsymbol{u}_p^T\boldsymbol{C}\boldsymbol{u}_p\boldsymbol{C}\boldsymbol{u}_p\boldsymbol{u}_p^T + \boldsymbol{0} + 3(\boldsymbol{u}_p^T\boldsymbol{C}\boldsymbol{u}_p)^2\boldsymbol{u}_p\boldsymbol{u}_p^T\Big] \\
&= \lambda_p\boldsymbol{C} - \lambda_p^2\boldsymbol{u}_p\boldsymbol{u}_p^T.
\end{aligned}$$

For $q < p$ we have

$$\begin{aligned}
\boldsymbol{S}_{pq} &= \Big[(\boldsymbol{C}\boldsymbol{u}_p\boldsymbol{u}_q^T\boldsymbol{C} + \boldsymbol{C}\boldsymbol{u}_q\boldsymbol{u}_p^T\boldsymbol{C})(\boldsymbol{I} - 2\sum_{k=1}^{q-1}\boldsymbol{u}_k\boldsymbol{u}_k^T) - \boldsymbol{u}_q^T\boldsymbol{C}\boldsymbol{u}_q\boldsymbol{C}\boldsymbol{u}_p\boldsymbol{u}_q^T\Big] \\
&+ \Big[(-2\sum_{j=1}^{p-1}\boldsymbol{u}_j\boldsymbol{u}_j^T)(\boldsymbol{C}\boldsymbol{u}_p\boldsymbol{u}_q^T\boldsymbol{C} + \boldsymbol{C}\boldsymbol{u}_q\boldsymbol{u}_p^T\boldsymbol{C}) \\
&+ 4(\sum_{j=1}^{p-1}\boldsymbol{u}_j\boldsymbol{u}_j^T)(\boldsymbol{C}\boldsymbol{u}_p\boldsymbol{u}_q^T\boldsymbol{C} + \boldsymbol{C}\boldsymbol{u}_q\boldsymbol{u}_p^T\boldsymbol{C})\cdot(\sum_{k=1}^{q-1}\boldsymbol{u}_k\boldsymbol{u}_k^T) + 2\boldsymbol{u}_q^T\boldsymbol{C}\boldsymbol{u}_q(\sum_{j=1}^{p-1}\boldsymbol{u}_j\boldsymbol{u}_j^T)\boldsymbol{C}\boldsymbol{u}_p\boldsymbol{u}_q^T\Big] \\
&+ \Big[-\boldsymbol{u}_p^T\boldsymbol{C}\boldsymbol{u}_p\boldsymbol{u}_p\boldsymbol{u}_q^T\boldsymbol{C} + 2\boldsymbol{u}_p^T\boldsymbol{C}\boldsymbol{u}_p\boldsymbol{u}_q^T\boldsymbol{C}(\sum_{k=1}^{q-1}\boldsymbol{u}_k\boldsymbol{u}_k^T) + \boldsymbol{u}_p^T\boldsymbol{C}\boldsymbol{u}_p\boldsymbol{u}_q^T\boldsymbol{C}\boldsymbol{u}_q\boldsymbol{u}_p\boldsymbol{u}_q^T\Big] \\
&= -\lambda_p\lambda_q\boldsymbol{u}_q\boldsymbol{u}_p^T.
\end{aligned}$$

References

[1] N. L. Owsley, Adaptive data orthogonalization, Proc. ICASSP '87, Dallas, TX, 6-9 April 1987, pp. 109-112.

[2] V. U. Reddy, B. Egardt, T. Kailath, Least squares type algorithm for adaptive implementation of Pisarenko's harmonic retrieval method, IEEE Trans. Acoust., Speech, Signal Processing, ASSP-30 (3) (June 1982) 399-405.

[3] E. Oja, Principal components, minor components and linear neural networks, Neural Networks, 5 (6) (1992) 927-935.

[4] B.Yang, Projection approximation subspace tracking, IEEE Trans. Signal Processing, 43 (1) (January 1995) 95-107.

[5] H. Sakai, K. Shimizu, A new adaptive algorithm for minor component analysis, Signal Processing, 71 (3) (December 1998) 301-308.

[6] V. Solo, X. Kong, Performance analysis of adaptive eigenanalysis algorithms, IEEE Trans. Signal Processing, 46 (3) (March 1998) 636-646.

[7] B. Yang, F.Gersemsky, Asymptotic distribution of recursive subspace estimator, Proc. ICASSP '96, Atlanta, GA, 7-9 May 1996, pp. 2856-2859.

[8] A. Benveniste et al., Adaptive Algorithms and Stochastic Approximations, Springer-Verlag, Berlin Heidelberg, 1990.

[9] J. P. Delmas, J. F. Cardoso, Performance analysis of an adaptive algorithm for tracking dominant subspaces, IEEE Trans. Signal Processing, 46 (11) (November 1998) 3045-3057.

[10] S. C. Douglas, S. Y. Kung, S. Amari, On the numerical stabilities of principal, minor, and independent component analysis algorithms, Proc. of the First Int. Workshop on Independent Component Analysis and Signal Separation, Aussois, France, 11-15 January 1999 pp. 419-424.

[11] J.R.Mabnus, H.Neudecker, Matrix Differential Calculus with Applications in Statistics and Econometrics, Revised Edition, Wiley, Chichester, 1999.

CONVERGENCE ANALYSIS OF THE DELAYLESS SUBBAND ADAPTIVE FILTER BASED ON THE FREQUENCY DOMAIN EXPRESSION

Shigeyuki Miyagi and Hideaki Sakai

Department of Systems Science, Graduate School of Informatics, Kyoto University, Japan

ABSTRACT

The upper limit of the step size and the variance of error signal for a two band delayless subband adaptive filter are theoretically evaluated in the frequency domain. The averaging method and the ordinary differential equation (ODE) method are used for this purpose. It is shown that the calculated result of upper limit of the step size has a similar form of that of the fullband LMS adaptive filter. In the ODE analysis, not only the convergence condition for the adaptive filter but also the variance of the error signal can be derived. The proposed method is also applied to a half band delayless subband adaptive filter. We demonstrate that these theoretical results give good approximations for simulation results.

1. INTRODUCTION

We consider the convergence condition and the error analysis of the delayless subband adaptive filter (ADF) which has been originally proposed by Morgan and Thi[1]. In the configuration of delayless subband ADFs, it is necessary to generate the tap coefficients of a fullband ADF from the tap coefficients of subband ADFs. In Morgan's work, the fast Fourier transformation (FFT) and the inverse FFT are used for the tap conversion.

In our previous work[2], it has been shown that this tap conversion may be singular and the fullband filter may not converge to an optimum Wiener filter. Additionally, a new tap conversion method using the Hadamard transform was proposed. In this paper, we consider our method in [2].

Here we study the updating equation of the subband ADF in the frequency domain and apply the averaging method and ODE method to obtain the upper limit of μ, the convergence condition and the variance of a error signal.

As a special case of the two band delayless subband ADF, we also consider a half band delayless subband ADF. In some practical applications, the adaptive filter in the highpass band can be neglected if the power of the highpass band of an unknown system is small. The analytical results of the two band case can be straightforwardly applied to this half band case. We show that the positive real condition plays an important role in our problems. We demonstrate the validity of the results by some simulations.

2. THE FREQUENCY DOMAIN EXPRESSION

The two band delayless subband adaptive filter is shown in Fig.1. The symbol of the signal at each point is written

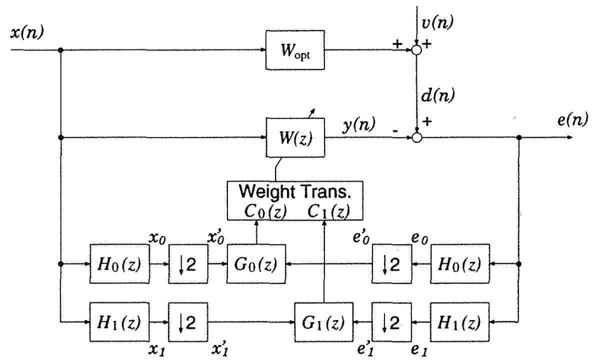

Figure 1: Structure of a delayless subband adaptive filter

by a lower case letter in Fig.1. The signal vector $\boldsymbol{x}(n)$ is defined by

$$\boldsymbol{x}(n) = [x(n),\ x(n-1),\ \cdots,\ x(n-N+1)]^T$$

where n is the time index in the subband and N is the tap length of the filter $W(z)$ and $W_{\rm opt}(z)$. Other signal vectors such as $\boldsymbol{x}_i(n)$ and $\boldsymbol{x}'_i(k)$ can be also defined by the same manner, where k in $\boldsymbol{x}'_i(k)$ denotes the time index in the subband and the length of $\boldsymbol{x}'_i(k)$ is N_g which is the tap length of the filter $G_i(z)$.

The tap vector of the fullband adaptive filter $W(z)$ is defined as

$$\boldsymbol{w}(n) = [w_0(n),\ w_1(n),\ \cdots,\ w_{N-1}(n)]^T.$$

Other tap vectors such as $\boldsymbol{w}_{\rm opt}$, $\boldsymbol{h}_i$, $\boldsymbol{c}_i$ and $\boldsymbol{g}_i(k)$ corresponding to $W_{\rm opt}(z)$, $H_i(z)$, $C_i(z)$, respectively and $G_i(z)$ are defined by the same way. We assume that the tap lengths N_h, N_c and N_g for $H_i(z)$, $C_i(z)$ and $G_i(z)$ are sufficiently smaller than N

A capital bold letter such as $\boldsymbol{W}_{\rm opt}$, $\boldsymbol{W}(n)$, $\boldsymbol{X}(n)$, etc. means the N point discrete Fourier transformation(DFT) of the corresponding vector, by applying N point DFT matrix

$$\boldsymbol{F} = \left[\exp\left(-\mathrm{i}\frac{2\pi lm}{N}\right)\right] \quad l, m = 0, 1, \cdots, N-1.$$

The each element of a vector in the frequency domain is denoted by the corresponding capital letter.

The error signal $e(n)$ is calculated by

$$\begin{aligned} e(n) &= d(n) - y(n) \\ &= -\boldsymbol{x}^\dagger(n)(\boldsymbol{w}(n) - \boldsymbol{w}_{\rm opt}) + v(n) \end{aligned} \quad (1)$$

where $\dagger$ denotes the complex conjugate transpose of a vector or a matrix. By using the DFT matrix $\boldsymbol{F}$, (1) can be expressed as

$$e(n) = -\frac{1}{N}\boldsymbol{X}^\dagger(n)\Delta\boldsymbol{W}(n) + v(n) \quad (2)$$

where $\Delta\boldsymbol{W}(n) = \boldsymbol{W}(n) - \boldsymbol{W}_{\rm opt}$. From (2), the variance of the error signal is calculated as

$$\mathrm{E}[|e(n)|^2] = \frac{1}{N^2}\mathrm{E}[\boldsymbol{X}^\dagger(n)\Delta\boldsymbol{W}(n)\Delta\boldsymbol{W}^\dagger(n)\boldsymbol{X}(n)] + \sigma_v^2 \quad (3)$$

where σ_v^2 is the variance of additive white noise $v(n)$.

3. THE FREQUENCY DOMAIN DESCRIPTION OF THE ADAPTIVE FILTER

The tap conversion from the subband filters $G_0(z)$ and $G_1(z)$ to the fullband filter $W(z)$ by using the Hadamard transform, is given in the z domain by

$$W(z) = \frac{1}{2}\left[(1+z^{-1})G_0(z^2) + (1-z^{-1})G_1(z^2)\right] \quad (4)$$

In the time domain, (4) can be generalized to the following equation,

$$\boldsymbol{w}(n) = \boldsymbol{c}_0 * (\boldsymbol{U}\boldsymbol{g}_0(k)) + \boldsymbol{c}_1 * (\boldsymbol{U}\boldsymbol{g}_1(k)), \quad k = n/2 \quad (5)$$

where $*$ denotes the convolution and $\boldsymbol{U}$ is an $N \times N_g$ up-sampling matrix defined by

$$\boldsymbol{U} = \left[\ \boldsymbol{e}_1,\ \boldsymbol{0},\ \boldsymbol{e}_2,\ \boldsymbol{0},\ \cdots, \boldsymbol{e}_{N_g},\ \boldsymbol{0}\ \right]^T$$

where $\boldsymbol{e}_i$ is the N_g row vector whose i-th element is one and other elements are zero. For (4), we take $\boldsymbol{c}_0 = 1/2[1,1]^T$ and $\boldsymbol{c}_1 = 1/2[1,-1]^T$. Generally speaking, however, $\boldsymbol{c}_0$ and $\boldsymbol{c}_1$ can be set to a lowpass filter and a high pass filter respectively. In our configuration, for simplicity, the tap length of each subband adaptive filter is half of that of the fullband adaptive filter so that $N_g = N/2$.

Applying the DFT matrix $\boldsymbol{F}$ to (5), then the frequency domain description of (5) is given by

$$\boldsymbol{W}(n) = \Lambda_{C_0}\boldsymbol{F}(\boldsymbol{U}\boldsymbol{g}_0(k)) + \Lambda_{C_1}\boldsymbol{F}(\boldsymbol{U}\boldsymbol{g}_1(k)) \quad (6)$$

where

$$\Lambda_{C_i} = \mathrm{diag}[\ C_{i,0},\ C_{i,1},\ \cdots,\ C_{i,N-1}\ ] \quad i = 0, 1.$$

Two coefficient vectors of the subband ADFs are updated by the following LMS algorithm,

$$\boldsymbol{g}_i(k+1) = \boldsymbol{g}_i(k) + \mu\boldsymbol{x}_i'(k)e_i'(k), \quad i = 0, 1. \quad (7)$$

By substituting (7) into (6), the recursive equation for $\Delta\boldsymbol{W}(n)$ is given by

$$\Delta\boldsymbol{W}(n) = \Delta\boldsymbol{W}(n-2) + \mu\sum_{i=0}^{1}\Lambda_{C_i}\boldsymbol{F}\boldsymbol{U}\boldsymbol{x}_i'(k-1)e_i'(k-1).$$

By replacing $\boldsymbol{x}_0'(k-1)$ and $e_0'(k-1)$ to $\boldsymbol{x}_i(n-2)$ and $e_i(n-2)$ with $N_g \times N$ down-sampling matrix $\boldsymbol{D}$ defined as $\boldsymbol{D} = \boldsymbol{U}^T$, and using the DFT matrix $\boldsymbol{F}$, the following recursive equations for $\Delta\boldsymbol{W}(n)$ is obtained,

$$\Delta\boldsymbol{W}(n) = \Delta\boldsymbol{W}(n-2) + \mu\boldsymbol{K}(\boldsymbol{X}_i(n-2), \Delta\boldsymbol{W}) \quad (8)$$

$$\boldsymbol{K}(\boldsymbol{X}_i(n-2), \Delta\boldsymbol{W}) \quad (9)$$

$$\equiv \frac{1}{N^2}\sum_{i=0}^{1}\Lambda_{C_i}\boldsymbol{F}\boldsymbol{U}\boldsymbol{D}\boldsymbol{F}^\dagger\boldsymbol{X}_i(n-2)\boldsymbol{B}^\dagger(n-2)\boldsymbol{H}_i$$

where $\boldsymbol{B}(n) = \boldsymbol{F}(\boldsymbol{d}(n) - \boldsymbol{y}(n))$.

4. THE CONVERGENCE ANALYSIS BY THE AVERAGING METHOD

We consider the upper limit of the step size μ based on the averaging method [3]. The averaged system corresponding to (8) is given by

$$\Delta\bar{\boldsymbol{W}}(n) = \Delta\bar{\boldsymbol{W}}(n-2) \quad (10)$$

$$-\frac{\mu}{N^2}\sum_{i=0}^{1}\Lambda_{C_i}\boldsymbol{F}\boldsymbol{U}\boldsymbol{D}\boldsymbol{F}^\dagger\Lambda_{H_i}^*\boldsymbol{Q}\Lambda_{H_i}\Delta\bar{\boldsymbol{W}}(n-2)$$

where

$$\Lambda_{H_i} = \mathrm{diag}[\ H_{i,0},\ H_{i,1},\ \cdots,\ H_{i,N-1}\ ] \quad i = 0, 1$$

and $\boldsymbol{Q}$ is the covariance matrix of $\boldsymbol{X}(n)$. When N is sufficiently large, each element of $\boldsymbol{X}(n)$ has almost no correlation each other so that $\boldsymbol{Q}$ becomes a diagonal matrix $\mathrm{E}[\boldsymbol{X}(n)\boldsymbol{X}^\dagger(n)] = \boldsymbol{Q} = \mathrm{diag}[Q_0,\ Q_1,\ \cdots,\ Q_{N-1}]$. The detailed derivation of (10) is omitted due to space limitation.

When the filters $C_0(z)$, $H_0(z)$, $C_1(z)$ and $H_1(z)$ are sufficiently close to an ideal lowpass filter and an ideal highpass filter respectively, the following approximation holds.

$$\Lambda_{C_i}\boldsymbol{F}\boldsymbol{U}\boldsymbol{D}\boldsymbol{F}^\dagger\Lambda_{H_i}^* \simeq (N/2)\Lambda_{C_i}\Lambda_{H_i}^* \quad i = 0, 1. \quad (11)$$

By substituting (11) into (10), the averaged system is finally obtained as

$$\Delta\bar{\boldsymbol{W}}(n) \simeq \left[1 - \frac{\mu}{2N}\sum_{i=0}^{1}\Lambda_{C_i}\Lambda_{H_i}^*\boldsymbol{Q}\Lambda_{H_i}\right]\Delta\bar{\boldsymbol{W}}(n-2) \quad (12)$$

All the matrices in (12) are diagonal so that (12) can be decomposed to the recursive equations for each element of $\Delta\bar{\boldsymbol{W}}(n)$. For these equations to converge, we require

$$\left|1 - \frac{\mu}{2N}Q_l\sum_{i=0}^{1}C_{i,l}|H_{i,l}|^2\right| < 1 \quad (l = 0, 1, \cdots, N-1) \quad (13)$$

From (13), the inequality with respect to the step size μ can be derived as

$$0 < \mu < 4N\frac{\sum_{i=0}^{1}|H_{i,l}|^2\mathrm{Re}[C_{i,l}]}{Q_l\left|\sum_{i=0}^{1}|H_{i,l}|^2C_{i,l}\right|^2} \quad (l = 0, 1, \cdots, N-1) \quad (14)$$

The upper limit of μ is determined as the minimum value of RHS in (14). From this the positive reality of $C_i(z)$ is required.

5. SECOND ORDER ANALYSIS

We can evaluate the covariance matrix for $\Delta\boldsymbol{W}$ by using the ordinary differential equation (ODE) method[4]. The variance of the error signal can be estimated by using this result and the averaging principle[5].

First, let us consider the ODE corresponding to (8). By using similar approximations in the Section 4, the ODE is obtained as,

$$\frac{\mathrm{d}\Delta\boldsymbol{W}}{\mathrm{d}t} = -\frac{1}{2N}\boldsymbol{Q}\sum_{i=0}^{1}\boldsymbol{\Lambda}_{C_i}\boldsymbol{\Lambda}_{H_i}^{*}\boldsymbol{\Lambda}_{H_i}\Delta\boldsymbol{W} \equiv \boldsymbol{J}(\Delta\boldsymbol{W}). \quad (15)$$

From (15), the equilibrium point is obviously $\Delta\boldsymbol{W}_* = \boldsymbol{0}$. The differential matrix $\boldsymbol{H}(\Delta\boldsymbol{W})$ for (15) can be calculated as

$$\boldsymbol{H}(\Delta\boldsymbol{W}) = \frac{\mathrm{d}\boldsymbol{J}(\Delta\boldsymbol{W})}{\mathrm{d}\Delta\boldsymbol{W}^T} = -\frac{1}{2N}\boldsymbol{Q}\sum_{i=0}^{1}\boldsymbol{\Lambda}_{C_i}\boldsymbol{\Lambda}_{H_i}^{*}\boldsymbol{\Lambda}_{H_i}. \quad (16)$$

$\boldsymbol{H}(\Delta\boldsymbol{W})$ must be a stable matrix for $\Delta\boldsymbol{W}$ to asymptotically converge to the equilibrium point, so that the condition $\sum_{i=0}^{1}|H_{i,l}|^2\mathrm{Re}[C_{i,l}] > 0$ is required.

Next we calculate the following matrix

$$\boldsymbol{S}(\Delta\boldsymbol{W}) = \sum_{n=-\infty}^{\infty}\mathrm{E}[\boldsymbol{K}(\boldsymbol{X}_i(n),\Delta\boldsymbol{W})\boldsymbol{K}^{\dagger}(\boldsymbol{X}_i(0),\Delta\boldsymbol{W})] \quad (17)$$

By substituting (9) into (17) and making some approximations we can obtain the matrix $\boldsymbol{S}$ at the equilibrium point $\Delta\boldsymbol{W}_* = \boldsymbol{0}$ as

$$\boldsymbol{S}(\boldsymbol{0}) = \frac{\sigma_v^2}{4}\sum_{i=0}^{1}\sum_{j=0}^{1}\boldsymbol{\Lambda}_{C_i}\boldsymbol{\Lambda}_{H_i}^{*}\boldsymbol{\Lambda}_{H_i}\boldsymbol{Q}\boldsymbol{\Lambda}_{H_j}^{*}\boldsymbol{\Lambda}_{H_j}\boldsymbol{\Lambda}_{C_j}^{*}. \quad (18)$$

By substituting (16) and (18) into the Liapunov equation $\boldsymbol{H}\boldsymbol{Y}+\boldsymbol{Y}\boldsymbol{H}^{\dagger} = -\boldsymbol{S}(\boldsymbol{0})$ and solving it with respect to $\boldsymbol{Y}$, we obtain

$$\begin{aligned} \boldsymbol{Y} &= \mathrm{diag}[Y_0\ Y_1\ \cdots\ Y_{N-1}] \quad (19) \\ Y_l &= \frac{\sigma_v^2 N}{4}\frac{\sum_{i=0}^{1}|H_{i,l}|^4|C_{i,l}|^2}{\sum_{i=0}^{1}|H_{i,l}|^2\mathrm{Re}[C_{i,l}]} \end{aligned}$$

under the condition that $H_0(z)$ and $H_1(z)$ are a lowpass filter and a highpass filter respectively. From [4](p.108, Theorem 2), the covariance matrix of $\Delta\boldsymbol{W}$ can be evaluated as $\mathrm{E}[\Delta\boldsymbol{W}\Delta\boldsymbol{W}^{\dagger}] = \mu\boldsymbol{Y}$. Applying the averaging principal to (3), the variance of the error signal can be obtained,

$$\mathrm{E}[|e(n)|^2] = \frac{1}{N^2}\mathrm{Tr}[\boldsymbol{Q}\mu\boldsymbol{Y}] + \sigma_v^2 = \sigma_v^2(1+\mu N\zeta)$$

$$\zeta = \frac{1}{4N^2}\sum_{l=0}^{N-1}\frac{Q_l\sum_{i=0}^{1}|C_{i,l}|^2|H_{i,l}|^4}{\sum_{i=0}^{1}|H_{i,l}|^2\mathrm{Re}[C_{i,l}]}$$

6. HALF BAND DELAYLESS SUBBAND ADAPTIVE FILTER

A half band delayless subband adaptive filter is a special case of a two band delayless ADF. Two types of the half band delayless ADF are shown in Fig.2(a) and (b).

In the configuration in Fig.2(a), by using the stationary condition of the cross spectrum $S_{e_0'x_0'}(z)$ between the subband signal x_0' and the subband error signal e_0', the optimal filter of $W(z)$ can be calculated as

$$\begin{aligned} W(z) &= C_0(z)G_0(z^2) \quad (20) \\ &= C_0(z)\frac{|H_0(z)|^2S_{dx}(z)+|H_0(-z)|^2S_{dx}(-z)}{|H_0(z)|^2C_0(z)S_x(z)+|H_0(-z)|^2C_0(-z)S_x(-z)} \\ &\simeq \begin{cases} S_{dx}(z)/S_x(z) = W_{\mathrm{opt}}(z) & |\omega| \le \pi/2 \\ 0 & \pi/2 < |\omega| \le \pi \end{cases} \end{aligned}$$

where S_{dx} is the cross spectrum between the desired signal d and the input signal x. If $C_0(z)$ is close to an ideal lowpass filter, $W(z)$ gives the Wiener filter in the lowpass band. Let us apply the previous discussion to this configuration. By setting $H_1(z)$ to zero, the upper limit of μ, the stability condition and ζ_a in the variance of error signal are obtained as $0 < \mu < (4N\ \mathrm{Re}[C_{0,l}])/(Q_l|H_{0,l}|^2|C_{0,l}|^2)$, $\mathrm{Re}[C_{0,l}] > 0$ and

$$\zeta_a = \frac{1}{4N^2}\sum_{l=0}^{N-1}\frac{Q_l|H_{0,l}|^2|C_{0,l}|^2}{\mathrm{Re}[C_{0,l}]}. \quad (21)$$

From (20), we can omit the lowpass filter for the error signal. This is the reason why another configuration shown in Fig.2(b) is considered. The optimal filter of $W(z)$ for this configuration is given by

$$\begin{aligned} W(z) &= C_0(z)G_0(z^2) \\ &= C_0(z)\frac{H_0(z^{-1})S_{dx}(z)+H_0(-z^{-1})S_{dx}(-z)}{H_0(z^{-1})C_0(z)S_x(z)+H_0(-z)C_0(-z)S_x(-z)}. \end{aligned}$$

$W(z)$ also gives the Wiener filter in the lowpass band like (20) if $C_0(z)$ is close to an ideal lowpass filter. To apply the previous discussion, we must slightly modify (8). In a similar manner, the upper limit of μ, the stability condition and ζ_b in the variance of error signal can be obtained as $0 < \mu < (4N\ \mathrm{Re}[C_{0,l}H_{0,l}^*])/(Q_l|C_{0,l}|^2|H_{0,l}|^2)$, $\mathrm{Re}[C_{0,l}H_{0,l}^*] > 0$ and

$$\zeta_b = \frac{1}{4N^2}\sum_{l=0}^{N-1}\frac{Q_l|C_{0,l}H_{0,l}^*|^2}{\mathrm{Re}[C_{0,l}H_{0,l}^*]}. \quad (22)$$

7. SIMULATION RESULTS

We check the stability conditions in the half band delayless ADF. The simulation results for the two configurations are summarized in Table 1. The eight tap lowpass filter of CQF bank is used as $H_0(z)$. Three sorts of lowpass filters are used as $C_0(z)$. $(1+z^{-1})/2$ corresponds to the Hadamard transform. The "fir2-16" is a 16 taps lowpass filter generated by fir2 function in MATLAB. All the simulation results in Tables 1 coincide with the theoretical stability conditions except of the case No.a-1. For $C_0(z) = (1+z^{-1})/2$, the stability condition holds except $l = N/2$.

The frequency responses of the adaptive filter in No.a-1 and b-2 are shown in Fig.3. The frequency response of the unknown system is plotted by a solid line. The frequency responses for both cases coincide with that for the unknown system in the lowpass band. The frequency response of No.b-2 is more sharply cut off than that of No.a-1 at $\omega = \pi/2$.

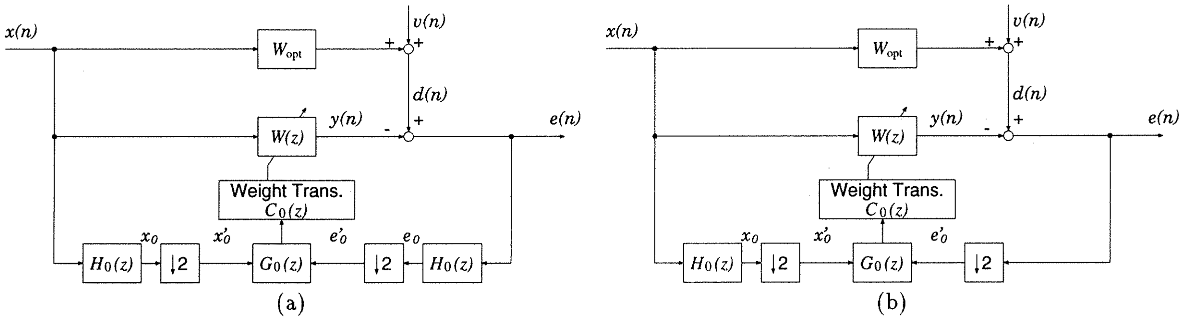

Figure 2: Configurations of half band delayless ADFs

$C_0(z)$	No.	Stability condition $\mathrm{Re}[C_{0,l}] > 0$	Stability in the simulation	No.	Stability condition $\mathrm{Re}[C_{0,l}H^*_{0,l}] > 0$	Stability in the simulation
$(1+z^{-1})/2$	a-1	marginal	stable	b-1	not satisfied	unstable
CQF8tap	a-2	not satisfied	unstable	b-2	satisfied	stable
fir2-16	a-3	not satisfied	unstable	b-3	not satisfied	unstable

Table 1: Simulation results for the configuration (a) and (b). The eight tap lowpass filter in CQF bank is used as $H_0(z)$

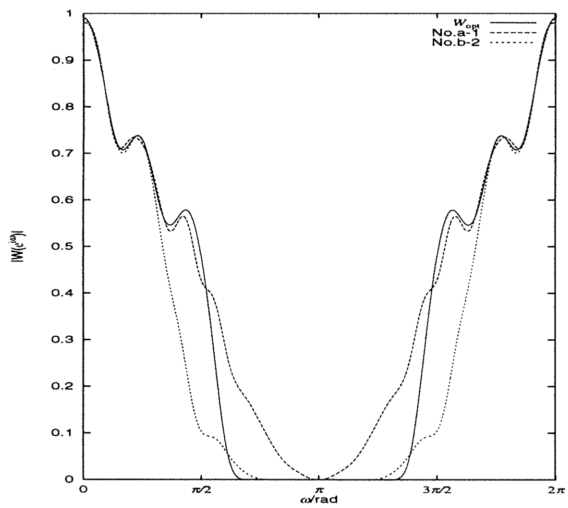

Figure 3: Frequency responses of $W(z)$ in No.a-1 and b-2.

For the cases of No.a-1 and b-2, the variances of the error signals are evaluated. We assume that the input signal is a white noise and W_{opt} is a 128 taps FIR filter. From (21) and (22), the theoretical values ζ_a and ζ_b are evaluated as 0.125 in each case. We calculate some variances of the error signal for each μ in $0.0008 \sim 0.008$. By applying a linear regression equation to these values, ζ_a and ζ_b can be estimated. As a result, $\zeta_a = 0.09127$ and $\zeta_b = 0.1074$ are obtained. These results are considerably close to the theoretical values, respectively.

8. CONCLUSION

We have derived the upper limit of the step size, stability condition and the variance of the error signal in a two band delayless subband ADF by means of the averaging method and the ODE method. We also have shown that these results can be applied to the half band delayless subband ADF. Some simulations have demonstrated the validity of these results in the half band case.

9. REFERENCES

[1] D. R. Morgan and J. C. Thi, "A delayless subband adaptive filter architecture," IEEE Trans. Signal Processing, vol. 43, pp.1819–1830, Aug. 1995.

[2] N. Hirayama, H. Sakai, and S. Miyagi, "Delayless subband adaptive filtering using the Hadamard transform," IEEE Trans. Signal Processing, vol. 47, pp.1731–1734, June 1999.

[3] V. Solo and X. Kong, Adaptive Signal Processing Algorithms – Stability and Performance –, Prentice Hall, New Jersey, 1995.

[4] A. Benveniste, M. Métivier and P. Priouret, Adaptive Algorithms and Stochastic Approximations, Springer-Verlag, Berlin Heidelberg, 1990.

[5] C. G. Samson and V. U. Reddy, "Fixed point error analysis of the normalized ladder algorithm," IEEE Trans. Acoustic Speech and Signal Processing, vol. ASSP-31, pp.1177–1191, Oct. 1983.

PERFORMANCE ANALYSIS OF AN ADAPTIVE ALGORITHM FOR MINOR COMPONENT ANALYSIS

Hideaki Sakai, Shigeyuki Miyagi and Kouji Minamiyama
Dept. of Systems Science, Graduate School of Informatics, Kyoto University, Japan
e-mail: hsakai@i.kyoto-u.ac.jp, miyagi@i.kyoto-u.ac.jp

ABSTRACT

The single minor component extraction algorithm proposed by Douglas *et al.* is extended to a multiple minor components extraction algorithm by combining the deflation technique and the Gram-Schmidt orthogonalization. The second order analysis for the multiple case is presented by applying the averaging method or the ordinary differential equation (ODE) method. The error covariances of the estimated minor components are derived and the validity of these evaluations is demonstrated by simulations.

1 INTRODUCTION

The minor component analysis (MCA) plays an important role in many parameter estimation problems such as MUSIC algorithm and the Pisarenko's method. As an adaptive algorithm for MCA, Oja's algorithms[1] is well known. Recently, Sakai and Shimizu[2] proposed another adaptive algorithm for extracting multiple minor components by combining the deflation technique and the Gram-Schmidt (GS) orthonormalization. This algorithm is obtained by modifying the PASTd algorithm due to Yang[3] for principal component analysis (PCA) or signal subspace filtering. Although the GS step is unnecessary in PCA, it is shown in [2] that the GS step is indispensable in MCA. This complicates the resulting algorithm and the associated performance analysis.

Solo and Kong [4] have presented the performance analysis of the algorithms for a single minor component corresponding to the minimum eigenvalue by using the averaging method or the ODE method[5]. In this paper we present the result for the multiple minor components case.

2 MULTIPLE MINOR COMPONENT ANALYSIS

The multiple minor components analysis is extracting the some eigenvectors corresponding to the smaller eigenvalues of the covariance matrix $\boldsymbol{C}$ of the input signal vector $\boldsymbol{x}(k)$. We assume that $\boldsymbol{x}(k)$ is an n-dimensional stochastic input signal and independent, identically normal distributed with zero mean. Let the eigen decomposition of $\boldsymbol{C}$ be

$$\boldsymbol{C} = \boldsymbol{U}\boldsymbol{\Lambda}\boldsymbol{U}^T, \quad \boldsymbol{U}\boldsymbol{U}^T = \boldsymbol{I},$$
$$\boldsymbol{U} = [\, \boldsymbol{u}_1, \cdots, \boldsymbol{u}_n \,], \quad \boldsymbol{\Lambda} = \mathrm{diag}[\, \lambda_1, \cdots, \lambda_n \,]$$

where $\boldsymbol{u}_i$ is the eigenvector corresponding to the eigenvalue λ_i and $\lambda_1 > \lambda_2 > \cdots > \lambda_{n-2} > \lambda_{n-1} > \lambda_n > 0$.

As a fundamental building block of our MCA, we use the following algorithm with a sufficiently small positive constant gain μ for extracting $\boldsymbol{u}_n$ corresponding to the minimum eigenvalue λ_n due to Douglas et al.[6].

$$\begin{aligned} \boldsymbol{v}_n(k) &= \boldsymbol{v}_n(k-1) - \mu \boldsymbol{A}_0(k)\boldsymbol{v}_n(k-1) \qquad (1)\\ \boldsymbol{A}_0(k) &= \|\boldsymbol{v}_n(k-1)\|^4 \boldsymbol{x}(k)\boldsymbol{x}^T(k) \\ &\quad - \boldsymbol{I}\left\{\boldsymbol{v}_n^T(k-1)\boldsymbol{x}(k)\right\}^2 \end{aligned}$$

This algorithm can be extended to extract up to the i-th ($i = 2, 3, \cdots, n$) minor component by combining the deflation technique and the orthogonalization as follows.

- deflation step

$$\boldsymbol{x}_n(k) = \boldsymbol{x}(k)$$
$$\boldsymbol{x}_{n-(i-1)}(k) = \left(\boldsymbol{I} - \sum_{j=1}^{i-1} \boldsymbol{v}_{n-j+1}(k)\boldsymbol{v}_{n-j+1}^T(k) \right) \boldsymbol{x}(k)$$

- updating the weight vector

$$\begin{aligned} \boldsymbol{\psi}_{n-(i-1)}(k) &= \boldsymbol{v}_{n-(i-1)}(k-1) \\ &\quad - \mu \boldsymbol{A}_{i-1}(k)\boldsymbol{v}_{n-(i-1)}(k-1) \qquad (2)\\ \boldsymbol{A}_{i-1}(k) &= \|\boldsymbol{v}_{n-(i-1)}(k-1)\|^4 \boldsymbol{x}_{n-(i-1)}(k)\boldsymbol{x}_{n-(i-1)}^T(k) \\ &\quad - \boldsymbol{I}\left\{\boldsymbol{v}_{n-(i-1)}^T(k-1)\boldsymbol{x}_{n-(i-1)}(k)\right\}^2 \end{aligned}$$

- orthogonalization

$$\boldsymbol{v}_{n-(i-1)}(k) = \left(\boldsymbol{I} - \sum_{j=1}^{i-1} \frac{\boldsymbol{v}_{n-j+1}(k)\boldsymbol{v}_{n-j+1}^T(k)}{\|\boldsymbol{v}_{n-j+1}(k)\|^2} \right) \boldsymbol{\psi}_{n-(i-1)}(k) \qquad (3)$$

The covariance matrix of a deflated signal $\boldsymbol{x}_{n-(i-1)}$ is defined as

$$\boldsymbol{C}_{n-(i-1)} = \mathrm{E}\left[\boldsymbol{x}_{n-(i-1)}(k)\boldsymbol{x}^T_{n-(i-1)}(k)\right]$$

which is used in a later discussion.

3 SUMMARY OF THE ODE METHOD

A general form of an adaptive algorithm is expressed as

$$\boldsymbol{\theta}(k) = \boldsymbol{\theta}(k-1) - \mu(k)\boldsymbol{h}(\boldsymbol{\theta}(k-1), \boldsymbol{x}(k))$$

where $\boldsymbol{\theta}(k)$, $\boldsymbol{x}(k)$, and $\mu(k)$ denote a parameter vector, an input signal vector, and a step gain, respectively. Under some regularity conditions, the corresponding ODE is given by

$$\frac{\mathrm{d}\boldsymbol{\theta}(t)}{\mathrm{d}t} = \tilde{\boldsymbol{h}}(\boldsymbol{\theta}(t))$$

with $\tilde{\boldsymbol{h}}(\boldsymbol{\theta}) = \lim_{k\to\infty} \mathrm{E}[\boldsymbol{h}(\boldsymbol{\theta}, \boldsymbol{x}(k))]$. Here we assume that $\boldsymbol{\theta}(t) \to \boldsymbol{\theta}_*$, so that $\boldsymbol{\theta}(k) \to \boldsymbol{\theta}_*$ in some sense. The derivative matrix is defined by

$$\boldsymbol{H}(\boldsymbol{\theta}) = \frac{\partial \tilde{\boldsymbol{h}}(\boldsymbol{\theta})}{\partial \boldsymbol{\theta}^T}.$$

Under the appropriate conditions, for $\mu(k) = \mu = \text{const}$, the following theorem holds[5].

Theorem 1 *If all the eigenvalues of $\boldsymbol{H}(\theta_*)$ have negative real parts and if the matrix*

$$\boldsymbol{S}(\boldsymbol{\theta}) = \sum_{k=-\infty}^{\infty} \mathrm{E}\left[\boldsymbol{h}(\boldsymbol{\theta}, \boldsymbol{x}(k))\boldsymbol{h}^T(\boldsymbol{\theta}, \boldsymbol{x}(0))\right]$$

exists, $\mu^{-1/2}[\boldsymbol{\theta}(k) - \boldsymbol{\theta}_*]$ converges asymptotically ($k \to \infty$ and $\mu \to 0$) to a zero mean normal distributed random vector weakly with a covariance matrix $\boldsymbol{D}$, which is the solution of the Lyapunov equation

$$\boldsymbol{H}(\boldsymbol{\theta}_*)\boldsymbol{D} + \boldsymbol{D}\boldsymbol{H}^\dagger(\boldsymbol{\theta}_*) = -\boldsymbol{S}(\boldsymbol{\theta}_*). \tag{4}$$

4 ANALYSIS OF A SINGLE MINOR COMPONENT EXTRACTION

We derive the ODE corresponding to (1) and evaluate the covariance matrix $\boldsymbol{D}$. From (1),

$$\boldsymbol{h}_0(\boldsymbol{v}_n, \boldsymbol{x}(k)) = -\boldsymbol{A}_0(k)\boldsymbol{v}_n \tag{5}$$

holds. By averaging the above equation, the ODE corresponding to (1) can be obtained as

$$\frac{\mathrm{d}\boldsymbol{v}_n}{\mathrm{d}t} = -\left[\|\boldsymbol{v}_n\|^4 \boldsymbol{C} - \boldsymbol{I}(\boldsymbol{v}_n^T\boldsymbol{C}\boldsymbol{v}_n)\right]\boldsymbol{v}_n \equiv \tilde{\boldsymbol{h}}_0(\boldsymbol{v}_n). \tag{6}$$

The derivative matrix $\boldsymbol{H}(\boldsymbol{v}_n)$ is calculated from (6) as

$$\begin{aligned}\boldsymbol{H}(\boldsymbol{v}_n) &= \frac{\partial}{\partial \boldsymbol{v}_n^T}\tilde{\boldsymbol{h}}_0(\boldsymbol{v}_n) \\ &= -\|\boldsymbol{v}_n\|^4 \boldsymbol{C} - 4\|\boldsymbol{v}_n\|^2 \boldsymbol{C}\boldsymbol{v}_n\boldsymbol{v}_n^T \\ &\quad + \boldsymbol{I}(\boldsymbol{v}_n^T\boldsymbol{C}\boldsymbol{v}_n) + 2\boldsymbol{v}_n\boldsymbol{v}_n^T\boldsymbol{C}. \end{aligned} \tag{7}$$

The value of the derivative matrix $\boldsymbol{H}(\boldsymbol{v}_n)$ at an equilibrium point, $\boldsymbol{v}_n^* = \boldsymbol{u}_n$ is calculated by

$$\boldsymbol{H}(\boldsymbol{v}_n^*) = -2\lambda_n\boldsymbol{u}_n\boldsymbol{u}_n^T + \sum_{j=1}^{n-1}(-\lambda_j + \lambda_n)\boldsymbol{u}_j\boldsymbol{u}_j^T. \tag{8}$$

From this result, all eigenvalues of $\boldsymbol{H}(\boldsymbol{v}_n^*)$ are negative, so that Theorem 1 can be applied. Under the assumption that the input signal $\boldsymbol{x}(k)$ is independently, identically and normally distributed, the definition of matrix $\boldsymbol{S}(\boldsymbol{v}_n)$ is reduced to

$$\boldsymbol{S}(\boldsymbol{v}_n) = \mathrm{E}\left[\boldsymbol{h}_0(\boldsymbol{v}_n, \boldsymbol{x}(0))\boldsymbol{h}_0^T(\boldsymbol{v}_n, \boldsymbol{x}(0))\right]. \tag{9}$$

By substituting (5) into (9), $\boldsymbol{S}(\boldsymbol{v}_n^*)$ is calculated as

$$\boldsymbol{S}(\boldsymbol{v}_n^*) = \lambda_n\boldsymbol{C} - \lambda_n^2\boldsymbol{u}_n\boldsymbol{u}_n^T. \tag{10}$$

By substituting (8) and (10) into (4) and solving it, the covariance matrix $\boldsymbol{D}$ is obtained as

$$\boldsymbol{D} = \frac{1}{2}\sum_{j=1}^{n-1}\frac{\lambda_j\lambda_n}{\lambda_j - \lambda_n}\boldsymbol{u}_j\boldsymbol{u}_j^T.$$

5 ANALYSIS OF A MULTIPLE MINOR COMPONENT EXTRACTION

We derive the ODE corresponding to the multiple minor components extraction algorithm described in Section 2. The ODE might be obtained from tedious calculation of the recursive equations, however, this process is considerably complex. Therefore we simplify (2) and (3) by discarding the terms that do not affect the evaluation of the matrices $\boldsymbol{H}$ and $\boldsymbol{S}$ at an equilibrium point and the terms of order μ^2, the following recursive equation is obtained.

$$\begin{aligned}
&\boldsymbol{v}_{n-(i-1)}(k) \approx \boldsymbol{\psi}_{n-(i-1)}(k) \\
&\qquad - \sum_{j=1}^{i-1}\frac{\boldsymbol{\psi}_{n-j+1}(k)\boldsymbol{\psi}^T_{n-j+1}(k)}{\|\boldsymbol{\psi}_{n-j+1}(k)\|^2}\boldsymbol{\psi}_{n-(i-1)}(k) \\
&\approx \quad \boldsymbol{v}_{n-(i-1)}(k-1) \\
&\qquad +\mu\Bigg[\\
&\qquad -\left(\boldsymbol{I} - \sum_{j=1}^{i-1}\frac{\boldsymbol{v}_{n-j+1}(k-1)\boldsymbol{v}^T_{n-j+1}(k-1)}{\|\boldsymbol{v}_{n-j+1}(k-1)\|^2}\right)\boldsymbol{A}_{i-1}(k) \\
&\qquad + \sum_{j=1}^{i-1}\frac{\boldsymbol{A}_{j-1}(k)\boldsymbol{v}_{n-j+1}(k-1)\boldsymbol{v}^T_{n-j+1}(k-1)}{\|\boldsymbol{v}_{n-j+1}(k-1)\|^2} \\
&\qquad + \sum_{j=1}^{i-1}\frac{\boldsymbol{v}_{n-j+1}(k-1)\boldsymbol{v}^T_{n-j+1}(k-1)\boldsymbol{A}^T_{j-1}(k)}{\|\boldsymbol{v}_{n-j+1}(k-1)\|^2} \\
&\qquad - 2\sum_{j=1}^{i-1}\left(\frac{\boldsymbol{v}^T_{n-j+1}(k-1)\boldsymbol{A}^T_{j-1}(k)\boldsymbol{v}_{n-j+1}(k-1)}{\|\boldsymbol{v}_{n-j+1}(k-1)\|^4}\right) \\
&\qquad \boldsymbol{v}_{n-j+1}(k-1)\boldsymbol{v}^T_{n-j+1}(k-1)\Bigg]\boldsymbol{v}_{n-(i-1)}(k-1) \qquad (11) \\
&\equiv \quad \boldsymbol{v}_{n-(i-1)}(k-1) \\
&\qquad + \mu\boldsymbol{h}_{i-1}(\boldsymbol{v}_{n-(i-1)}, \boldsymbol{x}_{n-(i-1)}(k-1)).
\end{aligned}$$

The ODE corresponding to (11) is given by

$$\frac{\mathrm{d}\boldsymbol{v}_{n-(i-1)}}{\mathrm{d}t} \tag{12}$$
$$= \left[-\left(\boldsymbol{I} - \sum_{j=1}^{i-1} \frac{\boldsymbol{v}_{n-j+1}\boldsymbol{v}_{n-j+1}^T}{\|\boldsymbol{v}_{n-j+1}\|^2} \right) \boldsymbol{A}_{i-1} \right.$$
$$+ \sum_{j=1}^{i-1} \frac{\boldsymbol{A}_{j-1}\boldsymbol{v}_{n-j+1}\boldsymbol{v}_{n-j+1}^T + \boldsymbol{v}_{n-j+1}\boldsymbol{v}_{n-j+1}^T\boldsymbol{A}_{j-1}^T}{\|\boldsymbol{v}_{n-j+1}\|^2}$$
$$- 2\sum_{j=1}^{i-1} \left(\frac{\boldsymbol{v}_{n-j+1}^T \boldsymbol{A}_{j-1}^T \boldsymbol{v}_{n-j+1}}{\|\boldsymbol{v}_{n-j+1}\|^4} \right)$$
$$\left. \boldsymbol{v}_{n-j+1}\boldsymbol{v}_{n-j+1}^T \right] \boldsymbol{v}_{n-(i-1)}$$
$$\equiv \tilde{\boldsymbol{h}}_{i-1}(\boldsymbol{v}_{n-(i-1)})$$

with

$$\boldsymbol{A}_{i-1} = \|\boldsymbol{v}_{n-(i-1)}\|^4 \boldsymbol{C}_{n-(i-1)} - \boldsymbol{I}\left(\boldsymbol{v}_{n-(i-1)}^T \boldsymbol{C}_{n-(i-1)} \boldsymbol{v}_{n-(i-1)}\right).$$

If we define the vectors such as

$$\boldsymbol{v}^T \equiv \left[\boldsymbol{v}_n^T, \boldsymbol{v}_{n-1}^T, \cdots, \boldsymbol{v}_{n-(i-1)}^T \right]^T$$
$$(\boldsymbol{v}^*)^T \equiv \left[\boldsymbol{u}_n^T, \boldsymbol{u}_{n-1}^T, \cdots, \boldsymbol{u}_{n-(i-1)}^T \right]^T$$
$$\boldsymbol{h}(\boldsymbol{v}, \boldsymbol{x}_n(k-1), \cdots, \boldsymbol{x}_{n-(i-1)}(k-1)) \equiv \begin{bmatrix} \boldsymbol{h}_0(\boldsymbol{v}_n, \boldsymbol{x}_n(k-1)) \\ \vdots \\ \boldsymbol{h}_{i-1}(\boldsymbol{v}_{n-(i-1)}, \boldsymbol{x}_{n-(i-1)}(k-1) \end{bmatrix}$$
$$\tilde{\boldsymbol{h}}^T \equiv \left[\tilde{\boldsymbol{h}}_0^T(\boldsymbol{v}_n), \tilde{\boldsymbol{h}}_1^T(\boldsymbol{v}_{n-1}), \cdots, \tilde{\boldsymbol{h}}_{i-1}^T(\boldsymbol{v}_{n-(i-1)}) \right]^T,$$

then the ODE (12) can be rewritten as

$$\frac{\mathrm{d}\boldsymbol{v}}{\mathrm{d}t} = \tilde{\boldsymbol{h}}.$$

The derivative matrix for the above ODE is defined by

$$\boldsymbol{H}(\boldsymbol{v}) = \frac{\partial \tilde{\boldsymbol{h}}}{\partial \boldsymbol{v}^T} = \begin{pmatrix} \frac{\partial \tilde{\boldsymbol{h}}_0(\boldsymbol{v}_n)}{\partial \boldsymbol{v}_n^T} & \cdots & \frac{\partial \tilde{\boldsymbol{h}}_0(\boldsymbol{v}_n)}{\partial \boldsymbol{v}_{n-(i-1)^T}} \\ & \ddots & \\ \frac{\partial \tilde{\boldsymbol{h}}_{i-1}(\boldsymbol{v}_{n-(i-1)})}{\partial \boldsymbol{v}_n^T} & \cdots & \frac{\partial \tilde{\boldsymbol{h}}_{i-1}(\boldsymbol{v}_{n-(i-1)})}{\partial \boldsymbol{v}_{n-(i-1)^T}} \end{pmatrix}$$
$$\equiv [\boldsymbol{H}_{p,q}] \quad (p = 1, \cdots, i \quad q = 1, \cdots, i).$$

From (12), each block of the derivative matrix at an equilibrium point is evaluated as follows;

$$\boldsymbol{H}_{p,q}^* = \boldsymbol{H}_{p,q}|_{\boldsymbol{v}=\boldsymbol{v}^*} \tag{13}$$
$$= \begin{cases} \sum_{j=1}^{n-p}(-\lambda_j + \lambda_{n-(p-1)})\boldsymbol{u}_j\boldsymbol{u}_j^T \\ -2\lambda_{n-(p-1)}\boldsymbol{u}_{n-(p-1)}\boldsymbol{u}_{n-(p-1)}^T & (p = q) \\ (\lambda_{n-(p-1)} - \lambda_{n-(q-1)}) \\ \quad \boldsymbol{u}_{n-(q-1)}\boldsymbol{u}_{n-(p-1)}^T & (p > q) \\ \boldsymbol{0} & (p < q) \end{cases}$$
$$(p = 1, \cdots, i \quad q = 1, \cdots, i).$$

The matrix $\boldsymbol{S}(\boldsymbol{v})$ is defined by

$$\boldsymbol{S}(\boldsymbol{v}) = \mathrm{E}\left[\boldsymbol{h}(\boldsymbol{v}, \boldsymbol{x}_n(0), \cdots, \boldsymbol{x}_{n-(i-1)}(0)) \boldsymbol{h}^T(\boldsymbol{v}, \boldsymbol{x}_n(0), \cdots, \boldsymbol{x}_{n-(i-1)}(0))\right]$$
$$\equiv [\boldsymbol{S}_{p,q}] \quad (p = 1 \cdots i \quad q = 1 \cdots i).$$

From (11), each block of the matrix $\boldsymbol{S}(\boldsymbol{v}^*)$ at an equilibrium point $\boldsymbol{v}^*$ is evaluated as

$$\boldsymbol{S}_{p,q}^* = \boldsymbol{S}_{p,q}|_{\boldsymbol{v}=\boldsymbol{v}^*} \tag{14}$$
$$= \begin{cases} \lambda_{n-(p-1)}\boldsymbol{C} - \lambda_{n-(p-1)}^2 \boldsymbol{u}_{n-(p-1)}\boldsymbol{u}_{n-(p-1)}^T \\ \qquad (p = q) \\ -\lambda_{n-(p-1)}\lambda_{n-(q-1)}\boldsymbol{u}_{n-(q-1)}\boldsymbol{u}_{n-(p-1)}^T \\ \qquad (p \neq q) \end{cases}$$
$$(p = 1, \cdots, i \quad \text{and} \quad q = 1, \cdots, i).$$

By substituting (13) and (14) into the Lyapunov equation and solving it, the covariance matrix

$$\boldsymbol{D} = \frac{\mathrm{E}\left[(\boldsymbol{v} - \boldsymbol{v}^*)(\boldsymbol{v} - \boldsymbol{v}^*)^T\right]}{\mu} \equiv \begin{bmatrix} \boldsymbol{D}_{1,1} & \cdots & \boldsymbol{D}_{1,i} \\ & \ddots & \\ \boldsymbol{D}_{i,1} & \cdots & \boldsymbol{D}_{i,i} \end{bmatrix}$$

is obtained as

$$\boldsymbol{D}_{p,q} = \begin{cases} \frac{1}{2}\sum_{j=1}^{n-1} \frac{\lambda_j\lambda_n}{\lambda_j - \lambda_n}\boldsymbol{u}_j\boldsymbol{u}_j^T & (p = q = 1) \\ \frac{1}{2}\sum_{j=1}^{n-p} \frac{\lambda_j\lambda_{n-(p-1)}}{\lambda_j - \lambda_{n-(p-1)}}\boldsymbol{u}_j\boldsymbol{u}_j^T \\ + \sum_{j=n-(p-2)}^{n} k_{p,j}\boldsymbol{u}_j\boldsymbol{u}_j^T & (p = q \neq 1) \\ -\frac{1}{2}\frac{\lambda_{n-(p-1)}\lambda_{n-(q-1)}}{|\lambda_{n-(p-1)} - \lambda_{n-(q-1)}|}\boldsymbol{u}_{n-(q-1)}\boldsymbol{u}_{n-(p-1)}^T \\ \qquad (p \neq q) \end{cases}$$
$$(p = 1, \cdots, i \quad q = 1, \cdots, i) \tag{15}$$

In (15), there are indeterminate terms in the diagonal blocks except $\boldsymbol{D}_{1,1}$. These terms are expressed by the parameter $k_{p,j}$, which can be determined from the constraint related to the i-th minor component

$$\boldsymbol{v}_{n-(i-1)}^T(k)\boldsymbol{v}_{n-(l-1)}(k) = 0 \quad (l = 1, \cdots, i-1). \tag{16}$$

The vector $\boldsymbol{v}_{n-(i-1)}$ is expressed as

$$\boldsymbol{v}_{n-(i-1)}(k) = \boldsymbol{u}_{n-(i-1)} - \Delta\boldsymbol{v}_{n-(i-1)}(k) \tag{17}$$

where $\Delta\boldsymbol{v}_{n-(i-1)}(k)$ denotes an estimation error. By substituting (17) into the constraint (16), expanding it, and ignoring the second order term with respect to $\Delta\boldsymbol{v}_{n-(i-1)}(k)$, the constraint is modified as

$$\boldsymbol{u}_{n-(i-1)}^T\Delta\boldsymbol{v}_{n-(l-1)}(k) + \Delta\boldsymbol{v}_{n-(i-1)}^T\boldsymbol{u}_{n-(l-1)}(k) \simeq 0. \tag{18}$$

	v^*_{10}		v^*_9		v^*_8	
	simulation	theoretical	simulation	theoretical	simulation	theoretical
1	4.370×10^{-3}	5.056×10^{-3}	5.776×10^{-2}	5.625×10^{-2}	1.367×10^{-1}	1.286×10^{-1}
2	3.715×10^{-3}	5.063×10^{-3}	5.244×10^{-2}	5.714×10^{-2}	1.422×10^{-1}	1.333×10^{-1}
3	4.089×10^{-3}	5.725×10^{-3}	4.094×10^{-2}	5.833×10^{-2}	1.129×10^{-1}	1.400×10^{-1}
4	5.743×10^{-3}	5.085×10^{-3}	7.324×10^{-2}	6.000×10^{-2}	1.149×10^{-1}	1.500×10^{-1}
5	5.762×10^{-3}	5.102×10^{-3}	6.904×10^{-2}	6.250×10^{-2}	1.756×10^{-1}	1.667×10^{-1}
6	6.097×10^{-3}	5.128×10^{-3}	7.442×10^{-2}	6.667×10^{-2}	1.620×10^{-1}	2.000×10^{-1}
7	4.424×10^{-3}	5.172×10^{-3}	7.505×10^{-2}	7.500×10^{-2}	2.546×10^{-1}	3.000×10^{-1}
8	7.398×10^{-3}	5.263×10^{-3}	1.088×10^{-1}	1.000×10^{-1}	2.660×10^{-4}	0
9	5.039×10^{-3}	5.556×10^{-3}	6.956×10^{-4}	0	1.075×10^{-1}	1.000×10^{-1}
10	1.199×10^{-3}	0	4.921×10^{-3}	5.556×10^{-3}	7.291×10^{-3}	5.263×10^{-3}

Table 1: The estimated and theoretical variances of the eigenvectors for the proposed algorithm of the multiple minor component analysis. The adaptive gain μ is 0.001. The iteration number is 100000.

By multiplying $\Delta \boldsymbol{v}^T_{n-(i-1)}(k)\boldsymbol{u}_{n-(l-1)}$ to (18) and taking the average, we have the following equation,

$$\boldsymbol{u}^T_{n-(i-1)}\boldsymbol{D}_{l,i}\boldsymbol{u}_{n-(l-1)} + \boldsymbol{u}^T_{n-(l-1)}\boldsymbol{D}_{i,i}\boldsymbol{u}_{n-(l-1)} \simeq 0 \quad (19)$$

where a relation

$$\mathrm{E}\left[\Delta \boldsymbol{v}_{n-(p-1)}(k)\Delta \boldsymbol{v}^T_{n-(q-1)}(k)\right] = \mu \boldsymbol{D}_{p,q}$$
$$(p = 1,\cdots,i \quad q = 1,\cdots,i)$$

is employed. By substituting (15) into (19), $k_{i,j}$ is obtained as

$$k_{i,j} = \frac{1}{2}\frac{\lambda_{n-(i-1)}\lambda_j}{\lambda_{n-(i-1)} - \lambda_j} \quad (j = n-(i-2),\cdots,n).$$

As a result, $\boldsymbol{D}_{p,q}$ is finally given by

$$\boldsymbol{D}_{p,q} = \begin{cases} \frac{1}{2}\sum_{j=1}^{n-1}\frac{\lambda_j\lambda_n}{\lambda_j-\lambda_n}\boldsymbol{u}_j\boldsymbol{u}_j^T & (p=q=1) \\ \frac{1}{2}\sum_{j=1}^{n-p}\frac{\lambda_j\lambda_{n-(p-1)}}{\lambda_j-\lambda_{n-(p-1)}}\boldsymbol{u}_j\boldsymbol{u}_j^T \\ \quad +\frac{1}{2}\sum_{j=n-(p-2)}^{n}\frac{\lambda_{n-(p-1)}\lambda_j}{\lambda_{n-(p-1)}-\lambda_j}\boldsymbol{u}_j\boldsymbol{u}_j^T \\ & (p=q\neq 1) \\ -\frac{1}{2}\frac{\lambda_{n-(p-1)}\lambda_{n-(q-1)}}{|\lambda_{n-(p-1)}-\lambda_{n-(q-1)}|}\boldsymbol{u}_{n-(q-1)}\boldsymbol{u}^T_{n-(p-1)} \\ & (p\neq q) \end{cases}$$
$$(p=1,\cdots,i \quad q=1,\cdots,i). \quad (20)$$

6 SIMULATION RESULTS

The estimated covariances of some eigenvectors extracted by the algorithm for multiple minor component analysis described in Section 2 are compared with the theoretical values calculated by (20). Ten dimensional random vectors with zero mean and the covariance matrix $\boldsymbol{C} = \mathrm{diag}[\,0.9,\ 0.8,\ \cdots,\ 0.1,\ 0.01\,]$ are generated as an input signals. The adaptive gain μ is set to 0.001. In our simulation, we fix $i = 3$, that is, three minor components are extracted. The number of independent trials is 30. In each trial, the covariance is calculated after 100000 iterations and whole estimated values are averaged. These results are shown in Tab.1. These theoretical results are roughly close to the theoretical values. This implies that the analysis with ODE approach gives a reasonable result.

7 CONCLUSION

The multiple minor component extraction algorithm based on the algorithm proposed by Douglas *et al.* has been proposed by applying the deflation technique. We have analyzed the asymptotic behavior of the algorithm by the ODE method and demonstrated that the estimated covariances by the simulations were close to the theoretical values.

References

[1] E. Oja, "Principal components, minor components and linear neural networks," *Neural Networks*, vol. 5, pp. 927-935, 1992.

[2] H. Sakai and K. Shimizu, "A new adaptive algorithm for minor component analysis," *Signal Processing*, vol. 71, pp. 301-308, 1998.

[3] B. Yang, "Projection approximation subspace tracking," *IEEE Trans. Signal Processing*, vol. 43, pp.95-107, Jan. 1995.

[4] V. Solo and X. Kong, "Performance analysis of adaptive eigenanalysis algorithms," IEEE Trans. Signal Processing, vol. 46, pp. 636-646, March 1998.

[5] A. Benveniste, M. Méitivier, and P. Priouret, *Adaptive Algorithms and Stochastic Approximations*, Springer-Verlag, 1990.

[6] S. C. Douglas, S. Y. Kung, and S. Amari, "On the numerical stabilities of principal, minor, and independent component analysis algorithm," *Proc. of the First Int. Workshop on Independent Component Analysis and Signal Processing*, pp. 419-424, 1999.

PERFORMANCE COMPARISON BETWEEN THE FILTERED-ERROR LMS AND THE FILTERED-X LMS ALGORITHMS

Shigeyuki Miyagi and Hideaki Sakai

Dept. of Systems Science, Graduate School of Informatics, Kyoto University
Yoshida, Sakyou-ku, Kyoto, 606-8501 Japan.
miyagi@i.kyoto-u.ac.jp, hsakai@i.kyoto-u.ac.jp

ABSTRACT

Several properties of the filtered-error (filtered-E) least mean square (LMS) algorithm, such as the stability condition, the upper limit of the step size and the variance of the error signal are quantitatively evaluated and compared with the those of the filtered-X LMS algorithm. For this purpose, the averaging method and the ordinary differential equation (ODE) method are applied to the frequency domain expression of both algorithms. From the averaged system, it is demonstrated that the stability condition and the upper limit of the step size of the filtered-E LMS algorithm are same with those of the filtered-X LMS algorithm. On the other hand, from the ODE analysis, it is shown that the excess mean square error of the filtered-E LMS algorithm is two thirds of that of the filtered-X LMS algorithm.

1. INTRODUCTION

Adaptive feedforward control systems are used in active noise control (ANC). The filtered-X LMS algorithm [1] is one of the most popular method to adapt the controller. As an alternative, the filtered-E LMS algorithm has been proposed by Wan[2]. It has been demonstrated by some simulations in [2] that this method has identical performance about the convergence and the misadjustment with those of the filtered-X LMS algorithm. The theoretical stability condition of the filtered-E LMS algorithm has been derived by Feintuch et al.[3]. In [3], a frequency domain technique is used to analyze the filtered-E type LMS algorithm. The stability condition of the mean weight vector and the second order stability are examined.

In this paper, we also use a similar technique, but we directly obtain the frequency domain expression of the algorithm by converting the time domain algorithm with the discrete Fourier transform unlike the method in [3]. By applying the averaging method[4] and ODE method[5] to the frequency domain expression, we can obtain the clear formulas of the stability condition, the upper limit of the step size and the expression of the excess mean square error. These results are compared with those of the filtered-X LMS algorithm.

2. THE AVERAGING METHOD AND THE ODE METHOD

Here we give a brief review of the averaging method in [4] and the ODE method in [5]. Consider the following general adaptive algorithm with appropriate regularity conditions

$$\boldsymbol{\theta}(k+1) = \boldsymbol{\theta}(k) + \mu \boldsymbol{h}(\boldsymbol{\theta}(k), \boldsymbol{x}(k)) \tag{1}$$

where $\boldsymbol{\theta}$ is a parameter vector, $\boldsymbol{x}$ is a random input signal and μ is the adaptive gain. The averaged system corresponding to (1) is

$$\bar{\boldsymbol{\theta}}(k+1) = \bar{\boldsymbol{\theta}}(k) + \mu \tilde{\boldsymbol{h}}(\bar{\boldsymbol{\theta}}(k)) \tag{2}$$

with $\tilde{\boldsymbol{h}}(\boldsymbol{\theta}) = \mathrm{E}\left[\boldsymbol{h}(\boldsymbol{\theta}, \boldsymbol{x}(k))\right]$. The convergence property of (1) can be examined by examining that of the averaged system (2).

On the other hand, the ODE corresponding to (1) is given by $\mathrm{d}\boldsymbol{\theta}(t)/\mathrm{d}t = \tilde{\boldsymbol{h}}(\boldsymbol{\theta}(t))$. It is assumed that an equilibrium point of the ODE exists and is denoted by $\boldsymbol{\theta}_*$. Under some regularity conditions, if all the eigenvalues of the derivative matrix $\boldsymbol{H}(\boldsymbol{\theta}_*)$ defined by

$$\boldsymbol{H}(\boldsymbol{\theta}_*) = \left.\frac{\mathrm{d}\tilde{\boldsymbol{h}}(\boldsymbol{\theta})}{\mathrm{d}\boldsymbol{\theta}^T}\right|_{\boldsymbol{\theta}=\boldsymbol{\theta}_*} \tag{3}$$

have negative real parts and if the matrix

$$\boldsymbol{S}(\boldsymbol{\theta}) = \sum_{k=-\infty}^{\infty} \mathrm{E}\left[\boldsymbol{h}(\boldsymbol{\theta}, \boldsymbol{x}(k))\boldsymbol{h}^\dagger(\boldsymbol{\theta}, \boldsymbol{x}(0))\right] \tag{4}$$

exists, $\mu^{-1/2}[\boldsymbol{\theta}(k) - \boldsymbol{\theta}_*]$ converges asymptotically ($k \to \infty$ and $\mu \to 0$) to a zero mean normal distributed random vector weakly with a covariance matrix $\boldsymbol{Y}$, which is the solution of the Lyapunov equation

$$\boldsymbol{H}(\boldsymbol{\theta}_*)\boldsymbol{Y} + \boldsymbol{Y}\boldsymbol{H}^\dagger(\boldsymbol{\theta}_*) = -\boldsymbol{S}(\boldsymbol{\theta}_*) \tag{5}$$

where † denotes the transpose of the complex conjugate vector or matrix.

3. STABILITY CONDITION BY THE AVERAGING METHOD

The block diagram of the ANC system using the filtered-E LMS algorithm is depicted in Fig.1(a) where $P(z)$ denotes the transfer function of the cascade of the primary path and the secondary path. The N-dimensional vector whose elements are coefficients of $P(z)$ is expressed by $\boldsymbol{p}$. $S(z)$ denotes the transfer function of the secondary path. In the filtered-E LMS algorithm, the error signal $e(k)$ is filtered

0-7803-6685-9/01/$10.00©2001 IEEE

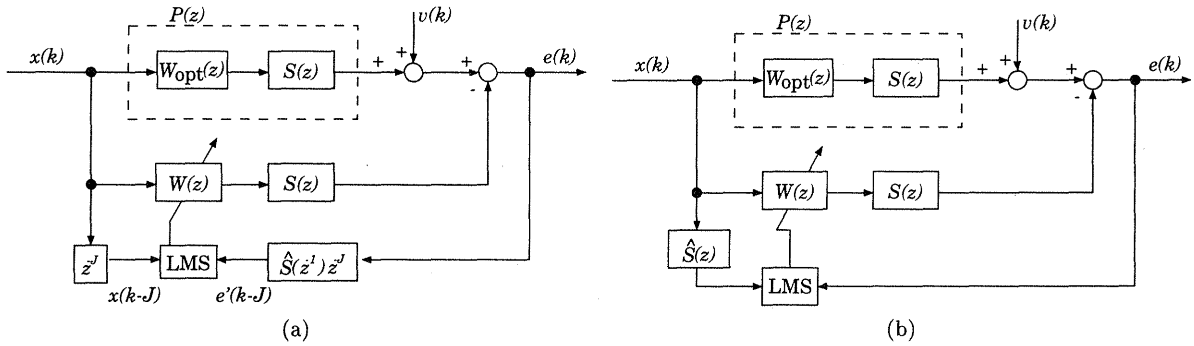

Figure 1: Block diagram of ANC with (a) the filtered-E LMS algorithm where J is the order of $\hat{S}(z)$ and (b) the filtered-X LMS algorithm.

by $\hat{S}(z^{-1})z^{-J}$ where J is the order of $\hat{S}(z)$ and $\hat{S}(z^{-1})$ denotes the time reversed version of the estimated secondary path transfer function $\hat{S}(z)$. The delay z^{-J} is introduced to retrieve the causality in the filtering operation. The tap vectors of $S(z)$ and $\hat{S}(z)$ are described by $\boldsymbol{s}$ and $\hat{\boldsymbol{s}}$ with the tap length N_s where $J = N_s - 1$ and it is assumed that N_s is sufficiently smaller than N. The tap vector of the adaptive transfer function $W(z)$ is expressed as $\boldsymbol{w}(k)$ whose tap length is $N - N_s + 1$ where k is the time index.

The tap vector $\boldsymbol{w}(k)$ is updated by

$$\boldsymbol{w}(k+1) = \boldsymbol{w}(k) + \mu \boldsymbol{x}'(k-J)e'(k-J) \tag{6}$$

where μ is the step size, $e'(k)$ is the error signal filtered by $\hat{S}(z^{-1})$, that is

$$e'(k) = \sum_{i=0}^{N_s-1} \hat{s}_i e(k+i), \tag{7}$$

and $\boldsymbol{x}'(k)$ is defined by $\boldsymbol{x}'(k) = [\ x(k),\ x(k-1),\ \cdots,\ x(k-N+N_s)\ ]^T$.

The output signal $y(k)$ is calculated as $y(k) = \sum_{i=0}^{N_s-1} s_i \sum_{j=0}^{N-N_s} w_j(k-i)x(k-i-j)$. Since $w_j(k-i)$ is slowly varying, we replace $w_j(k-i)$ by $w_j(k)$ and $y(k)$ is approximated by

$$y(k) \simeq (\boldsymbol{w}(k) * \boldsymbol{s})^T \boldsymbol{x}(k) \tag{8}$$

where $*$ denotes a vector convolution and the input signal vector, $\boldsymbol{x}(k)$, is defined by $\boldsymbol{x}(k) = [\ x(k),\ x(k-1),\ \cdots,\ x(k-N+1)\ ]^T$. The above approximation is justified as follows. Since from (6) the difference between $w_j(k-i)$ and $w_j(k)$ is of $O(\mu)$, its effect through $e'(k)$ in (6) is of $O(\mu^2)$ and this can be discarded.

From (8), the error signal $e(k)$ is given by

$$e(k) \simeq \boldsymbol{p}^T \boldsymbol{x}(k) - (\boldsymbol{w}(k) * \boldsymbol{s})^T \boldsymbol{x}(k) + v(k). \tag{9}$$

By applying the discrete Fourier transform (DFT) matrix $\boldsymbol{F} = [\exp(-i2\pi lm/N)]\quad l, m = 0, 1, \cdots, N-1$, the N point DFTs of $\boldsymbol{x}(k)$, $\boldsymbol{x}'(k)$, $\boldsymbol{p}$, $\boldsymbol{s}$, $\hat{\boldsymbol{s}}$, $\boldsymbol{w}(k)$ are denoted as $\boldsymbol{X}(k)$, $\boldsymbol{X}'(k)$, $\boldsymbol{P}$, $\boldsymbol{S}$, $\hat{\boldsymbol{S}}$, $\boldsymbol{W}(k)$, respectively. Since the lengths of $\boldsymbol{s}$, $\hat{\boldsymbol{s}}$, $\boldsymbol{x}'(k)$ and $\boldsymbol{w}(k)$ are less than N, $N - N_s$ or $N_s - 1$ zeros are padded. Hence, (9) is rewritten as

$$e(k) \simeq -\frac{1}{N}\boldsymbol{X}^\dagger(k)\boldsymbol{F}(\Delta\boldsymbol{w}(k) * \boldsymbol{s}) + v(k)$$

where we assume that $P(z) = W_{\rm opt}(z)S(z)$, that is $\boldsymbol{p} = \boldsymbol{w}_{\rm opt} * \boldsymbol{s}$ and $\Delta\boldsymbol{w}(k) = \boldsymbol{w}(k) - \boldsymbol{w}_{\rm opt}$. From the property of DFT, we have

$$e(k) \simeq -\frac{1}{N}\boldsymbol{X}^\dagger(k)\boldsymbol{\Lambda}_S \Delta\boldsymbol{W}(k) + v(k) \tag{10}$$

where $\boldsymbol{\Lambda}_S$ is a diagonal matrix defined by $\boldsymbol{\Lambda}_S = \mathrm{diag}[\ S_0,\ S_1,\ \cdots,\ S_{N-1}\ ]$ whose each element corresponds to each element in $\boldsymbol{S}$. From (10), the variance of $e(k)$ is calculated as

$$\mathrm{E}[|e(k)|^2] = \frac{1}{N^2}\mathrm{E}\left[\boldsymbol{X}^\dagger(k)\boldsymbol{\Lambda}_S\Delta\boldsymbol{W}(k)\Delta\boldsymbol{W}^\dagger(k)\boldsymbol{\Lambda}_S^\dagger\boldsymbol{X}(k)\right] + \sigma_v^2, \tag{11}$$

since we assume that $v(k)$ is white noise with zero mean and the variance σ_v^2 and is uncorrelated with $\boldsymbol{X}(k)$ and $\Delta\boldsymbol{W}(k)$. By applying the DFT matrix to (6), the following adaptive algorithm is obtained,

$$\begin{aligned}\Delta\boldsymbol{W}(k+1) &= \Delta\boldsymbol{W}(k) + \mu\boldsymbol{F}\boldsymbol{x}'(k-J)e'(k-J) \qquad (12)\\ &\equiv \Delta\boldsymbol{W}(k) + \mu h(\Delta\boldsymbol{W}(k-J), \boldsymbol{X}(k), v(k)).\end{aligned}$$

This is an adaptive (time-varying) algorithm about the discrete frequency response of the original adaptive filter. To analyze this, let us consider the averaged system corresponding to (12). By substituting (10) into (7), the following approximation is obtained,

$$e'(k) \simeq -\frac{1}{N}\sum_{j=0}^{N_s-1}\hat{s}_j\boldsymbol{X}^\dagger(k+j)\boldsymbol{\Lambda}_S\Delta\boldsymbol{W}(k) + \sum_{j=0}^{N_s-1}\hat{s}_j v(k+j) \tag{13}$$

From the above approximation and $\boldsymbol{F}\boldsymbol{x}'(k) \simeq \boldsymbol{X}(k)$, the average of $\boldsymbol{F}\boldsymbol{x}'(k)e'(k)$ for fixed $\Delta\bar{\boldsymbol{W}}(k)$ is given by

$$\mathrm{E}[\boldsymbol{F}\boldsymbol{x}'(k)e'(k)] = -\frac{1}{N}\sum_{j=0}^{N_s-1}\hat{s}_j\mathrm{E}\left[\boldsymbol{X}(k)\boldsymbol{X}^\dagger(k+j)\right]\boldsymbol{\Lambda}_S\Delta\bar{\boldsymbol{W}}(k). \tag{14}$$

The (m,l)-th element of $\mathrm{E}\left[\boldsymbol{X}(k)\boldsymbol{X}^\dagger(k+j)\right]$ is

$$\begin{aligned}&\mathrm{E}\left[X_m(k)X_l^*(k+j)\right]\\ &\quad = e^{i\frac{2\pi jl}{N}}\mathrm{E}\left[\sum_{p=0}^{N-1}x(k-p)e^{-\frac{i2\pi pm}{N}}\sum_{q=-j}^{N-1-j}x(k-q)e^{\frac{i2\pi ql}{N}}\right]\end{aligned}$$

where $X_m(k)$ is the m-th element of $\boldsymbol{X}(k)$. From the theorem related to the cumulant of finite Fourier transform of time series in [7], we have

$$\mathrm{E}\left[X_m(k)X_l^*(k+j)\right] \simeq \mathrm{e}^{\mathrm{i}\frac{2\pi jl}{N}}(N-j)f_x(\omega_l)\delta_{lm} \quad (15)$$

where $f_x(\omega)$ is the spectral density of the input signal and $\omega_l = 2\pi l/N$. Since the maximum value of j, that is $N_s - 1$ is sufficiently smaller than N, (15) is further approximated as

$$\mathrm{E}\left[X_m(k)X_l^*(k+j)\right] \simeq \mathrm{e}^{\mathrm{i}\frac{2\pi jl}{N}}Q_l\delta_{lm}. \quad (16)$$

where Q_l is a diagonal element of $\boldsymbol{Q} \equiv \mathrm{E}[\boldsymbol{X}(k)\boldsymbol{X}^\dagger(k)]$ and $f_x(\omega_l) \simeq Q_l/N$ is used. Since each element of $\boldsymbol{X}(k)$ is independent from each other as $N \to \infty$ due to the property of stationary processes, $\boldsymbol{Q}$ is approximately expressed as a diagonal matrix, $\boldsymbol{Q} = \mathrm{diag}[\, Q_0,\ Q_1,\ \cdots,\ Q_{N-1}\,]$. By substituting (16) into (14), the averaged system corresponding to (12) is obtained as

$$\Delta\bar{\boldsymbol{W}}(k+1) = \Delta\bar{\boldsymbol{W}}(k) - \frac{\mu}{N}\boldsymbol{Q}\boldsymbol{\Lambda}_{\hat{S}}^*\boldsymbol{\Lambda}_S\Delta\bar{\boldsymbol{W}}(k-J) \quad (17)$$

where we use $\boldsymbol{\Lambda}_{\hat{S}} = \mathrm{diag}\left[\,\hat{S}_0,\ \hat{S}_1,\ \cdots,\ \hat{S}_{N-1}\,\right]$.

All the matrices in (17) are diagonal so that (17) can be decomposed into the recursive equation for each element of $\Delta\bar{\boldsymbol{W}}(k)$. The characteristic equation for each recursive equation is obtained as $z - 1 + \alpha_l z^{-J} = 0$, $l = 0,\ 1,\ \cdots,\ N-1$ where $\alpha_l = \mu\hat{S}_l^* Q_l S_l/N$. By substituting $z = 1+\varepsilon$ into the above equation, the approximated solution, $\varepsilon \simeq -\alpha_l/(1-\alpha_l J) \simeq -\alpha_l$ is obtained where $O(\mu^2)$ and higher order terms are discarded. From the condition $|1+\varepsilon| < 1$, the upper limit of μ is obtained as

$$\mu < \frac{2\mathrm{Re}[\hat{S}_l^* S_l]}{f_x(\omega_l)|\hat{S}_l^* S_l|^2}, \quad l = 0,\ 1,\ \cdots,\ N-1.$$

This bound coincides with the upper limit of the step size of the filtered-X LMS algorithm. To keep μ positive,

$$\mathrm{Re}[\hat{S}_l^* S_l] > 0 \quad (18)$$

is required. This implies that the phase difference between $S(z)$ and $\hat{S}(z)$ must be less than $\pi/2$, which coincides with the stability condition of the filtered-X LMS algorithm[1].

4. SECOND ORDER ANALYSIS BY THE ODE

The ODE corresponding to (12) is given by

$$\frac{\mathrm{d}\Delta\boldsymbol{W}}{\mathrm{d}t} = -\frac{1}{N}\boldsymbol{\Lambda}_{\hat{S}}^*\boldsymbol{Q}\boldsymbol{\Lambda}_S\Delta\boldsymbol{W} \equiv \bar{h}(\Delta\boldsymbol{W}) \quad (19)$$

with an equilibrium point $\Delta\boldsymbol{W}_* = \boldsymbol{0}$.

To evaluate the covariance matrix of $\Delta\boldsymbol{W}(k)$, let us begin to calculate the two matrices in (3) and (4). From (19), $\boldsymbol{H}(\Delta\boldsymbol{W})$ is easily calculated as

$$\boldsymbol{H}(\Delta\boldsymbol{W}) = -\frac{1}{N}\boldsymbol{\Lambda}_{\hat{S}}^*\boldsymbol{Q}\boldsymbol{\Lambda}_S. \quad (20)$$

This is a stable matrix under (18). From (12) and (13) with $\Delta\boldsymbol{W}_* = \boldsymbol{0}$, we have

$$\boldsymbol{h}(\Delta\boldsymbol{W}_*, \boldsymbol{X}(k), v(k)) = \boldsymbol{X}'(k-J)\sum_{j=0}^{N_s-1}\hat{s}_j v(k-J+j).$$

Using the property $\boldsymbol{F}\boldsymbol{F}^\dagger/N = \boldsymbol{I}$, the (m, m')-th element of $\boldsymbol{S}(\Delta\boldsymbol{W}_*)$ is described as

$$\frac{1}{N^2}\sum_{k=-\infty}^{\infty} A_{mm'}\mathrm{e}^{\mathrm{i}(\omega_m-\omega_{m'})J} \sum_{j=0}^{N-1}\hat{S}_j\sum_{j'=0}^{N-1}\hat{S}_{j'}^* B_{jj'}\mathrm{e}^{-\mathrm{i}(\omega_m-\omega_j)k}\mathrm{e}^{-\mathrm{i}(\omega_j-\omega_{j'})J} \quad (21)$$

where

$$A_{mm'} = \mathrm{E}\left[\sum_{p=-k+J}^{-k+N-N_s+J} x(-p)\mathrm{e}^{-\mathrm{i}\omega_m p}\sum_{p'=J}^{N-N_s+J} x(-p')\mathrm{e}^{\mathrm{i}\omega_{m'}p'}\right]$$

$$B_{jj'} = \mathrm{E}\left[\sum_{l=-k+J}^{-k+J-N+1} v(-l)\mathrm{e}^{\mathrm{i}\omega_j l}\sum_{l'=J}^{J-N+1} v(-l')\mathrm{e}^{-\mathrm{i}\omega_{j'}l'}\right].$$

By applying the theorem in [7] again and using $N_s \ll N$, we obtain the following approximations

$$A_{mm'} \simeq \begin{cases} (N-|k|)f_x(\omega_m)\delta_{mm'} & |k| \le N \\ 0 & \text{otherwise} \end{cases}$$

$$B_{jj'} \simeq \begin{cases} (N-|k|)f_v(\omega_j)\delta_{jj'} & |k| \le N \\ 0 & \text{otherwise} \end{cases},$$

where $f_v(\omega)$ is the spectral density of the additive noise $v(n)$. By using the above approximations, (21) is further approximated as

$$\begin{aligned}(21) \quad &\simeq \quad \frac{1}{N^2}\delta_{mm'}f_x(\omega_m)\sum_{j=0}^{N-1}\hat{S}_j\hat{S}_j^* f_v(\omega_j) \\ &\qquad \times \sum_{k=-N}^{N}(N-|k|)^2\mathrm{e}^{-\mathrm{i}(\omega_m-\omega_j)k} \\ &\simeq \quad \frac{2}{3}Q_m\hat{S}_m\hat{S}_m^* f_v(\omega_m)\delta_{mm'}\end{aligned}$$

where we use $(2N/3)\delta_{mj}$ as the approximation of the sum with respect to k as $N \to \infty$. From the assumption that $\{v(k)\}$ is white with the variance σ_v^2, $f_v(\omega_m)$ is replaced by σ_v^2. As a result, the matrix $\boldsymbol{S}(\Delta\boldsymbol{W}_*)$ can be approximately evaluated as

$$\boldsymbol{S}(\Delta\boldsymbol{W}_*) = \frac{2}{3}\sigma_v^2\boldsymbol{\Lambda}_{\hat{S}}^*\boldsymbol{Q}\boldsymbol{\Lambda}_{\hat{S}} \quad (22)$$

From (20) and (22), the solution of the corresponding Lyapunov equation in (5) is given by

$$\boldsymbol{Y} = \mathrm{diag}[\, Y_0,\ Y_1,\ \cdots,\ Y_{N-1}\,], \quad Y_l = \frac{N\sigma_v^2|\hat{S}_l|^2}{3\mathrm{Re}[\hat{S}_l^* S_l]}.$$

By using $\mathrm{E}[\Delta\boldsymbol{W}(k)\Delta\boldsymbol{W}^\dagger(k)] = \mu\boldsymbol{Y}$, the variance of the error signal is rewritten as

$$\begin{aligned}\mathrm{E}[|e(k)|^2] \quad &= \quad \frac{1}{N^2}\mathrm{Tr}\left[\boldsymbol{\Lambda}_S\mu\boldsymbol{Y}\boldsymbol{\Lambda}_S^\dagger\boldsymbol{Q}\right] + \sigma_v^2 = \sigma_v^2(1+\zeta\mu N) \\ \zeta \quad &= \quad \frac{1}{3N^2}\sum_{l=0}^{N-1}\frac{|\hat{S}_l S_l|^2 Q_l}{\mathrm{Re}[\hat{S}_l^* S_l]}.\end{aligned} \quad (23)$$

N_s	filtered-E LMS theoretical ζ	simulation $N=128$ filtered-E LMS ζ_a	FXLMS ζ_f	ζ_a/ζ_f	simulation $N=256$ Filtered-E LMS ζ_a	FXLMS ζ_f	ζ_a/ζ_f
2	0.1667	0.3219	0.3222	0.9991	0.2580	0.2670	0.9663
3	0.1202	0.1965	0.1995	0.9850	0.1271	0.1809	0.7026
4	0.1047	0.1993	0.2624	0.7595	0.1457	0.1617	0.9011
8	0.1628	0.2920	0.3455	0.8452	0.2644	0.3153	0.8386
12	0.1762	0.3329	0.3639	0.9148	0.2389	0.3416	0.6994

Table 2: Comparison of the excess mean square errors in the filtered-E LMS (ζ_a) with those in the filtered-X LMS (ζ_f).

$\hat{s}_1$	simulation	$\hat{s}_1$	simulation
0.9	stable	1.0	stable
0.925	stable	1.025	stable
0.95	stable	1.05	unstable
0.975	stable	1.075	unstable
		1.1	unstable

Table 1: Verification of the stability for some cases of $\hat{s}_1$. The theoretical stability condition is $\hat{s}_1 < 1.0$.

A similar argument can be also made to the filtered-X LMS algorithm shown in Fig.1(b) and the same form of the ODE is obtained. However, the coefficient 2/3 in (22) disappears. This result implies that the excess mean square error of the filtered-E LMS algorithm is reduced as compared with that of the filtered-X LMS algorithm.

5. SIMULATION RESULTS

First, we verify the stability condition for a simple case in which we assume that the orders of filters $S(z)$ and $\hat{S}(z)$ are one, that is $S(z) = s_0 + s_1 z^{-1}$ and $\hat{S}(z) = \hat{s}_0 + \hat{s}_1 z^{-1}$. In this case, the stability condition (18) can be rewritten as $s_0\hat{s}_0 + s_1\hat{s}_1 > s_0\hat{s}_1 + \hat{s}_0 s_1$. We set the variance of the input signal, the variance of the additive noise and the step size to 1.0, 1.0×10^{-4} and 0.002, respectively. An FIR filter with the tap length 64 is used as $W_{\mathrm{opt}}(z)$. The tap coefficients s_0, s_1 and $\hat{s}_0$ are fixed to 1.0, 0.5 and 1.0. From these values, the theoretical limit of the stability condition is given by $\hat{s}_1 < 1.0$. Some simulations are performed for various values of $\hat{s}_1$ between 0.9 and 1.1 in every 0.025 steps and the results are listed in Table 1. The marginal value 1.025 is considerably close to the theoretical value 1.0.

Second, we evaluate the excess mean square errors of the filtered-E LMS algorithm and compare them with those in the filtered-X LMS algorithm. FIR filters with tap length 128 and 256 are used as the transfer function W_{opt} which has the impulse response simulating the characteristics of a duct in [1]. For convenience, we assume that $S(z) = \hat{S}(z)$ and $S(z)$, $\hat{S}(z)$ are lowpass filters with cut off frequency $3\pi/5$. The variance of the input signal, the variance of the additive noise and the step size are set to 1.0, 1.0×10^{-4} and 0.001. Under each condition, 20 trials are performed and the empirical values of ζ are evaluated. These results are listed in Table 2. All the excess mean square errors of the filtered-E LMS, ζ_a's are almost equal or smaller than those of the filtered-X LMS, ζ_f's. These simulation results correspond to the theoretical result that ζ of the filtered-E LMS is reduced by a factor 1/3. It seems that ζ_a's tend to theoretical values as N becomes larger.

6. CONCLUSION

From the averaging analysis, it has been shown that the filtered-E LMS algorithm has the identical stability condition and the upper limit of the step size with the filtered-X LMS algorithm. From the ODE method, it has been demonstrated that the filtered-E LMS algorithm is slightly superior to the filtered-X LMS algorithm in the excess mean square error. These results have been verified by some simulations. It is a future work to extend these results to the multiple-input-multiple-output case.

7. REFERENCES

[1] S. M. Kuo and D. R. Morgan, Active Noise Control Systems. John Wiley & Sons Inc., 1996.

[2] E. A. Wan, "Adjoint LMS: an efficient alternative to the filtered-X LMS and multiple error LMS algorithm," Proc. ICASSP96, Atlanta, vol.3, pp.1843-1846.

[3] P. L. Feintuch, N. J. Bershad and A. K. Lo, "A frequency domain model for "filtered" LMS algorithms – stability analysis, design, and elimination of the training mode," IEEE Trans. Signal Processing, vol.41, No.4, pp.1518-1531, April, 1993.

[4] V. Solo and X. Kong, Adaptive Signal Processing Algorithms – Stability and Performance –. Prentice Hall, 1995.

[5] A. Benveniste, M. Métivier and P. Priouret, Adaptive Algorithms and Stochastic Approximations. Springer-Verlag, 1990.

[6] S. Miyagi and H. Sakai, "Convergence analysis of the delayless subband adaptive filter based on the frequency domain expression," Proc. ICASSP 2000, Istanbul, vol.1, pp.368-371.

[7] D. R. Brillinger, Time Series – Data Analysis and Theory –, New York: Holt, Rinehart and Wintston, 1975.

ANALYSIS OF THE ADAPTIVE FILTER ALGORITHM FOR FEEDBACK-TYPE ACTIVE NOISE CONTROL

Hideaki Sakai and Shigeyuki Miyagi

Dept. of Systems Science, Graduate School of Informatics, Kyoto University
Yoshida, Sakyou-ku, Kyoto, 606-8501 Japan
E-mail: hsakai@i.kyoto-u.ac.jp

ABSTRACT

The feedback-type active noise control (ANC) system uses only one microphone to provide necessary signals for adjusting the adaptive filter. Due to the complicated nature of the whole adaptive filter structure there have been no theoretical results about its convergence properties. In this paper, first a stationary point of the adaptive filter using the filtered-X LMS algorithm is obtained by the averaging method combined with the frequency domain technique. Then the local convergence condition is derived. This is a counterpart of the well-known 90° condition for the feedforward-type ANC. Finally, the convergence condition is explicitly given for a simple example and its validity is shown by some simulations.

1. INTRODUCTION

Recently there have been growing interests in the feedback-type active noise control (ANC) system in Fig.1 where only one microphone is used to provide necessary signals for adjusting the adaptive filter in ANC [1]. This is in contrast with the conventional feedforward-type ANC system where two microphones are used to pick up the reference signal to the primary path and the error signal at the end of the secondary path [2]. The convergence condition of the latter type ANC is well-known. The so-called 90° condition says that the phase difference between the transfer functions of the secondary path and its estimate should lie in the interval $(-\pi/2, \pi/2)$ [2]. However, as far as the authors are aware, there have been no theoretical results about the convergence properties of the feedback-type ANC algorithms. In this paper, we present some results about the stationary point of the adaptive filter and the convergence condition using the averaging method in [3] with the frequency domain technique developed in [4]. This technique converts adaptive algorithms into those in the discrete frequency domain by the discrete Fourier transform (DFT) and is successfully applied to the analysis of rather complicated adaptive systems such as the delayless subband adaptive filter where fixed filters, decimators and upsamples for rate conversion are included.

The configuration we are treating is due to [5] and is shown in Fig.2 where only the error signal picked up by the microphone is available. To generate a "reference" signal to the adaptive filter, the "feedback control" filter is inserted to recover the original external noise $w(n)$. But its transfer

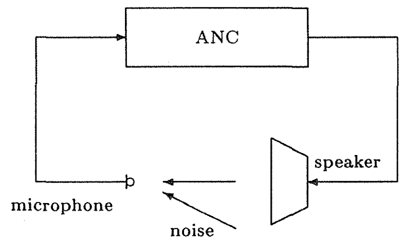

Fig. 1. Feedback-type active noise control system

function $\hat{B}(z)$ may be different from that of the (physical) feedback path $B(z)$ so that in general the artificially generated reference signal $x(n)$ is not exactly equal to $w(n)$. The weights in the adaptive filter are updated according to the filtered-X LMS algorithm. The idea behind this is that if $w(n)$ is available, the original problem becomes the optimal prediction of $w(n)$ by the output of the cascade of the adaptive filter and the physical feedback path $B(z)$ with the input $w(n)$. Interchanging the filters in the cascade and replacing $B(z)$, $w(n)$ by $\hat{B}(z)$, $x(n)$, respectively, we have the filtered-X LMS algorithm.

2. DERIVATION OF THE STATIONARY POINT OF THE ADAPTIVE FILTER

Since we are essentially dealing with the prediction problem of a zero mean stationary process $w(n)$, as stated in [6] some cares are needed to insure the causality of the steady state transfer function of the adaptive filter when the analysis is performed in the discrete frequency domain. We use the technique in [4] to analyze the scheme in Fig.2. The relations of the signals in Fig.2 are written as

$$e(n) = w(n) - \sum_{i=0}^{N_b-1} b_i x'(n-i) \quad (1)$$

$$x'(n) = \sum_{i=0}^{N-1} h_i(n) x(n-i) \quad (2)$$

$$x(n) = e(n) + \sum_{i=0}^{N_b-1} \hat{b}_i x'(n-i) \quad (3)$$

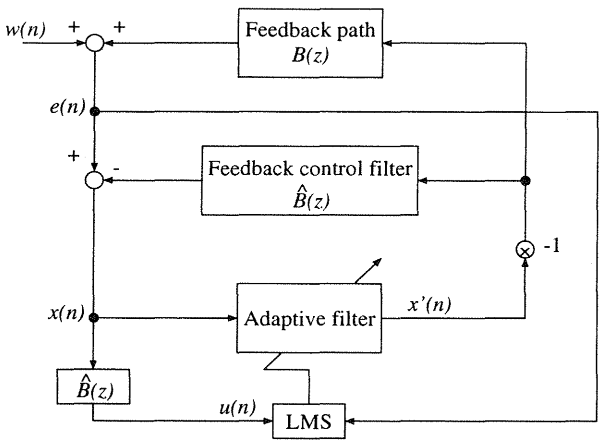

Fig. 2. Block diagram of the adaptive filter for feedback-type ANC

where N is the number of the tap coefficients $\{h_i(n)\}$ of the adaptive filter, $N_b - 1$ is the order of the transfer functions of $B(z)$ and $\hat{B}(z)$ whose impulse responses are $\{b_i\}$ and $\{\hat{b}_i\}$, respectively. We also assume that $N_b \ll N$. Then the error signal $e(n)$ is given by

$$e(n) = w(n) - \sum_{i=0}^{N_b-1} b_i \sum_{k=0}^{N-1} h_k(n-i)x(n-i-k). \qquad (4)$$

Since the tap weight $h_i(n)$ $(i = 0, 1, \cdots, N-1)$ is updated by the filtered-X LMS algorithm

$$h_i(n+1) = h_i(n) + \mu u(n-i)e(n) \qquad (5)$$

with a small positive gain μ, the difference between $h_k(n)$ and $h_k(n-i)$ is of $O(\mu)$. So its effect through $e(n)$ in (5) is of $O(\mu^2)$ and can be discarded. Hence, the second term in (4) can be regarded as the output of the cascade filter of the adaptive filter with the fixed $\{h_i(n)\}$ and the feedback path where the input is $x(n)$. So $e(n)$ is approximately expressed as

$$e(n) \simeq w(n) - \sum_{l=0}^{N-1} \left(\sum_{i=0}^{N_b-1} b_i h_{l-i}(n) \right) x(n-l). \qquad (6)$$

Next, we define the following L-dimensional vectors as

$$\begin{aligned} \boldsymbol{h}(n) &= [\ h_0(n),\ \cdots,\ h_{N-1}(n),\ \boldsymbol{0}^T\ ]^T \qquad (7) \\ \boldsymbol{x}(n) &= [\ x(n),\ \cdots,\ x(n-N+1),\ \boldsymbol{0}^T\ ]^T \end{aligned}$$

where "$\boldsymbol{0}$" denotes the $(L-N)$-dimensional zero vector and $L \geq 2N$. The reason why $L-N$ zeros are padded in (7) is that the N-point DFT of $\{h_i(n)\}$ $(i = 0, \cdots, N-1)$ results in the N-period sequence in the discrete frequency domain and this in turn introduces the N-periodicity in $\{h_i(n)\}$ through the inverse DFT. Thus $h_i(n)$ for negative i becomes non-zero. To avoid this and insure the causality zero padding is introduced [6]. Similarly we define the L-dimensional vectors for other signals and the vectors $\boldsymbol{b}$, $\hat{\boldsymbol{b}}$ with $(L - N_b)$ zeros padded for tap coefficients of $B(z)$ and $\hat{B}(z)$, respectively. Then (6) can be written as

$$e(n) \simeq w(n) - (\boldsymbol{b} \otimes \boldsymbol{h}(n))^{\dagger}\boldsymbol{x}(n) \qquad (8)$$

where "$\dagger$" and "$\otimes$" denote the complex conjugate transpose and the convolution, respectively. Also, $(\boldsymbol{b} \otimes \boldsymbol{h}(n))$ is made L-dimensional by deleting the extra zeros. Then the adaptive rule can be written as

$$\boldsymbol{h}(n+1) = \boldsymbol{h}(n) + \mu\boldsymbol{u}(n)e(n) \qquad (9)$$

Also, we define the L-point DFT matrix by

$$\boldsymbol{F} = \left[\exp\left(-\mathrm{j}\frac{2\pi lm}{L}\right)\right] \quad l, m = 0, 1, \cdots, L-1$$

and the L-point DFT of $\boldsymbol{w}$, $\boldsymbol{e}$, $\boldsymbol{x}$, $\boldsymbol{x}'$, $\boldsymbol{u}$, $\boldsymbol{h}$, $\boldsymbol{b}$, $\hat{\boldsymbol{b}}$ are denoted by the corresponding capital letters as $\boldsymbol{W}$, $\boldsymbol{E}$, $\boldsymbol{X}$, $\boldsymbol{X}'$, $\boldsymbol{U}$, $\boldsymbol{H}$, $\boldsymbol{B}$, $\hat{\boldsymbol{B}}$, respectively. Also the following diagonal matrix is defined for $\boldsymbol{H}(n) = (\ H_0(n),\ H_1(n),\ \cdots,\ H_{L-1}(n)\ )^T$ as

$$\boldsymbol{\Lambda}_{\boldsymbol{H}(n)} = \mathrm{diag}[\ H_0(n),\ H_1(n),\ \cdots,\ H_{L-1}(n)]$$

and similarly for $\boldsymbol{B}$, $\hat{\boldsymbol{B}}$ as $\boldsymbol{\Lambda}_B$, $\boldsymbol{\Lambda}_{\hat{B}}$. Noting that

$$\boldsymbol{F}^{\dagger}\boldsymbol{F} = L\boldsymbol{I}$$

where $\boldsymbol{I}$ denotes the $L \times L$ identity matrix and using this in (8) we have

$$\begin{aligned} e(n) &\simeq w(n) - \frac{1}{L}\boldsymbol{x}^{\dagger}(n)\boldsymbol{F}^{\dagger}\boldsymbol{F}(\boldsymbol{b} * \boldsymbol{h}(n)) \\ &\simeq w(n) - \frac{1}{L}\boldsymbol{X}^{\dagger}(n)\boldsymbol{\Lambda}_{\boldsymbol{B}}\boldsymbol{H}(n) \qquad (10) \end{aligned}$$

Applying $\boldsymbol{F}$ to (9) and using (10), we have

$$\boldsymbol{H}(n+1) = \boldsymbol{H}(n) + \mu\boldsymbol{U}(n)\left[w(n) - \frac{1}{L}\boldsymbol{X}^{\dagger}(n)\boldsymbol{\Lambda}_B\boldsymbol{H}(n)\right]. \qquad (11)$$

Since

$$u(n) = \sum_{i=0}^{N_b-1} \hat{b}_i x(n-i),$$

the l-th element of $\boldsymbol{U}(n)$ can be written as

$$(\boldsymbol{U}(n))_l = \sum_{i=0}^{N_b-1} \hat{b}_i e^{\mathrm{j}\frac{2\pi li}{L}} \sum_{k=i}^{L-1+i} x(n-k)e^{-\mathrm{j}\frac{2\pi lk}{L}}.$$

But the index i moves from 0 to $N_b - 1$ and $N_b \ll L$ so that we can replace the range of the second summation with $0 \leq k \leq L-1$ by neglecting the "end effects". Thus we have the approximate relation

$$\boldsymbol{U}(n) \simeq \boldsymbol{\Lambda}_{\hat{B}}^{*}\boldsymbol{X}(n), \qquad (12)$$

where "$*$" denotes the complex conjugate. Similarly the corresponding approximate expressions for (1)-(3) are

$$\begin{aligned} \boldsymbol{E}(n) &\simeq \boldsymbol{W}(n) - \boldsymbol{\Lambda}_B^{*}\boldsymbol{X}'(n) \\ \boldsymbol{X}'(n) &\simeq \boldsymbol{\Lambda}_{H(n)}^{*}\boldsymbol{X}(n) \qquad (13) \\ \boldsymbol{X}(n) &\simeq \boldsymbol{E}(n) + \boldsymbol{\Lambda}_{\hat{B}}^{*}\boldsymbol{X}'(n). \end{aligned}$$

Hence by eliminating $\boldsymbol{E}(n)$ and $\boldsymbol{X}'(n)$ in (13) we have

$$\boldsymbol{X}(n) \simeq \boldsymbol{Q}(n)\boldsymbol{W}(n) \tag{14}$$

with

$$\boldsymbol{Q}(n) = \left[\, \boldsymbol{I} + \boldsymbol{\Lambda}^*_{H(n)} \left(\boldsymbol{\Lambda}^*_B - \boldsymbol{\Lambda}^*_{\hat{B}}\right) \,\right]^{-1}. \tag{15}$$

Substituting (12) and (14) into (11) we have the discrete frequency domain expression of (9) as

$$\begin{aligned}\boldsymbol{H}(n+1) \simeq \boldsymbol{H}(n) + \mu &\left[\boldsymbol{\Lambda}^*_{\hat{B}}\boldsymbol{Q}(n)\boldsymbol{W}(n)w(n)\right.\\ &\left. - \frac{1}{L}\boldsymbol{\Lambda}^*_{\hat{B}}\boldsymbol{Q}(n)\boldsymbol{W}(n)\boldsymbol{W}^\dagger(n)\boldsymbol{Q}^\dagger(n)\boldsymbol{\Lambda}_B\boldsymbol{H}(n)\right]. \end{aligned} \tag{16}$$

Since L is large and $w(n)$ is a zero-mean stationary process, the element of $\boldsymbol{W}(n)$, that is, the DFT of $w(n)$ is uncorrelated with each other. Hence,

$$\mathrm{E}\left[\boldsymbol{W}(n)\boldsymbol{W}^\dagger(n)\right] \simeq L\mathrm{diag}\left[\, S_0,\ S_1,\ \cdots,\ S_{N-1} \,\right] \equiv L\boldsymbol{\Lambda}_S \tag{17}$$

where $S(\mathrm{e}^{\mathrm{j}\omega})$ is the spectral density of $w(n)$ and $S_l = S(\mathrm{e}^{\mathrm{j}\frac{2\pi l}{L}})$. Also,

$$w(n) = \frac{1}{L}\sum_{l=0}^{L-1}\sum_{k=0}^{L-1} w(n-k)\mathrm{e}^{\mathrm{j}\frac{2\pi l}{L}k} = \frac{1}{L}\boldsymbol{W}^\dagger(n)\boldsymbol{\pi} \tag{18}$$

where $\boldsymbol{\pi}$ is an L-dimensional vector whose elements are all 1. So from (17) and (18)

$$\mathrm{E}\left[\boldsymbol{W}(n)w(n)\right] \simeq \boldsymbol{\Lambda}_S\boldsymbol{\pi} = \boldsymbol{S}. \tag{19}$$

We use the averaging method in [3] to analyze (16). By taking the average with respect to $\boldsymbol{W}(n)$ and $w(n)$ in the right hand side of (16), replacing $\boldsymbol{H}(n)$ with the corresponding deterministic quantity $\bar{\boldsymbol{H}}(n)$ and using (17), (19), the averaged system is given by

$$\begin{aligned}\bar{\boldsymbol{H}}(n+1) = \bar{\boldsymbol{H}}(n) + \mu &\left[\boldsymbol{\Lambda}^*_{\hat{B}}\bar{\boldsymbol{Q}}(n)\boldsymbol{S}\right.\\ &\left. - \boldsymbol{\Lambda}^*_{\hat{B}}\bar{\boldsymbol{Q}}(n)\boldsymbol{\Lambda}_S\bar{\boldsymbol{Q}}^\dagger(n)\boldsymbol{\Lambda}_B\bar{\boldsymbol{H}}(n)\right]_+ \end{aligned} \tag{20}$$

where $\bar{\boldsymbol{Q}}(n)$ is given by (15) with $\boldsymbol{H}(n)$ replaced by $\bar{\boldsymbol{H}}(n)$ and $[\ ]_+$ indicates that the causal part is taken from the inverse transform of the quantity in a square bracket [6]. This operation is necessary to keep $\bar{\boldsymbol{H}}(n)$ to be causal. Since all the matrices in (20) are diagonal, the l-th element of (20) is written as the following scalar nonlinear difference equation

$$\bar{H}_l(n+1) = \bar{H}_l(n) + \mu\left[\frac{\hat{B}_l^* S_l}{1+\bar{H}_l{}^*(n)\epsilon_l^*} - \frac{\hat{B}_l^* S_l B_l \bar{H}_l(n)}{\left(1+\bar{H}_l(n)\epsilon_l\right)\left(1+\bar{H}_l{}^*(n)\epsilon_l^*\right)}\right]_+ \tag{21}$$

where $B_l = B(\mathrm{e}^{\mathrm{j}\frac{2\pi l}{L}})$, $\hat{B}_l = \hat{B}(\mathrm{e}^{\mathrm{j}\frac{2\pi l}{L}})$, and $\epsilon_l = B_l - \hat{B}_l$.

Thus the stationary point of the original filtered-X LMS algorithm in (5) is obtained by solving (21) with $\bar{H}_l(n+1) = \bar{H}_l(n) = H_l$. When $N \to \infty$ $(L \to \infty)$, we can replace the discrete frequencies with the continuous ones so that instead of H_l we use $H(z)$ where $z = \mathrm{e}^{\mathrm{j}\omega}$. Hence, it follows that the stationary point is determined by

$$\left[\hat{B}(z^{-1})S(z) - \frac{\hat{B}(z^{-1})S(z)B(z)H(z)}{1+H(z)\epsilon(z)}\right]_+ = 0 \tag{22}$$

where $\epsilon(z) = B(z) - \hat{B}(z)$ and $1 + H(z^{-1})\epsilon(z^{-1})$ is purely non-causal except the constant term so that from the denominator we can get rid of this. In general, it is very difficult to solve this "generalized Wiener-Hopf" equation. Let the spectral factorization of $S(z)$ be $S(z) = G(z)G(z^{-1})$ where $G(z)$ is of minimum phase. Then $G(z^{-1})$ can be factored out from the left hand side of (22).

Here we present two cases where we can have explicit solutions. The first case is that $B(z) = \hat{B}(z)$ $(\epsilon(z) = 0)$. Then we immediately have the solution

$$H_{\mathrm{opt}}(z) = \frac{1}{B_{\min}(z)G(z)}\left[\frac{B(z^{-1})G(z)}{B_{\min}(z^{-1})}\right]_+$$

where $B(z)B(z^{-1}) = B_{\min}(z)B_{\min}(z^{-1})$ and $B_{\min}(z)$ is a stable polynomial. A more interesting case is for $\epsilon(z) \neq 0$. Assume that $B(z) = z^{-d}C(z)$, $\hat{B}(z) = z^{-d}\hat{C}(z)$ where d is a positive integer denoting the delay and $C(z)$, $\hat{C}(z)$ are stable polynomials. Further assume for the moment that $1 + H(z)\epsilon(z)$ is of minimum phase. Then (22) can be simplified as

$$\left[z^dG(z)\right]_+ - \frac{G(z)C(z)H(z)}{1+H(z)\epsilon(z)} = 0$$

so that if we set $A(z) = \left[z^dG(z)\right]_+/G(z)$, we have the solution

$$H_{\mathrm{opt}}(z) = \frac{A(z)}{C(z) - z^{-d}(C(z)-\hat{C}(z))A(z)}, \tag{23}$$

provided that this is a stable transfer function. For (23) $1 + H(z)\epsilon(z)$ is of minimum phase. We also note that $A(z)$ is the transfer function of the optimal d-step ahead linear predictor of $w(n+d)$.

3. THE CONVERGENCE CONDITION OF THE ADAPTIVE ALGORITHM

The local stability of (21) around the stationary point is examined by calculating the derivative of (21). We use a special definition of the derivative with respect to a complex variable in [7] where we note that the following property $\partial\bar{H}_l^*(n)/\partial\bar{H}_l(n) = 0$ holds. Since $\bar{\boldsymbol{H}}(n+1)$ and $\bar{\boldsymbol{H}}(n)$ in (20) are causal, we can get rid of the operation $[\ ]_+$ from the right hand side of (20) by adding some purely noncausal vector which may be dependent on $\bar{\boldsymbol{H}}^*(n)$. Hence in calculating the derivative we discard the operation $[\ ]_+$ in (21) and obtain

$$\frac{\partial\bar{H}_l(n+1)}{\partial\bar{H}_l(n)} = 1 - \frac{\mu\hat{B}_l^*S_lB_l}{(1+\bar{H}_l(n)\epsilon_l)^2(1+\bar{H}_l^*(n)\epsilon_l^*)}. \tag{24}$$

Substituting the stationary point (23) of the second case we have

$$\left.\frac{\partial\bar{H}_l(n+1)}{\partial\bar{H}_l(n)}\right|_{\bar{H}_l(n)=H_{\mathrm{opt},l}} = 1 - \frac{\mu S_l\hat{C}_l^*\left|C_l - A_l\epsilon_l\right|^2(C_l - A_l\epsilon_l)}{|C_l|^2}. \tag{25}$$

For the (local) stability we require that the absolute value of the right hand side of (25) is less than 1. Since $0 < \mu \ll 1$ and $S_l > 0$, we have the condition

$$\mathrm{Re}\left[\hat{C}_l^*(C_l - A_l\epsilon_l)\right] > 0 \tag{26}$$

where $\epsilon_l = e^{-j\frac{2\pi l d}{L}}(C_l - \hat{C}_l)$. This is a counter-part of the so-called 90° condition in the feedforward-type ANC . However in the feedback-type ANC the condition (26) depends on the property of $w(n)$. Under (26) the transfer function of the adaptive filter converges to $H_{\rm opt}(z)$ in (23) at least locally for large N and in this steady state from (1), (2), (3) and (23) the error signal $e(n)$ is symbolically expressed as

$$\begin{aligned} e(n) &= \frac{1 - \hat{B}(z)H_{\rm opt}(z)}{1 + (B(z) - \hat{B}(z))H_{\rm opt}(z)} w(n) \\ &= (1 - z^{-d}A(z))w(n) \end{aligned}$$

where z^{-1} means the unit delay operator. This is the minimum variance d-step ahead prediction error of $w(n)$. That is, even if $\hat{B}(z)$ differs from $B(z)$ within some range, the scheme in Fig. 2 gives the optimal steady state performance.

4. A SIMPLE EXAMPLE

Here we consider a simple case where $B(z) = \gamma z^{-1}$, $\hat{B}(z) = \hat{\gamma} z^{-1}$ and $w(n)$ is a first order (lowpass) AR process with the innovation variance 1, that is, $G(z) = (1 - az^{-1})^{-1}$ with $0 < a < 1$. Then (23) becomes

$$H_{\rm opt}(z) = \frac{a}{\gamma\{1 - z^{-1}(1-\beta)a\}} \qquad (27)$$

with $\beta = \hat{\gamma}/\gamma$ and the corresponding impulse response

$$h_{{\rm opt},l} = a^{l+1}(1-\beta)^l/\gamma \quad (l \geq 0). \qquad (28)$$

The condition that (27) is the stationary point of the adaptive algorithm is $|(1-\beta)a| < 1$, that is, $1 - 1/a < \beta < 1 + 1/a$. Under this condition we consider (26) in this case, that is,

$$\beta\left\{1 - (1-\beta)a\cos\frac{2\pi l}{L}\right\} > 0 \quad (l = 0, \cdots, L-1).$$

But the quantity in the bracket is positive so that we have the overall local convergence condition as

$$0 < \beta < 1 + \frac{1}{a}. \qquad (29)$$

Some simulations have been made to check the theoretical findings. In Fig.3 the learning curve showing the empirical variance of the squared error $e^2(n)$ is presented for the case where $a = 0.9$, $\gamma = 1$, $\hat{\gamma} = 0.5$ ($\beta = 0.5$) with $N = 8$, and $\mu = 0.01$. The variance is obtained by averaging over 50 data sets and the steady state variance is 1.02879 which is very close to the minimum variance 1.0. In Table 1, the steady state first 4 impulse responses of the adaptive filter are presented together with the theoretical ones in (28). The agreements are good. Finally we have observed that for $\beta = -0.05$ and 2.2 the adaptive algorithm diverges. This coincide well with (29).

5. CONCLUSION

We have presented the analysis of the adaptive filter algorithm for feedback-type ANC concerning its stationary point and the local convergence condition using the averaging method combined with the frequency domain expression of the adaptive algorithm. The obtained theoretical results coincide well with the simulation results. A further study is needed about the property of the generalized Wiener-Hopf equation describing the stationary point.

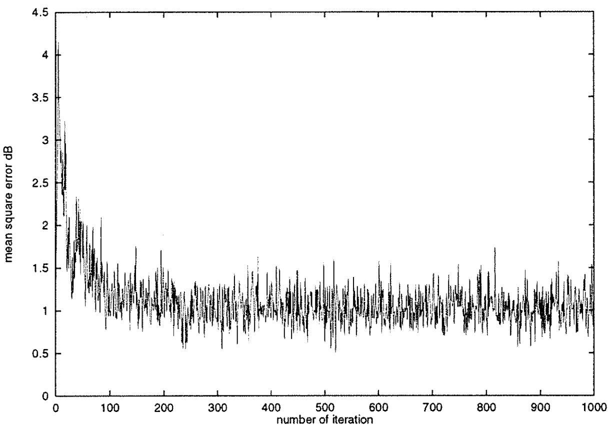

Fig. 3. Learning curve under the condition $a = 0.9$, $\gamma = 1$ and $\hat{\gamma} = 0.5$.

	h_0	h_1	h_2	h_3
empirical	0.870165	0.414190	0.201025	0.093168
theoretical	0.900000	0.405000	0.182250	0.082013

Table 1. Theoretical and estimated impulse responses.

6. REFERENCES

[1] S. J. Elliott and P. A. Nelson, "Active noise control," *IEEE Signal Processing Magazine*, pp.12-35, Oct. 1993.

[2] S. M. Kuo and D. R. Morgan, *Active Noise Control Systems*, John Wiley & Sons Inc., 1996.

[3] V. Solo and X. Kong, *Adaptive Signal Processing Algorithms -Stability and Performance-*, Prentice Hall,1995.

[4] S. Miyagi and H. Sakai, "Convergence analysis of the delayless subband adaptive filter based on the frequency domain expression", *Proc. ICASSP*, pp.368–371, Istanbul, June 2000.

[5] K. Fujii, "Filter structure for the feedback control of the noise," *Proc. Conf. Acoust. Soc. Japan*, pp. 513–516, March 1999. (in Japanese)

[6] S. J. Elliott and B. Rafaely, "Frequency-domain adaptation of causal digital filters," *IEEE Trans. Signal Processing*, pp.1354-1364, May 2000.

[7] S. Haykin, *Adaptive Filter Theory*, Third Edition, Prentice Hall, 1996.

Stabilisation of fast QRD inverse-updates adaptive filtering algorithm

H.Sakai and S.Hori

Abstract: A stabilisation method for the fast QRD inverse-updates adaptive filtering algorithm (Proudler, 1994) involving modification by leakage is proposed. A stability analysis of error propagation of the algorithm is presented using the averaging principle. It is shown that the proposed algorithm is stable if the variance of the one-step-ahead linear predictor of the input signal is less than that of the prediction error, with the forgetting factor and the leakage factor sufficiently close to 1, under additional assumptions on the leakage factor and the linear prediction coefficient.

1 Introduction

It is well known that the fast Kalman-type recursive least squares (RLS) adaptive filtering algorithms are numerically unstable. Slock [1] proposed a stabilisation method for the FTF algorithm and provided a general framework for the analysis of error propagation based on the averaging principle. Binde [2] also proposed a stabilisation method for the fast Kalman algorithm by leakage and presented a corresponding stability analysis. However, the discussion is limited to the diagonal blocks of the expected transition matrix of the linearised error system. To conclude that the algorithm is truly stable, it may be necessary to study the effects of the off-diagonal blocks, which are small but may not be neglected.

The fast QR decomposition (QRD) inverse-updates algorithm of Proudler [3] is also numerically unstable. In this paper, we propose its modification by leakage and present a more detailed and, in a sense, more accurate stability analysis of error propagation of the modified algorithm. It is shown that the modified algorithm is guaranteed to be stable under a certain condition.

2 Modified algorithm by leakage

We consider the following RLS adaptive filtering problem

$$\min_{w(n)} \sum_{t=1}^{n} \lambda^{n-t}(y(t) + w^T(n)x(t))^2$$

with (1)

$$x(n) = (x(n)x(n-1)\cdots x(n-p+1))^T$$

where $x(n)$, $y(n)$ and $\lambda(0 \le \lambda < 1)$ are the input signal, the desired signal and the forgetting factor, respectively. The original QRD algorithm by Proudler [3] for eqn. 1 is modified in the following eqns. 5 and 14:

initialisation: $\epsilon_f^{-2}(0) = 1,\ \epsilon_b^{-2}(0) = 1,\ \delta_p^{-1}(0) = 1,$ all other variables $= 0$

$$e_f(n) = w_f^T(n-1)x(n-1) + x(n) \tag{2}$$

$$\delta_{p+1}^{-1}(n) = \delta_p^{-1}(n-1) + \beta^{-2}\epsilon_f^{-2}(n-1)e_f^2(n) \tag{3}$$

$$\bar{c}_f = \frac{\delta_p^{-1}(n-1)}{\delta_{p+1}^{-1}(n)},\quad \bar{s}_f = \frac{\beta^{-2}e_f(n)\epsilon_f^{-2}(n-1)}{\delta_{p+1}^{-1}(n)} \tag{4}$$

$$w_f^T(n) = \tau\{w_f^T(n-1) + e_f(n)k^T(n-1)\} \tag{5}$$

$$v_f^T(n) = k^T(n-1) - \bar{s}_f w_f^T(n) \tag{6}$$

$$\mu_f(n) = -\bar{s}_f \tag{7}$$

$$\epsilon_f^{-2}(n) = \bar{c}_f\ \beta^{-2}\epsilon_f^{-2}(n-1) \tag{8}$$

$$[v_b^T(n)\ \mu_b(n)] = [\mu_f(n)\ v_f^T(n)] \tag{9}$$

$$e_b(n) = w_b^T(n-1)x(n) + x(n-p) \tag{10}$$

$$\delta_p^{-1}(n) = \delta_{p+1}^{-1}(n) - \beta^{-2}\epsilon_b^{-2}(n-1)e_b^2(n) \tag{11}$$

$$\bar{c}_b = \frac{\delta_p^{-1}(n)}{\delta_{p+1}^{-1}(n)},\quad \bar{s}_b = \frac{\beta^{-2}e_b(n)\epsilon_b^{-2}(n-1)}{\delta_{p+1}^{-1}(n)} \tag{12}$$

$$k(n) = \bar{c}_b^{-1}\{v_b(n) + \bar{s}_b\ w_b(n-1)\} \tag{13}$$

$$w_b^T(n) = \tau\{w_b^T(n-1) + e_b(n)k^T(n)\} \tag{14}$$

$$\epsilon_b^{-2}(n) = \bar{c}_b\ \beta^{-2}\epsilon_b^{-2}(n-1) \tag{15}$$

$$e(n) = w^T(n-1)x(n) + y(n) \tag{16}$$

$$w^T(n) = w^T(n-1) + k^T(n)e(n) \tag{17}$$

IEE Proceedings online no. 20010153
DOI: 10.1049/ip-vis:20010153
Paper first received 4th January and in revised form 5th October 2000

The authors are with the Department of Systems Science, Graduate School of Informatics, Kyoto University, Sakyo-ku Kyoto 606-8501, Japan

We set $\beta = \lambda^{\frac{1}{2}}$ and $\tau = \beta^r (0 < r \ll 1)$. Since $\tau < 1$, the 'leakage' effect is introduced in eqns. 5 and 14. For $r = 0$, the algorithm reduces to the original one of Proudler [3].

The above algorithm can be regarded as a nonlinear stochastic dynamical systems:

$$\boldsymbol{\psi}(n) = f(\boldsymbol{\psi}(n-1), x(n)) \tag{18}$$

with the (3p + 3)-dimensional state vector

$$\boldsymbol{\psi}(n) = (\boldsymbol{w}_f(n)\ \epsilon_f^2(n)\ \boldsymbol{w}_b(n)\ \epsilon_b^2(n)\ \boldsymbol{k}(n)\ \delta_p(n))^T$$

where $\boldsymbol{w}_f(n)$, $\epsilon_f^2(n)$, $\boldsymbol{w}_b(n)$, $\epsilon_b^2(n)$, $\boldsymbol{k}(n)$ and $\delta_p(n)$ are the forward linear prediction coefficient vector, the forward prediction residual energy, the backward linear prediction coefficient vector, the backward prediction residual energy, Kalman gain vector and the likelihood variable, respectively, and its output is $\boldsymbol{w}(n)$. As elsewhere [1, 2], the stability of error propagation of eqn. 18 can be examined by evaluating the eigenvalues of the expected transition matrix of the linearised system:

$$\boldsymbol{A} = \mathrm{E}\left[\frac{\delta\boldsymbol{\psi}(n)}{\delta\boldsymbol{\psi}^T(n-1)}\right] \tag{19}$$

in the limit $\lambda \to 1$. The justification of this approach is presented elsewhere [1]. We use the following assumptions to calculate $\boldsymbol{A}$ and guarantee that the modified algorithm is stable.

Assumption 1: $\lambda^{\frac{1}{2}} = \beta = 1 - \epsilon$ and $\tau = \beta^r \simeq 1 - r\epsilon$ for sufficiently small $\epsilon > 0$, where r is of order $\epsilon^{\zeta} (1/2 > \zeta)$ i.e. $r = 0(\epsilon^{\frac{1}{2}})$.
Assumption 2: The first element of the backward linear prediction coefficient vector for $\boldsymbol{x}(n)$ (defined in eqn. 70) is zero.
Assumption 3: The input signal $\{x(n)\}$ is a Gaussian stationary process with the exponentially decaying autocovariance function.
Assumption 4: The variance of the one-step-ahead linear predictor of $\{x(n)\}$ is less than that of the prediction error.

Hereafter, ε is used as the perturbation parameter to calculate $\boldsymbol{A}$ by a perturbation analysis.

3 Calculation of *A*

To calculate $\boldsymbol{A}$, we extensively use the averaging principle of Samson and Reddy [4]. Let $X(k)$ and $Y(k)$ be a slowly varying random variable and a rapidly changing random variable, respectively. The averaging principle then says that

$$\mathrm{E}[X(k)Y(k)] \simeq \mathrm{E}[X(k)]\mathrm{E}[Y(k)] \tag{20}$$

From

$$\mathrm{E}[Y(k)] = \mathrm{E}\left[X(k) \cdot \frac{Y(k)}{X(k)}\right] \simeq \mathrm{E}[X(k)]\ \mathrm{E}\left[\frac{Y(k)}{X(k)}\right] \tag{21}$$

we also use the following approximation:

$$\mathrm{E}\left[\frac{Y(k)}{X(k)}\right] \simeq \frac{\mathrm{E}[Y(k)]}{\mathrm{E}[X(k)]} \tag{22}$$

When there is no leakage effect, i.e. $\tau = 1$, it is shown [1] that

$$\mathrm{E}[\boldsymbol{k}(n)\boldsymbol{x}^T(n)] \simeq (\beta^2 - 1)I \tag{23}$$

where $\boldsymbol{I}$ denotes the identity matrix. In addition, the likelihood variable $\delta_p^{-1}(n)$ is defined by

$$\delta_p^{-1}(n) = 1 - \mathrm{tr}(\boldsymbol{k}(n)\boldsymbol{x}^T(n)), \quad \boldsymbol{k}(n) = \boldsymbol{R}^{-1}(n)\boldsymbol{x}(n),$$
$$\boldsymbol{R}(n) = \beta^2\boldsymbol{R}(n-1) + \boldsymbol{x}(n)\boldsymbol{x}^T(n) \tag{24}$$

Hence, in the steady state $\mathrm{E}[\boldsymbol{R}(n)] = \boldsymbol{R}/(1-\beta^2)$, where $\boldsymbol{R}$ is the covariance matrix of $\boldsymbol{x}(n)$, i.e.

$$\boldsymbol{R} = \mathrm{E}[\boldsymbol{x}(n)\boldsymbol{x}^T(n)] \tag{25}$$

Thus, $\mathrm{E}[\boldsymbol{R}(n)]$ is of order ϵ^{-1}. However by applying Lemma A of Stoica and Nehorai [5] to each element of $\boldsymbol{R}(n)$ with assumption 3, we see that $(1-\lambda)\boldsymbol{R}(n) \to \boldsymbol{R} + O(\sqrt{(1-\lambda)})$ and $n \to \infty$, where $O(\sqrt{(1-\lambda)})$ denotes a zero mean random variable vector whose covariance matrix tends to zero with the order of $(1-\lambda)$ as $\lambda \to 1$. This means that $\boldsymbol{R}(n)$ is of order ϵ^{-1} and $\boldsymbol{k}(n)$ is of order ϵ. We can then assume that $\delta_p(n) \simeq 1$ when elements of $\boldsymbol{A}$ are evaluated.

When the leakage factor $\tau \simeq 1 - r\epsilon$ is introduced, in eqn. 23 there will be a perturbation term of order $r\epsilon$. By assumption 2 about r, this term is small compared with the first term, which is of order ϵ, and so we discard this term and in the following calculations use eqn. 23. Thus, from eqn. 5 we get

$$\mathrm{E}\left[\frac{\partial\boldsymbol{w}_f(n)}{\partial\boldsymbol{w}_f^T(n-1)}\right] = \mathrm{E}[\tau\{I + \boldsymbol{k}(n-1)\boldsymbol{x}^T(n-1)\}]$$
$$\simeq \tau\beta^2\boldsymbol{I} \simeq \{1 - (r+2)\epsilon\}\boldsymbol{I} \tag{26}$$

From eqn. 13 we have

$$\frac{\partial\boldsymbol{k}(n)}{\partial\boldsymbol{k}^T(n-1)} = \frac{1}{\bar{c}_b}\frac{\partial\boldsymbol{v}_b(n)}{\partial\boldsymbol{k}^T(n-1)} \tag{27}$$

By using the shift matrix

$$\boldsymbol{S} = \begin{pmatrix} 0 & & & 0 \\ 1 & 0 & & \\ & \ddots & \ddots & \\ 0 & & 1 & 0 \end{pmatrix} \tag{28}$$

from eqns. 5, 6, 7 and 9 we can express $\boldsymbol{v}_b(n)$ as

$$\boldsymbol{v}_b(n) = \boldsymbol{S}(1 - \tau\bar{s}_f e_f(n))\boldsymbol{k}(n-1) - \tau\bar{s}_f\boldsymbol{S}\boldsymbol{w}_f(n-1) - \bar{s}_f\pi \tag{29}$$

$$\bar{s}_f \simeq 1 - \frac{\delta_p^{-1}(n-1)}{\delta_p^{-1}(n-1) + \beta^{-2}e_f(n)\epsilon_f^{-2}(n-1)}$$
$$= \frac{\beta^{-2}e_f(n)}{\beta^{-2}e_f(n) + \delta_p^{-1}(n-1)\epsilon_f^2(n-1)} \tag{30}$$

where $\pi = (1\ 0 \cdots 0)^T$. We can also write

$$\frac{1}{\bar{c}_b} = 1 + \frac{e_b^2(n)\delta_p(n)}{\beta^2\epsilon_b^2(n-1)} \tag{31}$$

Thus, we obtain

$$\mathrm{E}\left[\frac{\partial\boldsymbol{k}(n)}{\partial\boldsymbol{k}^T(n-1)}\right] = \mathrm{E}\left[\left(1 + \frac{e_b^2(n)\delta_p(n)}{\beta^2\epsilon_b^2(n-1)}\right)(1 - \tau\bar{s}_f e_f(n))\right]$$
$$\boldsymbol{S} \equiv \rho\boldsymbol{S} \tag{32}$$

From the structure of the algorithm there are several blocks that are identically zero. Thus, we have

$$A = \begin{pmatrix} \{1-(r+2)\varepsilon\}I & \mathbf{0} & 0 & \mathbf{0} & 0 & \mathbf{0} \\ * & * & * & * & \mathbf{0} & * \\ * & * & * & * & 0 & * \\ * & * & * & * & \mathbf{0} & * \\ * & * & * & * & \rho S & * \\ * & * & * & * & \mathbf{0} & * \end{pmatrix} \tag{33}$$

where * shows a non-zero block. As off-diagonal blocks in the first block row and the fifth block column of A are all zero, by considering the expansion of the determinant of $A - \lambda I$, the eigenvalues of A are equal to the eigenvalues of the first, the fifth diagonal blocks and those of

$$A' = \mathrm{E}\left[\begin{pmatrix} \frac{\partial\epsilon_f^2(n)}{\partial\epsilon_f^2(n-1)} & \frac{\partial\epsilon_f^2(n)}{\partial w_b^T(n-1)} & \frac{\partial\epsilon_f^2(n)}{\partial\epsilon_b^2(n-1)} & \frac{\partial\epsilon_f^2(n)}{\partial\delta_p(n-1)} \\ \frac{\partial w_b(n)}{\partial\epsilon_f^2(n-1)} & \frac{\partial w_b(n)}{\partial w_b^T(n-1)} & \frac{\partial w_b(n)}{\partial\epsilon_b^2(n-1)} & \frac{\partial w_b(n)}{\partial\delta_p(n-1)} \\ \frac{\partial\epsilon_b^2(n)}{\partial\epsilon_f^2(n-1)} & \frac{\partial\epsilon_b^2(n)}{\partial w_b^T(n-1)} & \frac{\partial\epsilon_b^2(n)}{\partial\epsilon_b^2(n-1)} & \frac{\partial\epsilon_b^2(n)}{\partial\delta_p(n-1)} \\ \frac{\partial\delta_p(n)}{\partial\epsilon_f^2(n-1)} & \frac{\partial\delta_p(n)}{\partial w_b^T(n-1)} & \frac{\partial\delta_p(n)}{\partial\epsilon_b^2(n-1)} & \frac{\partial\delta_p(n)}{\partial\delta_p(n-1)} \end{pmatrix}\right] \tag{34}$$

The eigenvalues of the (1,1) block of A are $1-(r+2)\varepsilon$. Obviously these are between 0 and 1 for $0<\varepsilon<1/(r+2)<1/2$. Since the (5,5) block is proportional to S, the corresponding eigenvalues are all zero.

4 Calculation of A'

We calculate the elements of the first row of A'. From eqns. 8, 3 and 4, we have

$$\epsilon_f^2(n) = \beta^2\epsilon_f^2(n-1) + e_f^2(n)\delta_p(n-1) \tag{35}$$

So

$$\mathrm{E}\left[\frac{\partial\epsilon_f^2(n)}{\partial\epsilon_f^2(n-1)}\right] = \beta^2 \simeq 1-2\varepsilon, \quad \mathrm{E}\left[\frac{\partial\epsilon_f^2(n)}{\partial w_b^T(n-1)}\right] = 0$$
$$\mathrm{E}\left[\frac{\partial\epsilon_f^2(n)}{\partial\epsilon_b^2(n-1)}\right] = 0, \quad \mathrm{E}\left[\frac{\partial\epsilon_f^2(n)}{\partial\delta_p(n-1)}\right] = \sigma^2 \tag{36}$$

where we define $\sigma^2 = \mathrm{E}[e_f^2(n)]$.

Next we calculate the elements of the second block row of A'. From eqns. 10 and 12–14, we have

$$\frac{\partial w_b(n)}{\partial w_b^T(n-1)} = \tau\left(I + k(n)x^T(n) + e_b(n)\frac{\bar{s}_b}{\bar{c}_b}I + e_b(n)w_b(n-1)\frac{\partial\left(\frac{\bar{s}_b}{\bar{c}_b}\right)}{\partial w_b^T(n-1)}\right) \tag{37}$$

We then take the expectation of each term. The second term is obtained from eqn. 23. From eqn. 12 the third term is

$$e_b(n)\frac{\bar{s}_b}{\bar{c}_b} = \frac{e_b^2(n)\delta_p(n)}{\beta^2\epsilon_b^2(n-1)} \tag{38}$$

From eqn. 15

$$\epsilon_b^2(n) = \bar{c}_b^{-1}\beta^2\epsilon_b^2(n-1) = \beta^2\epsilon_b^2(n-1) + e_b^2(n)\delta_p(n) \tag{39}$$

Thus, in the steady state $\mathrm{E}[\epsilon_b^2(n-1)]\ (1-\beta^2) = \mathrm{E}[e_b^2(n)\delta_p(n)]$ and, by a similar argument applied to $R(n)$, $\epsilon_b^2(n)$ and $\epsilon_f^2(n)$ in eqn. 35 are of order ε^{-1}. Since $\epsilon_b^2(n)$ varies slowly and $e_b^2(n)$ varies quickly, by the averaging principle (eqn. 22), we have

$$\mathrm{E}\left[\frac{e_b^2(n)\delta_p(n)}{\beta^2\epsilon_b^2(n-1)}\right] \simeq \frac{1}{\beta^2} - 1 \tag{40}$$

Next we evaluate the fourth term in eqn. 37. However, by the leakage factor in eqn. 14, a bias is introduced in $w_b(n)$. The expression for this bias is presented in the Appendix (Section 10.1). From eqn. 12 $\bar{s}_b/\bar{c}_b = e_b(n)\delta_p(n)/\beta^2\epsilon_b^2(n-1)$, and so the last term of eqn. 37 becomes

$$e_b(n)w_b(n-1)\frac{\partial\left(\frac{\bar{s}_b}{\bar{c}_b}\right)}{\partial w_b^T(n-1)} = \frac{e_b(n)w_b(n-1)}{\beta^2\epsilon_b^2(n-1)}\left[x^T(n) + e_b(n)\frac{\partial\delta_p(n)}{\partial w_b^T(n-1)}\right] \tag{41}$$

From eqns. 10, 70 and 74, since in the steady state $w_b(n-1) \simeq w_b$, we have

$$\begin{aligned} e_b(n) &\simeq x(n-p) + (1-\xi)w_0^T x(n) \\ &\simeq e_{b,0}(n) - \xi w_0^T x(n) \end{aligned} \tag{42}$$

Hence

$$\mathrm{E}[e_b(n)x^T(n)] \simeq -\xi w_0^T \mathrm{E}[x(n)x^T(n)] = -\xi w_0^T R \tag{43}$$

As $w_b(n)$ varies slowly and $e_b(n)$ and $x(n)$ vary quickly, by the averaging principle, from eqns. 71 and 74 we obtain

$$\begin{aligned} \mathrm{E}[e_b(n)w_b(n-1)x^T(n)] &\simeq w_b\mathrm{E}[e_b(n)x^T(n)] \\ &= -(1-\xi)w_0\xi w_0^T R \end{aligned} \tag{44}$$

In a similar way to that for w_b in Section 10.1, we can calculate the bias in $w_f(n)$ and it is same as that of $w_b(n)$. Therefore, the variance of $e_b(n)$ is equal to that of $e_f(n)$, since $\{x(n)\}$ is a stationary process, so that the statistics of the forward and the backward prediction errors are the same. Hence $\mathrm{E}[e_b^2(n)] = \mathrm{E}[e_f^2(n)] = \sigma^2$ and, from eqn. 39 and $\delta_p(n) \simeq 1$, $\mathrm{E}[\epsilon_b^2(n-1)] \simeq \sigma^2/(1-\beta^2)$. Hence from eqn. 77 in the Appendix (Section 10.2), the second term on the right-hand side of eqn. 41 is $2e_b^3(n)w_b(n)x^T(n)/\beta^4\epsilon_b^4(n-1)$ and of order ε^2, since $\epsilon_b^4(n-1)$ is of order ε^{-2} and other quantities are of order $O(1)$. Therefore, this term can be discarded. Combining eqns. 38, 40 and 44 with $\lambda = \beta^2$, we have

$$\begin{aligned} \mathrm{E}\left[\frac{\partial w_b(n)}{\partial w_b^T(n-1)}\right] &\simeq \tau\left\{1 + (\beta^2 - 1) + \left(\frac{1}{\beta^2} - 1\right)\right\}I \\ &\quad - \tau\left(\frac{1}{\beta^2} - 1\right)(1-\xi)\xi\frac{w_0 w_0^T R}{\sigma^2} \\ &\simeq (1 - r\varepsilon)I - 2\varepsilon(1-\xi)\xi\frac{w_0 w_0^T R}{\sigma^2} \end{aligned} \tag{45}$$

Other blocks of the second block row are calculated by similar approximations:

$$\mathrm{E}\left[\frac{\partial \boldsymbol{w}_b^T(n)}{\partial \epsilon_f^2(n-1)}\right] \simeq \frac{8\varepsilon^3}{\sigma^2}(1-\xi)\boldsymbol{w}_0 \tag{46}$$

$$\mathrm{E}\left[\frac{\partial \boldsymbol{w}_b(n)}{\partial \epsilon_b^2(n-1)}\right] \simeq -\frac{4\varepsilon^2}{\sigma^2}(1-\xi)\boldsymbol{w}_0,$$

$$\mathrm{E}\left[\frac{\partial \boldsymbol{w}_b(n)}{\partial \delta_p(n-1)}\right] \simeq 2\varepsilon(1-\xi)\boldsymbol{w}_0 \tag{47}$$

The derivations are a little complicated and are deferred to the Appendix (Sections 10.4).

The elements of the third row of $\boldsymbol{A}'$ are also calculated by similar approximations. From eqns. 39, 75, and the Appendix (Sections 10.2 and 10.3)

$$\begin{aligned}
\mathrm{E}\left[\frac{\partial \epsilon_b^2(n)}{\partial \epsilon_f^2(n-1)}\right] &= \mathrm{E}\left[e_b^2(n)\frac{\partial \delta_p(n)}{\partial \epsilon_f^2(n-1)}\right] \\
&\simeq \mathrm{E}\left[\frac{e_f^2(n)e_b^2(n)}{\beta^2\epsilon_f^4(n-1)}\right] \simeq 4\varepsilon^2 \\
\mathrm{E}\left[\frac{\partial \epsilon_b^2(n)}{\partial \boldsymbol{w}_b^T(n-1)}\right] &= \mathrm{E}\left[2e_b(n)\boldsymbol{x}^T(n) + e_b^2(n)\frac{\partial \delta_p(n)}{\partial \boldsymbol{w}_f^T(n-1)}\right] \\
&\simeq \mathrm{E}[2e_b(n)\boldsymbol{x}^T(n)] + \mathrm{E}\left[\frac{2e_b^3(n)\boldsymbol{x}(n)}{\beta^2\epsilon_b^2(n-1)}\right] \\
&\simeq -2\xi\boldsymbol{w}_0^T\boldsymbol{R}
\end{aligned} \tag{48}$$

$$\mathrm{E}\left[\frac{\partial \epsilon_b^2(n)}{\partial \epsilon_b^2(n-1)}\right] = \beta^2 \simeq 1-2\varepsilon,$$

$$\mathrm{E}\left[\frac{\partial \epsilon_b^2(n)}{\partial \delta_p(n-1)}\right] = \mathrm{E}[e_b^2(n)] = \sigma^2$$

To obtain eqn. 35, we note that from assumption 3 $\mathrm{E}[e_b^3(n)\boldsymbol{x}^T(n)] = 3\mathrm{E}[e_b^2(n)]\mathrm{E}[e_b(n)\boldsymbol{x}^T(n)]$ and use eqn. 43, but the second term is small compared with the first term and is discarded.

From Sections 10.2 and 10.3 eqn. 31 the elements of the fourth row of $\boldsymbol{A}'$ are given by

$$E\left[\frac{\partial \delta_p(n)}{\partial \epsilon_f^2(n-1)}\right] \simeq \frac{4\varepsilon^2}{\sigma^2} \qquad E\left[\frac{\partial \delta_p(n)}{\partial \boldsymbol{w}_b^T(n-1)}\right] \simeq -\frac{4\varepsilon}{\sigma^2}\xi\boldsymbol{w}_0^T\boldsymbol{R}$$

$$E\left[\frac{\partial \delta_p(n)}{\partial \epsilon_b^2(n-1)}\right] \simeq -\frac{4\varepsilon^2}{\sigma^2} \qquad E\left[\frac{\partial \delta_p(n)}{\partial \delta_p(n-1)}\right] \simeq 1 \tag{49}$$

Combining the above results, we finally have

$$\boldsymbol{A}' \simeq \begin{pmatrix} 1-2\varepsilon & 0 & 0 & \sigma^2 \\ \frac{8\varepsilon^3}{\sigma^2}(1-\xi)\boldsymbol{w}_0 & (1-r\varepsilon)I - \frac{2\varepsilon(1-\xi)\xi}{\sigma^2}\boldsymbol{w}_0\boldsymbol{w}_0^T\boldsymbol{R} & -\frac{4\varepsilon^2}{\sigma^2}(1-\zeta)\boldsymbol{w}_0 & 2\varepsilon(1-\zeta)_0 \\ 4\varepsilon^2 & -2\xi\boldsymbol{w}_0^T R & 1-2\varepsilon & \sigma^2 \\ \frac{4\varepsilon^2}{\sigma^2} & -\frac{4\varepsilon}{\sigma^2}\xi\boldsymbol{w}_0^T R & -\frac{4\varepsilon^2}{\sigma^2} & 1 \end{pmatrix} \tag{50}$$

In eqn. 46 for $\tau = 1 (r = 0)$ we have $\xi = 0$ and

$$E\left[\frac{\partial \boldsymbol{w}_b(n)}{\partial \boldsymbol{w}_b^T(n-1)}\right] \simeq \left(\frac{1}{\lambda} + \lambda - 1\right)\boldsymbol{I} \tag{51}$$

Since, in this case, the off-diagonal blocks of the second block column of $\boldsymbol{A}'$ in eqn. 50 are all zero, $1/\lambda + \lambda - 1 \simeq 1 + 4\varepsilon^2$ for $\lambda \simeq 1 - 2\varepsilon$ is the eigenvalue of $\boldsymbol{A}'$. This means that the original QRD algorithm of Proudler [3] is unstable. However, the corresponding eigenvalues of the fast Kalman algorithm are $1/\lambda \simeq 1 + 2\varepsilon$ [1], and so the degree of instability in Proudler's algorithm [3] is an order of magnitude less. This explains why it appears to be more difficult to find cases in which Proudler's algorithm diverges [3].

5 Stability Analysis

To calculate the eigenvalues of $\boldsymbol{A}'$, diagonalisation of the (2, 2) block in $\boldsymbol{A}'$ is considered. Since the (2, 2) block of $\boldsymbol{A}'$ is $(1 - r\varepsilon)I - 2\varepsilon(1-\xi)\xi\boldsymbol{w}_0\boldsymbol{w}_0^T\boldsymbol{R}/\sigma^2$, the eigenvectors are $\boldsymbol{w}_0$ and there is a set of linearly independent vectors $\boldsymbol{a}_i (i = 1, \ldots, p-1)$ such that $\boldsymbol{w}_0^T\boldsymbol{R}\boldsymbol{a}_i = 0$. Therefore, we can diagonalise it by using the matrix $\boldsymbol{U} = (\boldsymbol{a}_1 \cdots \boldsymbol{a}_{p-1}\ \boldsymbol{w}_0)$ as

$$\boldsymbol{U}^{-1}\left\{(1-r\varepsilon)\boldsymbol{I}_p - \frac{2\varepsilon(1-\xi)\xi}{\sigma^2}\boldsymbol{w}_0\boldsymbol{w}_0^T\boldsymbol{R}\right\}$$

$$\boldsymbol{U} = \begin{pmatrix} (1-r\varepsilon)\boldsymbol{I}_{p-1} & 0 \\ 0 & 1 - r\varepsilon - 2\varepsilon(1-\xi)\xi\gamma \end{pmatrix} \tag{52}$$

with $\gamma = \boldsymbol{w}_0^T\boldsymbol{R}\boldsymbol{w}_0/\sigma^2$. to emphasise the dimension of the identity matrix, $\boldsymbol{I}_p$ denotes the $p \times p$ identity matrix. Clearly, $\boldsymbol{U}^{-1}$ is expressed as

$$\boldsymbol{U}^{-1} = \left(\boldsymbol{b}_1 \cdots \boldsymbol{b}_{p-1}\ \frac{\boldsymbol{R}\boldsymbol{w}_0}{\boldsymbol{w}_0^T\boldsymbol{R}\boldsymbol{w}_0}\right)^T \tag{53}$$

with appropriate vectors $\boldsymbol{b}_i (i = 1, \ldots, p-1)$, such that $\boldsymbol{b}_i^T\boldsymbol{w}_0 = 0$. So

$$\boldsymbol{U}^{-1}\boldsymbol{w}_0 = \begin{pmatrix} 0 \\ 1 \end{pmatrix} \quad \text{and} \quad \boldsymbol{w}_0^T\boldsymbol{R}\boldsymbol{U} = \begin{pmatrix} 0 & \boldsymbol{w}^{\mathrm{T}}\boldsymbol{R}\boldsymbol{w}_0 \end{pmatrix} \tag{54}$$

Multiplying diag(1, $\boldsymbol{U}^{-1}$, 1, 1), diag(1, $\boldsymbol{U}$, 1, 1) from the left and the right, respectively, to eqn. 50 and using eqn. 54 we see that the eigenvalues of $\boldsymbol{A}'$ are $1 - r\varepsilon$ and those of the matrix

$$\boldsymbol{A}'' = \begin{pmatrix} 1-2\varepsilon & 0 & 0 & \sigma^2 \\ \frac{8\varepsilon^3}{\sigma^2}(1-\xi) & 1 - r\varepsilon - 2\varepsilon(1-\xi)\xi\gamma & -\frac{4\varepsilon^2}{\sigma^2}(1-\xi) & 2\varepsilon(1-\xi) \\ 4\varepsilon^2 & -2\xi\gamma\sigma^2 & 1-2\varepsilon & \sigma^2 \\ \frac{4\varepsilon^2}{\sigma^2} & -4\varepsilon\xi\gamma & -\frac{4\varepsilon^2}{\sigma^2} & 1 \end{pmatrix} \tag{55}$$

Thus, the stability of the algorithm depends on the location of the eigenvalues of $\boldsymbol{A}''$.

By putting $z=1+\varepsilon\eta$ in the characteristic equation $\det(A''-zI)=0$, a fourth-order equation is derived as follows:

$$\eta^4+\{r+4+2(1-\xi)\xi\gamma\}\eta^3+4\{r+1+2(1-\xi)\xi\gamma\}\eta^2$$
$$+4\{r-2(1-\xi)\xi\gamma+4\varepsilon(1+2(1-\xi)\xi\gamma)\}\eta$$
$$+16\varepsilon\{r-2(1-\xi)\xi\gamma\}=0 \quad (56)$$

When the Hurwitz stability condition holds, the real part of η is negative and the eigenvalues of A'' are inside the unit circle if ε is sufficiently small. In this case, the Hurwitz stability condition [6] is written as

$$\{r-2(1-\xi)\xi\gamma+4\varepsilon(1+2(1-\xi)\xi\gamma)\}$$
$$[\{r+4+2(1-\xi)\xi\gamma\}\{r+1+2(1-\xi)\xi\gamma\}$$
$$-\{r-2(1-\xi)\xi\gamma+4\varepsilon(1+2(1-\xi)\xi\gamma)\}]$$
$$-\varepsilon\{r-2(1-\xi)\xi\gamma\}\{r+4+2(1-\xi)\xi\gamma\}^2>0 \quad (57)$$

$$r+4+2(1-\xi)\xi\gamma>0 \quad (58)$$

$$r+1+2(1-\xi)\xi\gamma>0 \quad (59)$$

$$r-2(1-\xi)\xi\gamma+4\varepsilon(1+2(1-\xi)\xi\gamma)>0 \quad (60)$$

$$r-2(1-\xi)\xi\gamma>0 \quad (61)$$

Since from eqn. 74, $0<\xi<1$, eqns. 58 and 59 are always satisfied. In addition, if eqn. 61 is satisfied, so is eqn. 60. Thus, we consider the condition of γ under which eqn. 61 is satisfied.

From eqns. 71 and 42

$$\sigma^2\simeq \mathrm{E}[e_b^2(n)]=\sigma_0^2+\xi^2 w_0^T R w_0 \quad (62)$$

where $w_0^T R w_0$ is the variance of the (backward) predictor $w_0^T x(n)$ and $\sigma_0^2=\mathrm{E}[e_{b,0}^2(n)]$ is the variance of the prediction error. Denoting $\gamma_0=w_T 0 R w_0/\sigma_0^2$ and using eqn. 74, the left-hand side of eqn. 61 is

$$r-\frac{4r}{(r+2)^2}\frac{w_0^T R w_0/\sigma_0^2}{1+\xi^2 w_0^T R w_0/\sigma_0^2}$$
$$\simeq\frac{r}{(r+2)^2+r^2\gamma_0}\{(1+\gamma_0)r^2+4r+4(1-\gamma_0)\} \quad (63)$$

Therefore, by assumption 4, i.e.

$$\gamma_0=\frac{w_0^T R w_0}{\sigma_0^2}<1 \quad (64)$$

Eqn. 61 is satisfied. We show that eqn. 57 is also satisfied. For small ε and r, from eqn. 74 $\xi\simeq r/2$ and $1-\xi\simeq 1$. Thus, the main term of eqn. 57 is $\{r-r\gamma+\varepsilon(1+r\gamma)\}\times 4-\varepsilon(r-r\gamma)\times 4^2$. However, this is positive for small ε if eqn. 61 holds. Hence, we conclude that, by the perturbation analysis, the modified algorithm by leakage is guaranteed to be stable under assumptions 1–4.

Eqn. 64 is also expressed in the following way. First, from eqn. 70 we note that $\mathrm{E}[x^2(n-p)]=\mathrm{E}[x^2(n)]=\sigma_0^2+w_0^T R w_0$. Thus, eqn. 64 becomes

$$\frac{\mathrm{E}\,[x^2(n)]}{\sigma_0^2}<2 \quad (65)$$

From the well known fact in the linear prediction theory [7], eqn. 65 is written as

$$\frac{1}{(1-\kappa_1^2)(1-\kappa_2^2)\cdots(1-\kappa_p^2)}<2 \quad (66)$$

where κ_i is the ith partial autocorrelation coefficient of $\{x(n)\}$.

6 Simulation results

We show some simulation results of the modified algorithm. The system under investigation is a third-order FIR filter, such that the output $y(n)$ in response to the input time series $x(n)$ is

$$y(n)=2.0x(n)+1.0x(n-1)-0.5x(n-2)+v(n) \quad (67)$$

$v(n)$ is from a white unit-variance Gaussian noise source. The time series $x(n)$ is a nonwhite-noise sequence generated by the first-order AR process

$$x(n)=\alpha\, x(n-1)+u(n) \quad (68)$$

where $u(n)$ is a white unit-variance noise. In this case, $p=3$, $w_0=(0\ 0\ -\alpha)$ and assumption 2 is satisfied. In addition, $\kappa_1=-\alpha$, $\kappa_2=\kappa_3=0$. Thus to satisfy eqn. 64, from eqn. 66 the AR coefficient α must meet $1/2<1-\alpha^2$, i.e. $|\alpha|<1/\sqrt{2}$.

We choose a value of 0.999 for the forgetting factor λ, with $\alpha=0.707$. To check the expression for the bias in eqn. 74, a dotted line in Fig. 1 represents the plots of the third element of $w_b(n)$, together with the theoretical value, where we use $r=0.5$ to see the bias clearly. The time average of the parameter estimate in the steady state from $k=10000$ to 5000 is 0.566. This is very close to the theoretical value 0.565. The agreement is good even for this rather large r. Next we made simulations for $\alpha=0.6$, 0.7, 0.707 with $r=0.1$. The algorithm remains stable for 50000 iterations at least. The simulation result for $\alpha=$ 0.707 is shown in Fig. 2. The plotted quantities in Fig. 2 are the three coefficients of the adaptive filter. However, for $a=0.8$, sometimes it fails. One trial for $a=0.8$ is depicted in Fig. 3. Even in such a condition, by simulations we find that the modified algorithm can be stabilised by using a larger value of r. The simulation result with $r=0.2$ is shown in Fig. 4, where the algorithm is now stabilised.

We also generate the second-order AR process

$$x(n)=\alpha_1 x(n-1)+\alpha_2 x(n-2)+u(n) \quad (69)$$

where $\alpha_1=-(\kappa_1+\kappa_2\kappa_1)$ and $\alpha_2=-\kappa_2$ [7]. In this case, $w_0^T=(0-\alpha_1-\alpha_2)$ and assumption 2 is satisfied. The case $\kappa_1=\kappa_2=0.5$ satisfies eqn. 64, whereas the case $\kappa_1=0.5$, $\kappa_2=1/\sqrt{3}$ does not. For $\lambda=0.9998$ the former case is

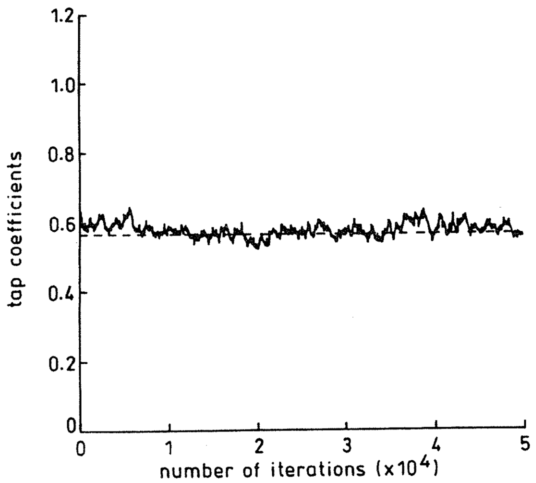

Fig. 1 *Plots of third element of $w_b(n)$ and theoretical bias value*
$\lambda=0.999$, $\alpha=0.707$, $r=0.5$

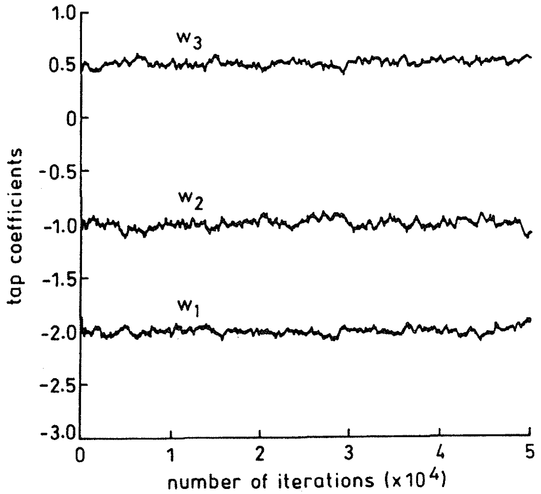

Fig. 2 *Plots of w(n) of modified fast QRD inverse-update algorithm*
$\lambda = 0.997$, $\alpha = 0.707$, $r = 0.1$

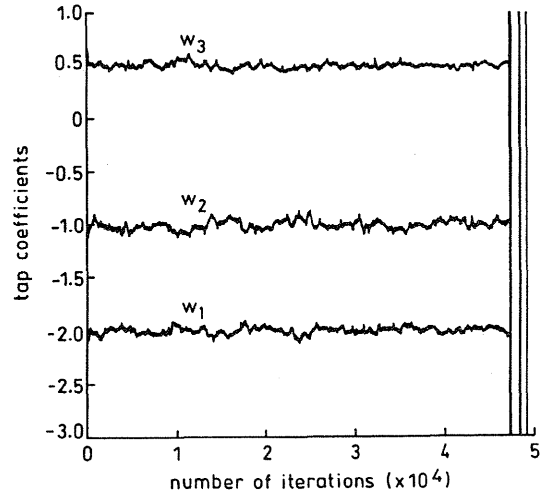

Fig. 3 *Plots of w(n) of modified fast QRD inverse-update algorithm*
$\lambda = 0.997$, $\alpha = 0.800$, $r = 0.1$

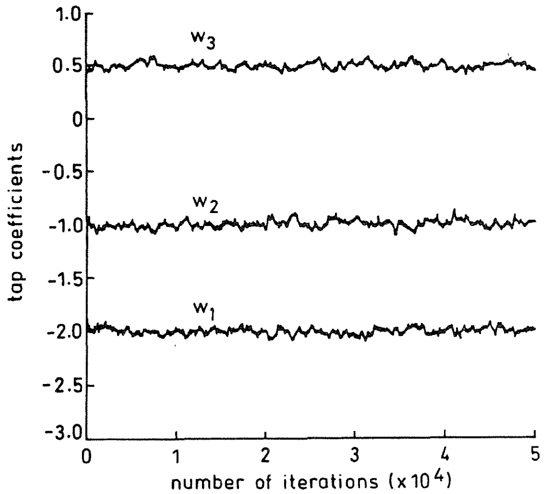

Fig. 4 *Plots of w(n) of modified fast QRD inverse-update algorithm*
$\lambda = 0.997$, $\alpha = 0.800$, $r = 0.2$

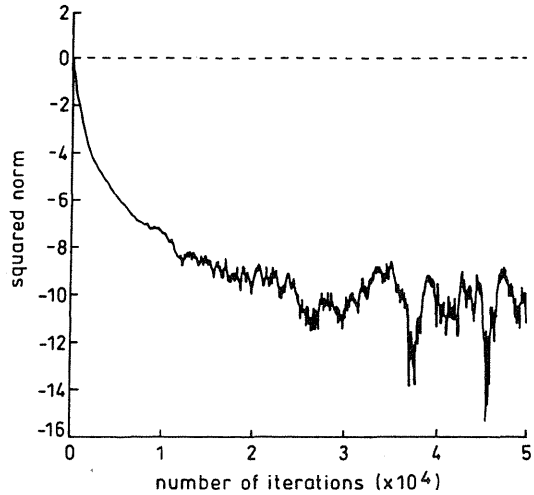

Fig. 5 *Plots of squared norm of difference between w(n) s of modified algorithm and conventional RLS algorithm in log scale*
$\lambda = 0.9998$, $\alpha_1 = 0.700$, $\alpha_2 = 0.400$, $r = 0.1$

stabilised for $r = 0.1$, whereas the latter case requires $r = 0.4$ for stabilisation. Thus, again we see that the simulation results somehow coincide with the conclusion derived by the perturbation analysis, but in this case we need to use much smaller ε.

Fig. 5 shows the plots of the squared norm of the difference between the weight vectors $w(n)$ by modified algorithm by leakage and the conventional numerically stable non-fast RLS algorithm. The plots are depicted in a log scale, which shows that the modified algorithm is numerically stable.

7 Conclusions

We have presented a stability analysis of error propagation of the modified fast QRD inverse-updates adaptive filtering algorithm by leakage. Theoretical findings and simulation results coincide well.

In future work, the case where the input signal is more correlated, i.e. γ_0 in eqn. 64 is greater than 1 will be examined.

8 Acknowledgment

The authors would like to thank the anonymous reviewers for their detailed comments.

9 References

1 SLOCK, D.T.M., and KAILATH, T.: 'Numerically stable fast transversal filters for recursive least squares adaptive filtering', *IEEE Trans. Signal Process.*, 1991, **39**, pp. 92–114
2 BINDE, S.: 'Stabilizing fast RLS algorithm by leakage', *Signal Process.*, 1998, **70**, pp. 1–21
3 PROUDLER, I.K.: 'Fast time-series adaptive-filtering algorithm based on the QRD inverse-updates method', *IEE Proc.-Vis. Image Signal Process.*, 1994, **141**, pp. 325–333
4 SAMSON, C.G., and REDDY, V.U.: 'Fixed point error analysis of the normalized ladder algorithm', *IEEE Trans. Acoust. Speech Signal Process.*, 1983, **ASSP-31**, (5), pp. 1177–1191
5 STOICA, P., and NEHORAI, A.: 'On the asymptotic distribution of exponentially weighted prediction error estimations', *IEEE Trans. Acoust. Speech Signal Process.*, 1988, **36**, (1), pp. 136–139
6 KUO, B.C.: 'Automatic control systems' (Prentice Hall, New Jersey, 1995, 7th edn.), Chap. 6
7 HAYKIN, S.: 'Adaptive filter theory' (Prentice Hall, New Jersey, 1996, 3rd edn.), Chap. 6

10 Appendix

10.1 Bias in $w_b(n)$

Here we examine a bias in $w_b(n)$. First, we express

$$x(n-p) = -w_0^T x(n) + e_{b,0}(n) \tag{70}$$

where $w_0 = (w_p \cdots w_1)^T$ is the (backward) optimal prediction coefficient vector, so that

$$E[e_{b,0}(n)x(n)] = 0 \tag{71}$$

From eqns. 10, 14 and 46 we have

$$w_b(n) = \tau\{w_b(n-1) + e_{b,0}(n)k(n) + k(n)x^T(n)(w_b(n-1) - w_0)\} \tag{72}$$

Define $w_b = E[w_b(n)]$. By using the averaging principle and eqn. 71, we note that $E[e_{b,0}(n)k(n)] = E[R^{-1}(n)x(n)e_{b,0}(n)] \simeq E[R^{-1}(n)]Ex(n)e_{b,0}(n)] = 0$. By taking the expectation of eqn. 72 and using eqn. 23, we have

$$\begin{aligned} w_b &= \tau\{w_b + (\beta^2 - 1)(w_b - w_0)\} \\ &= \frac{\tau - \tau\beta^2}{1 - \tau\beta^2} w_0 \end{aligned} \tag{73}$$

Setting $\beta = 1 - \varepsilon$, $\tau = 1 - r\varepsilon$ then gives

$$w_b \simeq (1 - \xi)w_0, \quad \xi = \frac{r}{r+2} \tag{74}$$

10.2 Partial derivatives of $\delta_p(n)$

Here we present the expressions of the partial derivatives of $\delta_p(n)$, which frequently appear. Since from eqns. 3 and 11

$$\delta_p(n) = \frac{\delta_p(n-1)}{1 + \left(\dfrac{e_f^2(n)}{\beta^2 \epsilon_f^2(n-1)} - \dfrac{e_b^2(n)}{\beta^2 \epsilon_b^2(n-1)}\right)\delta_p(n-1)} \tag{75}$$

we have

$$\frac{\partial \delta_p(n)}{\partial \epsilon_f^2(n-1)} = \frac{\delta_p^2(n)}{\delta_p(n-1)} \frac{e_f^2(n)}{\beta^2 \epsilon_f^4(n-1)} \simeq \frac{e_f^2(n)}{\beta^2 \epsilon_f^4(n-1)} \tag{76}$$

$$\frac{\partial \delta_p(n)}{\partial w_b^T(n-1)} = \frac{\delta_p^2(n)}{\delta_p(n-1)} \frac{2e_b(n)x(n)}{\beta^2 \epsilon_b^2(n-1)} \simeq \frac{2e_b(n)x(n)}{\beta^2 \epsilon_b^2(n-1)} \tag{77}$$

$$\frac{\partial \delta_p(n)}{\partial \epsilon_b^2(n-1)} = -\frac{\delta_p^2(n)}{\delta_p(n-1)} \frac{e_b^2(n)}{\beta^2 \epsilon_b^4(n-1)} \simeq -\frac{e_b^2(n)}{\beta^2 \epsilon_b^4(n-1)} \tag{78}$$

$$\begin{aligned} \frac{\partial \delta_p(n)}{\partial \delta_p(n-1)} &= \frac{\delta_p(n)}{\delta_p(n-1)} - \frac{\delta_p^2(n)}{\delta_p(n-1)} \left(\frac{e_f^2(n)}{\beta^2 \epsilon_f^2(n-1)} - \frac{e_b^2(n)}{\beta^2 \epsilon_b^2(n-1)}\right) \\ &\simeq 1 - \left(\frac{e_f^2(n)}{\beta^2 \epsilon_f^2(n-1)} - \frac{e_b^2(n)}{\beta^2 \epsilon_b^2(n-1)}\right) \end{aligned} \tag{79}$$

10.3 Higher order moments

Here we present the expressions of the higher order moments of $\epsilon_f^2(n)$ and $\epsilon_b^2(n)$. Squaring both sides of eqn. 35 with $\delta_p(n-1) \simeq 1$, we have

$$\epsilon_f^4(n) \simeq \beta^4 \epsilon_f^4(n-1) + 2\beta^2 \epsilon_f^2(n-1)\sigma^2 + e_f^4(n) \tag{80}$$

Taking the expectation, using the averaging principle and $E[\epsilon_f^2(n)] \simeq \sigma^2/(1\text{-}\beta^2)$ in the steady state, we have

$$E[\epsilon_f^4(n)] \simeq \frac{2\beta^2\sigma^4}{(1-\beta^2)(1-\beta^4)} \simeq \frac{\sigma^4 \varepsilon^{-2}}{4} \tag{81}$$

Similarly, we have

$$E[\epsilon_b^4(n)] \simeq \frac{\sigma^4 \varepsilon^{-2}}{4} \tag{82}$$

Next, multiplying both sides of eqns. 35 and 39 with $\delta_p(n) \simeq 1$, we have the recursion

$$\begin{aligned} \epsilon_f^2(n)\epsilon_b^2(n) \simeq{}& \lambda^2 \epsilon_f^2(n-1)\epsilon_b^2(n-1) + \lambda\epsilon_b^2(n-1)e_f^2(n-1) \\ &+ \lambda\epsilon_f^2(n-1)e_b^2(n) + e_f^2(n-1)e_b^2(n) \end{aligned} \tag{83}$$

Taking the expectation and using the averaging principle, we have

$$\begin{aligned} E[\epsilon_f^2(n)\epsilon_b^2(n)] &\simeq \frac{1}{1-\lambda^2}\sigma^2\{E[\epsilon_b^2(n-1)] + E[\epsilon_f^2(n-1)]\} \\ &\simeq \frac{\sigma^4}{4}\varepsilon^{-2} \end{aligned} \tag{84}$$

In entirely the same way from eqns. 80 and 39, we have

$$\begin{aligned} \epsilon_f^4(n)\epsilon_b^4(n) ={}& \lambda^3 \epsilon_f^4(n-1)\epsilon_b^2(n-1) \\ &+ 2\lambda^2 \epsilon_f^2(n-1)\epsilon_b^2(n-1)e_f^2(n-1) \\ &+ \lambda^2 \epsilon_f^4(n-1)e_b^2(n) \\ &+ 2\lambda\epsilon_f^2(n-1)e_f^2(n-1)e_b^2(n) + e_f^4(n-1)e_b^2(n) \end{aligned} \tag{85}$$

Hence from eqns. 81–84, we have

$$\begin{aligned} E[\epsilon_f^4(n)\epsilon_b^2(n)] \simeq{}& \frac{2\lambda^2}{1-\lambda^3} E[\epsilon_f^2(n-1)\epsilon_b^2(n-1)]\sigma^2 \\ &+ \frac{\lambda^2}{1-\lambda^3} E[\epsilon_f^4(n-1)]\sigma^2 \simeq \frac{\sigma^6}{8}\varepsilon^{-3} \end{aligned} \tag{86}$$

10.4 Derivation of eqns. 46 and 47

From eqn. 30 we note that $k(n)$ is of order ε In addition, from eqn. 44 $\bar{s}_f$ is of order ε, since $\epsilon_f^2(n)$ is of order ε^{-1}. Thus, from eqn. 29 $v_b(n)$ is of order ε

First, eqn. 46 is derived. From eqns. 13 and 14

$$\begin{aligned} \frac{\partial w_b(n)}{\partial \epsilon_f^2(n-1)} ={}& \tau e_b(n) \frac{\partial v_b(n)}{\partial \epsilon_f^2(n-1)} \frac{1}{\bar{c}_b} \\ &+ \tau e_b(n) \frac{\partial\left(\frac{1}{\bar{c}_b}\right)}{\partial \epsilon_f^2(n-1)} v_b(n) \\ &+ \tau e_b(n) \frac{\partial\left(\frac{\bar{s}_b}{\bar{c}_b}\right)}{\partial \epsilon_f^2(n-1)} w_b(n-1) \\ \equiv{}& T_1 + T_2 + T_3 \end{aligned} \tag{87}$$

From eqn. 29 we have

$$\begin{aligned} \frac{\partial v_b(n)}{\partial \epsilon_f^2(n-1)} ={}& -\frac{\partial \bar{s}_f}{\partial \epsilon_f^2(n-1)}(S\tau e_f(n)k(n-1) \\ &+ \tau S w_f(n-1) + \pi) \end{aligned} \tag{88}$$

However, the first term is small compared with the other terms. Hence, from eqn. 44 and $\delta_p(n-1) \simeq 1$

$$\frac{\partial \bar{s}_f}{\partial \epsilon_f^2(n-1)} \simeq -\frac{e_f(n)}{\delta_p^{-1}(n-1)\epsilon_f^4(n-1)} \tag{89}$$

and

$$\mathrm{E}[T_1] \simeq \mathrm{E}\left[\frac{e_f(n)e_b(n)}{\beta^2 \epsilon_f^4(n-1)}(\boldsymbol{S}\boldsymbol{w}_f(n-1)+\pi)\right] \tag{90}$$

Hence, by the averaging principle and eqn. 80, we have

$$\mathrm{E}[T_1] \simeq \frac{4(\boldsymbol{S}\boldsymbol{w}_f+\pi)\varepsilon^2}{\sigma^4}\mathrm{E}[e_f(n)e_b(n)] \tag{91}$$

where $\boldsymbol{w}_f = \mathrm{E}[\boldsymbol{w}_f(n)]$. As in eqn. 74 $\boldsymbol{w}_f = (1\text{-}\xi)\bar{\boldsymbol{w}}_0$ with $\bar{\boldsymbol{w}}_0 = (\boldsymbol{w}_1 \ldots \boldsymbol{w}_p)^T$. Thus, corresponding to eqn. 42

$$e_f(n) = e_{f,0}(n) - \xi\bar{\boldsymbol{w}}_0^T \boldsymbol{x}(n-1) \tag{92}$$

where $e_{f,0}(n) = x(n) + \bar{\boldsymbol{w}}_0^T \boldsymbol{x}(n-1)$. Under assumption 2 about the linear prediction coefficient, i.e. $\boldsymbol{w}_p = 0$, we have

$$\begin{aligned}&\mathrm{E}[e_{f,0}(n)e_{b,0}(n)]\\ &\quad = \mathrm{E}[(x(n)+\bar{\boldsymbol{w}}_0^T\boldsymbol{x}(n-1))(x(n-p)+\boldsymbol{w}_0^T\boldsymbol{x}(n))]\\ &\quad = \boldsymbol{w}_p\mathrm{E}[x(n-p)(x(n-p)+\boldsymbol{w}_0^T\boldsymbol{x}(n))] = 0\end{aligned} \tag{93}$$

Thus, from eqn. 74

$$\mathrm{E}[e_f(n)e_b(n)] = \xi^2\mathrm{E}[\bar{\boldsymbol{w}}_0^T\boldsymbol{x}(n-1)\boldsymbol{w}_0^T\boldsymbol{x}(n)] = O(r^2) \tag{94}$$

Therefore, if we take $r = O(\varepsilon^\zeta)(1/2 < \zeta)$ as in assumption 1, then $\mathrm{E}[T_1] \simeq o(\varepsilon^3)$ and this can be discarded.

From eqns. 31, 75 and $\epsilon_b^2(n) \simeq O(\varepsilon^{-1}), \varepsilon_f^4(n) \simeq O(\varepsilon^{-2})$, we note

$$\frac{\partial\left(\frac{1}{\bar{c}_b}\right)}{\partial\epsilon_f^2(n-1)} \simeq \frac{e_b^2(n)e_f^2(n)}{\beta^4\epsilon_b^2(n-1)\epsilon_f^4(n-1)} \simeq O(\varepsilon^3) \tag{95}$$

However, $\boldsymbol{v}_b(n)$ is of order ε so that T_2 is of order ε^4 and can be discarded.

Since from eqn. 12

$$e_b(n)\frac{\bar{s}_b}{\bar{c}_b} = \frac{1}{\bar{c}_b} - 1 \tag{96}$$

from eqns. 80, 95 and 86 and the averaging principle, we have

$$\mathrm{E}[T_3] \simeq \mathrm{E}\left[\frac{e_f^2(n)e_b^2(n)}{\epsilon_b^2(n-1)\epsilon_f^4(n-1)}\right]\boldsymbol{w}_b \simeq \frac{8\varepsilon^3}{\sigma^2}\boldsymbol{w}_b \tag{97}$$

where from assumption 3 we use $\mathrm{E}[e_f^2(n)e_b^2(n)] = \sigma^4 + 2(\mathrm{E}[e_f(n)e_b(n)])^2 \simeq \sigma^4$. Thus, eqn. 46 is shown.

In a similar way, eqn. 47 can be derived. From eqn. 13

$$\begin{aligned}\frac{\partial \boldsymbol{w}_b(n)}{\partial\epsilon_b^2(n-1)} &= \tau e_b(n)\frac{\partial\left(\frac{1}{\bar{c}_b}\right)}{\partial\epsilon_b^2(n-1)}\boldsymbol{v}_b(n)\\ &\quad + \tau e_b(n)\frac{\partial\left(\frac{\bar{s}_b}{\bar{c}_b}\right)}{\partial\epsilon_b^2(n-1)}\boldsymbol{w}_b(n-1)\\ &\equiv T_4 + T_5\end{aligned} \tag{98}$$

As in eqn. 95

$$\frac{\partial\left(\frac{1}{\bar{c}_b}\right)}{\partial\epsilon_b^2(n-1)} \simeq \frac{e_b^2(n)}{\beta^2\epsilon_b^4(n-1)}\left(1-\frac{e_b^2(n)}{\beta^4\epsilon_b^2(n-1)}\right) \simeq O(\varepsilon^2) \tag{100}$$

and $\boldsymbol{v}_b(n)$ is of order ε so that $T_4 \simeq \mathcal{O}(\varepsilon^3)$. From eqns. 96 and 100, $\mathrm{E}[T_5] \simeq -\mathrm{E}[\tau e_b^2(n)\boldsymbol{w}_b(n-1)/\beta^2\epsilon_b^4(n-1)] \simeq -4\varepsilon^2\boldsymbol{w}_b/\sigma^2$.

Also

$$\begin{aligned}\frac{\partial \boldsymbol{w}_b(n)}{\partial\delta_p(n-1)} &= \tau e_b(n)\frac{\partial\left(\frac{1}{\bar{c}_b}\right)}{\partial\delta_p(n-1)}\boldsymbol{v}_b(n)\\ &\quad + \tau e_b(n)\frac{\partial\left(\frac{\bar{s}_b}{\bar{c}_b}\right)}{\partial\delta_p(n-1)}\boldsymbol{w}_b(n-1)\\ &\equiv T_6 + T_7\end{aligned} \tag{101}$$

However, again from eqns. 31 and 75

$$\frac{\partial\left(\frac{1}{\bar{c}_b}\right)}{\partial\delta_p(n-1)} = \frac{e_b^2(n)}{\beta^2\epsilon_b^2(n-1)}\frac{\partial\delta_p(n)}{\partial\delta_p(n-1)} \simeq \frac{e_b^2(n)}{\beta^2\epsilon_b^2(n-1)} \tag{102}$$

so that T_6 is of order ε^2 and $\mathrm{E}[T_7] \simeq \mathrm{E}[\tau e_b^2(n)\boldsymbol{w}_b(n-1)/\beta^2\epsilon_b^2(n-1)] \simeq 2\varepsilon\boldsymbol{w}_b$.